Technische Universität München
Fakultät für Medizin

Analysis of CXCL11 expression in high-grade serous ovarian cancer and triple-negative breast cancer

Yulia Bauer

Vollständiger Abdruck der von der Fakultät für Medizin der Technischen Universität München zur Erlangung des akademischen Grades einer
Doktorin der Medizin (Dr. med.)
genehmigten Dissertation.

Vorsitz: Prof. Dr. Lars Mägdefessel
Prüfer*innen der Dissertation: 1. apl. Prof. Dr. Viktor Magdolen
2. Prof. Dr. Angela Krackhardt

Die Dissertation wurde am 01.09.2022 bei der Technischen Universität München eingereicht und durch die Fakultät für Medizin am 03.01.2023 angenommen

Table of Content

Abbreviation

ACS *American Cancer Society*
ADCC *antibody-dependent cellular cytotoxicity*
ADCP antibody-dependent cellular phagocytosis
AR *androgen receptors*
ATCC *American Type Culture Collection*
BC breast cancer
BRAF *murine sarcoma viral oncogene homolog B1*
BRCA1 *breast cancer type 1 susceptibility protein*
BRCA2 *breast cancer type 2 susceptibility protein*
BSC *breast-conserving surgery*
CA-125 *serum cancer antigen 125*
Ca2+ *calcium*
CDC *complement-dependent cytotoxicity*
CD4 *cluster of differentiation 4*
CD8 *cluster of differentiation 8*
CDK *cyclin-dependent kinases*
cDNA *complementary deoxyribonucleic acid*
CHEK2 *checkpoint kinase 2*
ChT *chemotherapy*
CI *confidence interval*
CISH *chromogenic in situ hybridization*
CTLs *cytotoxic lymphocytes*
CXCL11 *CXC motif ligand 11*
CXCR3 *CXC motif receptor 3*
DAB *diaminobenzidine*
DCIS *ductal carcinomas in situ*
DCs *dendritic cells*
DFS *disease-free survival*
DMEM *Dulbecco's modified eagle medium*
DMSO *dimethyl sulfoxid*
DNA *desoxy ribonucleic acid*
E *efficiency*
EGFR-CAR *epidermal growth factor receptor-CAR*
ELISA *enzyme linked immuno sorbent assay*
EOC *epithelial ovarian cancer*
EP *error propagation*
ER *estrogen-receptor*
ERL *glucine leucine arginine*
FBS *fetal bovine serum*
FFPE *formalin-fixed, paraffin-embedded*
FPKM *1fragments per kilobase million*
FGFs *fibroblast growth factors*
Egr-1 *early growth response protein 1*
FIGO *Féderation Internationale de Gynécologie et d'Obstétrique*
FISH *fluorescence in situ hybridization*
FoxP3 *forkhead box protein P3*
G *histologic grade*
GEPIA *gene expression profiling interactive analysis*
HE4 *human epididymis protein 4*
HEPES *4-(2-hydroxyethyl)-1-piperazineethanesulfonic acid*
HER-2 *epidermal growth factor receptor 2*
HGSOC *high-grade serous carcinomas*
HPRT *hypoxanthine-guaninephosphoribosyltransferase*
HR *hazard ratio*
ICB *immune checkpoint blockade*
IFN *interferon*
IHC *immunohistochemistry*
IL *interleukin*
IP-9 *interferon-gamma-inducible protein 9*
I-TAC *interferon-inducible T-cell alpha chemoattractant*
KRAS *Kirsten rat sarcoma-2 virus*
LCIS *lobular carcinomas in situ*
LGSOC *low-grade serous carcinomas*
LPBC *lymphocyte-predominant breast cancer*
MAPK *mitogen-activated protein kinase*
min *minute*
mRNA *messenger RNA*
NK *natural killer*

NK *natural killer T cells*
OC *ovarian cancer*
OS *overall survival*
PARPi *PARP inhibitors*
PBS *phosphate-buffered saline*
PDGF *platelet growth factor*
PFS *progression-free survival*
PTEN *phosphatase and tensin homolog*
qPCR *real time quantitative polymerase chain reaction*
RNA *ribonucleic acid*
ROMA *ovarian malignancy risk algorithm*
RPMI *medium from the Roswell Park Memorial Institute*
RT *room temperature*
SISH *silver-enhanced in situ hybridization*
TAAs *tumor-associated antigens*
Th1 *T-helper 1*
Th2 *T helper 2*
TCGA *The Cancer Genome Atlas*
TILs *tumor infiltrating lymphocytes*
TMAs *tissue microarrays*
TME *tumor-microenvironment*
TNBC *triple-negative breast cancer*
TNF *tumor necrosis factor*
TP53 *tumor protein p53*
Tregs *regulatory T lymphocytes*
VEGF *vascular endothelial growth factor*
WHO *World Health Organization*

List of Tables

List of Figures

1 Introduction

1.1 Ovarian cancer

1.1.1 Epidemiology

Ovarian cancer (OC) is the most common cause of mortality and one of the most common gynecologic cancers in the world (Momenimovahed et al., 2019). It holds the 8th place among the most common cancers in women. Globally, it occurs in around 250,000 females each year and causes around 140,000 annual deaths (Bray et al., 2018). According to the *International Agency for Research on Cancer* 294,414 cases of OC were diagnosed in 2018 and 184,799 patients died. Around 3.4% of all cancer cases in women occur due to OC (official page of the *International Agency for Research on Cancer*, https://gco.iarc.fr/).

OC is a typical "silent killer". In most cases, there are no symptoms even at later stages and also no specific subjective signs for this type of cancer. This explains its high mortality, which exceeds the rates for any other type of cancer of the female reproductive system (Gajjar et al., 2012). The rates of mortality for this type of cancer have been stagnant since 1980. According to the *American Cancer Society* 75-80% of the women afflicted with tumor stage III or IV have 5-year survival rates of 17-39% only (cancer.org; Karen et al., 2017).

1.1.2 Classification

1.1.2.1 Histopathological classification

OC is not a single entity, but in fact a heterogeneous group of diseases. Based on the most probable tissue of origin, the *World Health Organization* (WHO) created a histological classification for ovarian tumors by separating ovarian neoplasms into the following groups: epithelial, germ cell, sex cord-stromal, metastases, miscellaneous (**Figure 1**; Ehdaivand, 2020).

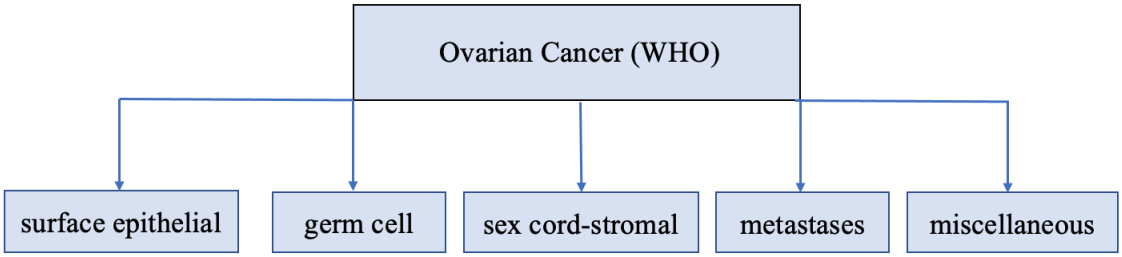

Figure 1. WHO classification of OC

Epithelial OC (EOC) accounts for 90% of the malignant ovarian tumors (Sundar et al., 2015). Epithelial ovarian tumors are grouped into histological types as follows: serous, mucinous,

endometrioid, clear cell tumors, transitional cell tumors (Brenner tumors), carcinosarcomas, mixed epithelial tumors, undifferentiated carcinomas, and others (**Figure 2**; Kaku et al., 2003). The major subtype is serous ovarian cancer, which includes approximately 70-80% of all EOC. Other groups are not as numerous, e.g., endometriod or mucinous tumors, which account for just ~5% or ~3%, respectively, of all EOC (Sundar et al., 2015).

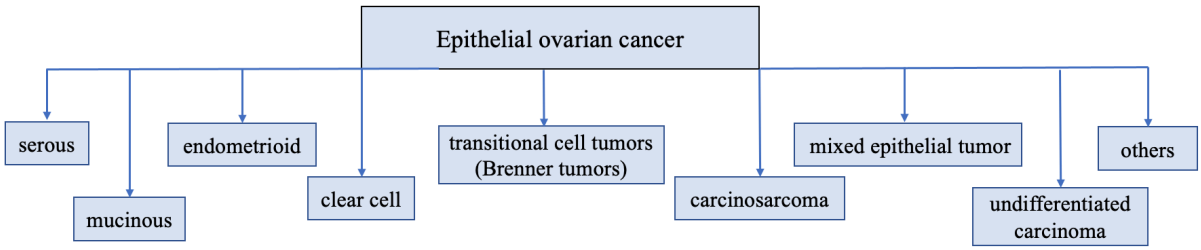

Figure 2. WHO classification of epithelial OC

1.2.2.2 Tumor staging

An important characteristic of all subtypes of OC is their respective stage describing the amount and extent of the spread of a tumor in the body. According to *International Federation of Gynecology and Obstetrics* (FIGO) there are four stages (**Figure 3**).

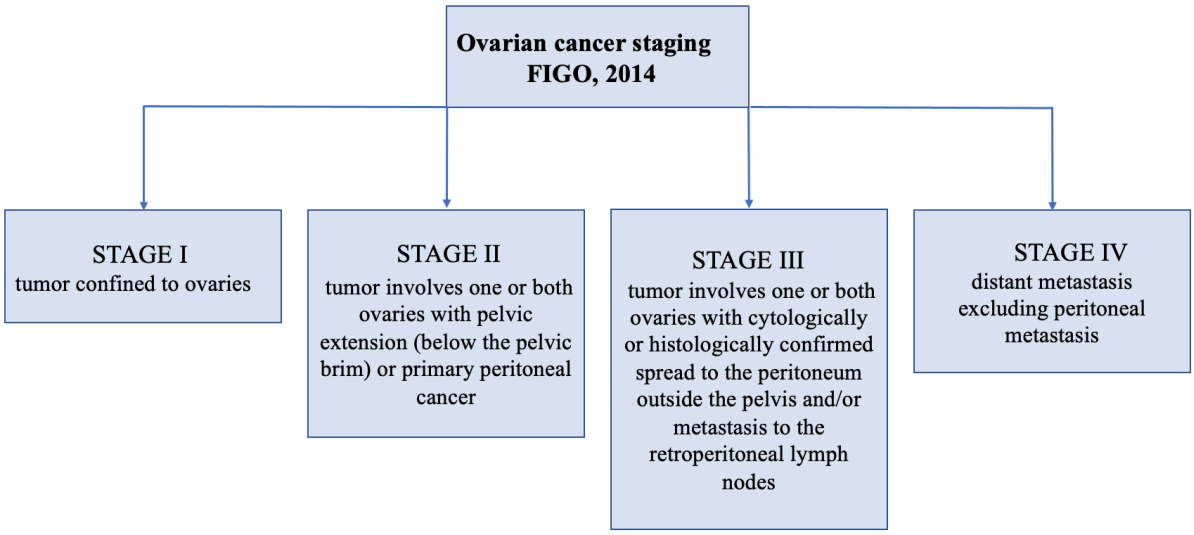

Figure 3. OC staging according to the FIGO

1.1.2.3 Clinical classification

Epithelial tumors can be subclassified by histologic grading**.** The grade of a tumor describes the morphological abnormality of the tumor cells when compared to healthy epithelial cells under a microscope (**Table 1**; Jonathan et al., 2018).

Table 1. Grading system for epithelial ovarian carcinoma according to the FIGO

GX	Grade cannot be assessed
G1	Well differentiated
G2	Moderately differentiated
G3	Poorly differentiated

G - histologic grade

Especially for serous carcinomas, a 2-tiered grading system has been established, in which tumors are divided into being low-grade and high-grade (**Figure 4**). This system is mainly based on the estimation of nuclear atypia including mitotic rates as a secondary feature (Malpica et al., 2004).

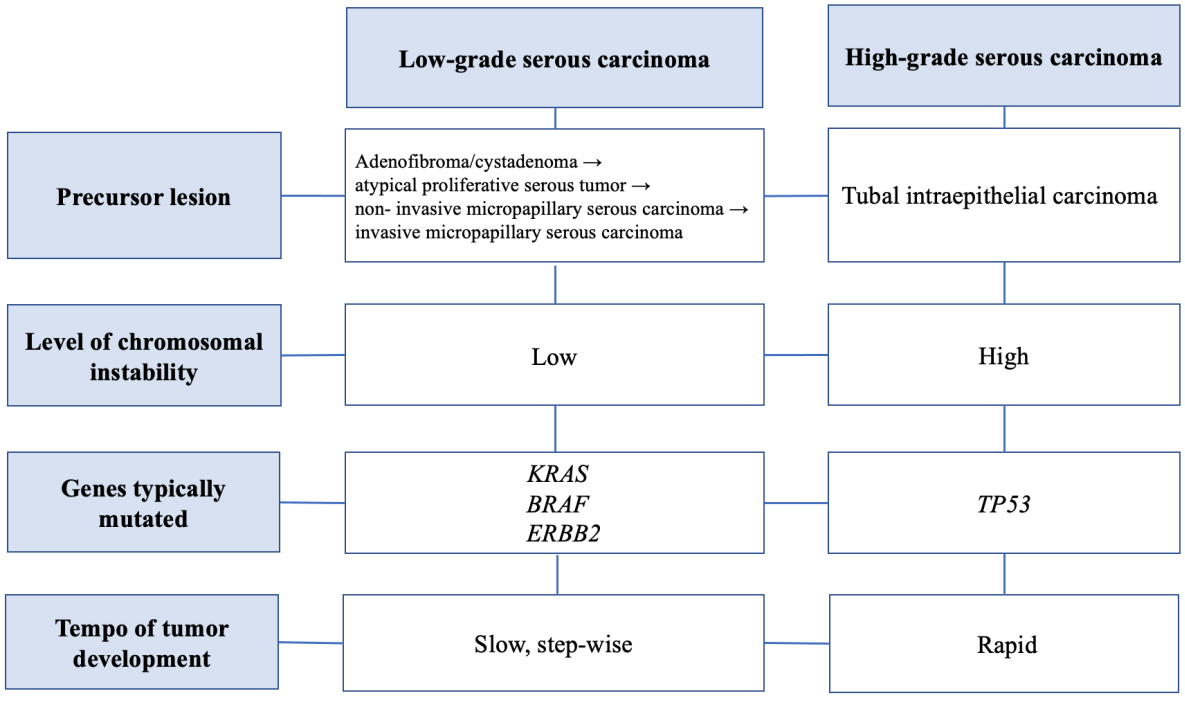

Modified from Vang et al., 2009

Figure 4. Pathogenesis of low-grade vs. high-grade ovarian serous carcinoma

Low-grade serous carcinomas (LGSOC) exhibit low-grade nuclei with a low mitotic index (up to 12 mitoses per 10 high power fields) and have frequent mutations of the human homolog of the Kirsten rat sarcoma-2 virus oncogene (*KRAS*), the murine sarcoma viral oncogene homolog

B1 (*BRAF*), or the epidermal growth factor receptor 2 (*ERBB2* or *HER-2)* genes, and lack tumor protein p53 (*TP53)* mutations. Mutations of *KRAS, BRAF*, and *ERBB2* result in the constitutive activation of the mitogen-activated protein kinase (MAPK) signal transduction pathway, which in turn leads to uncontrolled proliferation (Lee et al., 2020; Vang et al., 2009; Forgó and Longacre, 2021). The *TP53* gene product performs a tumor-suppressor function (Aubrey et al., 2016). Histologically, LGSOC is characterized by malignant glandular cells in clusters and singly, a moderate amount of finely vacuolated cytoplasm, enlarged hyperchromatic nuclei, the absence of significant nuclear pleomorphism (<3-fold change in size), and pronounced nucleoli (Forgó and Longacre, 2021). LGSOC, in rare cases, can develop into an invasive micropapillary serous borderline tumor and also progress to high-grade serous OC (HGSOC), sarcomatoid OC or carcinosarcoma (Forgo and Longacre, 2021; Gadducci and Cosio, 2020).

HGSOC generally displays high-grade nuclei and a high mitotic index (more than 12 mitotic figures per 10 high power fields). Recently, studies have shown that the majority of HGSOC originate from the fallopian tube, and not from the ovaries. This type is characterized by a rapid development. Typical for this subtype are *TP53* mutations and the lack of mutations of *KRAS, BRAF* or *ERBB2* (Vang et al., 2009; Forgo and Longacre, 2021). Histologically, HGSOC are characterized by three-dimensional clusters or single cells with scant cytoplasm, significant nuclear pleomorphism (more than 3x variation in size), and prominent nucleoli (Forgo and Longacre, 2021).

1.1.3 Diagnosis

Indefinite symptoms for OC include: bloating, pelvic or abdominal pain, decreased appetite, or urinary symptoms. The main problem is that symptoms are often overlooked. When the symptoms are covert, the identification of risk factors and screening plays a very important role. Increased risk includes older age, nullipara, early menarche or late menopause, menopausal hormone replacement therapy, endometriosis, *BRCA1/2* mutation, and Lynch syndrome. On the other hand, multiparity, lactation, hysterectomy, tubal ligation and using oral contraceptives is linked to a decreased risk of OC development (**Table 2**; Salehi et al., 2008; cancer.org).

Table 2. Risk factors for the development of OC

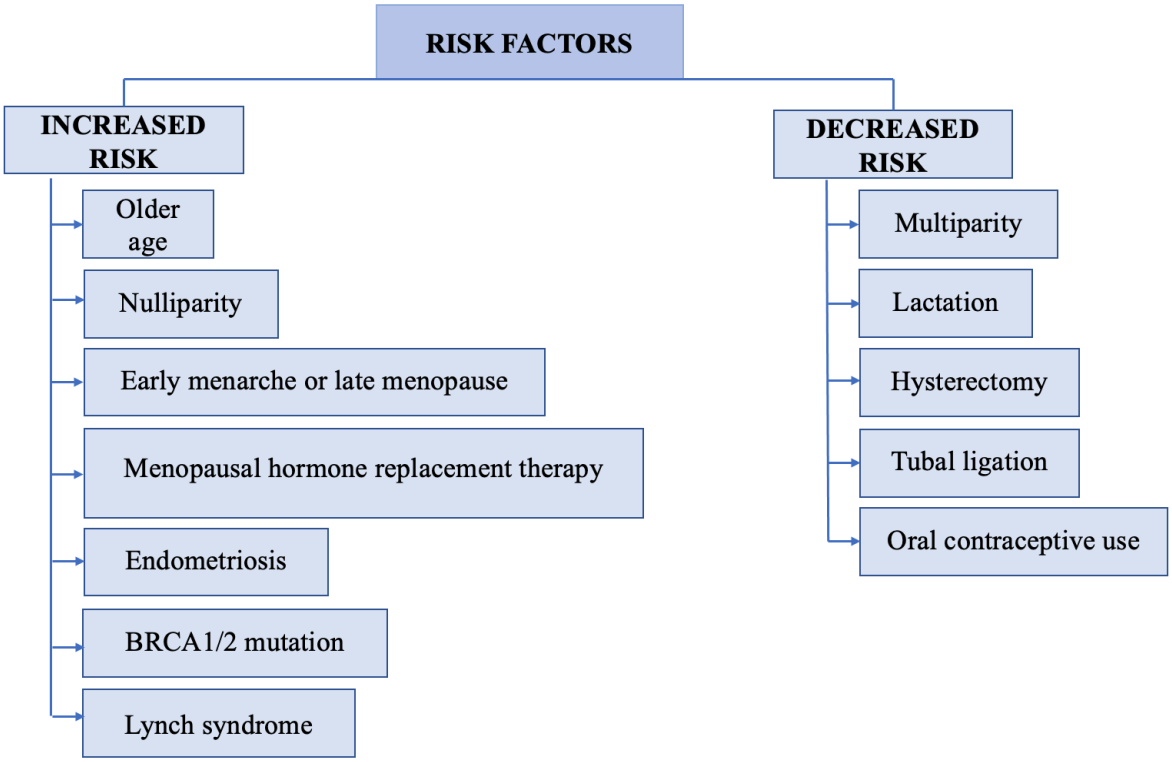

Diagnostic tools for OC detection are bimanual pelvic examination, transvaginal ultrasound, the determination of serum levels of carbohydrate antigen 125 (CA-125) as well as human epididymis protein 4 (HE4), and the calculation of the *Ovarian Malignancy Risk Algorithm* (ROMA) (Wei et al., 2016). Bimanual pelvic examination, however, lacks adequate sensitivity and specificity as a screening test and detects only one in 10,000 ovarian carcinomas in asymptomatic women. Transvaginal ultrasound can identify size and morphology changes of the ovary that may indicate a developing malignancy, but still has limited specificity and sensitivity. The serum level of the cancer antigen 125 (CA-125) is limited by its specificity. It is elevated in 80% of all ovarian carcinomas, but only in 50% of women with cancer limited to the ovary. It may also be found in women with a benign ovarian disease and in healthy women (Kamal et al., 2018; Jelovac et al., 2011). HE4, in contrast to CA-125, is more sensitive and specific, 72.9 and 95%, respectively. The ROMA index based on CA125 and HE4 serum levels as well as the menopausal status is also helpful for finding an ovarian malignancy (Wei et al., 2016). Due to the high prevalence, the high mortality rate and the limited possibilities of detection methods, there is an urgent need for additional diagnostic tools, especially at an early stage.

1.1.4 Treatment

The treatment not only depends on the type of OC and its stage, but also on the general health condition of the patient. Surgery and chemotherapy (ChT) are the standard treatments. For the stages I to IVA, the initial treatment is surgery. Few patients with stage IA or IB (grade 1), especially, serous, mucinous, endometrioid, and Brenner tumors, can be treated with surgery alone. Stages IC, II, III, and IV are usually treated with a combination of surgery and ChT (Jelovac et al., 2011; Grabosch et al., 2019; cancer.org). ChT can be applied before or after surgery and has different aims. Neoadjuvant ChT, or ChT before surgery, is given to reduce or stop the spread of cancer and makes surgery less invasive and more effective. Adjuvant or post-operative ChT is used to destroy any remaining cancer cells to reduce the chance of recurrence. OC can be highly sensitive to ChT, especially, to platinum-derived agents (carboplatin or cisplatin) and taxanes (paclitaxel or docetaxel), but despite this, recurrent metastatic lesions are common (Strandmann et al., 2016).

Radiotherapy is not widely used. Nevertheless, it remains an effective therapy for women with metastatic lesions, as well as for palliatives in advanced disease (Fields et al., 2017). The hormone therapy is used to treat ovarian sex-cord stromal tumors, but is seldom applied for EOC. (Knipprath-Mészáros et. Al., 2018).

Targeted therapy uses the molecular profile of cancer to develop a more effective therapy plan for the disease. Tumor angiogenesis is a complex and highly regulated process of blood vessel proliferation that promotes the survival, growth, invasion, and metastasis of tumor cells. Overexpression of pro-angiogenic factors, such as vascular endothelial growth factor (VEGF), fibroblast growth factors (FGFs), platelet growth factor (PDGF), and angiopoietins, have been reported in OC and are correlated with tumor progression and poor prognosis (Lopez et al., 2013). An example of targeted therapy is bevacizumab, which is a monoclonal antibody directed to VEGF and slows or stops cancer growth.

PARP inhibitors (PARPi) (olaparib, talazoparib) block PARP enzymes, which are normally involved in one pathway to help repair damaged DNA inside cells, including cancer cells. Blocking PARP may help to keep cancer cells away from repairing their damaged DNA. Currently, PARPi are used for metastatic *BRCA1/2*-mutant-associated cancers (cancer.org; Lopez et al., 2013; Sapiezynski et al., 2016; Pilié et al., 2019).

1.1.5 Immunology and ovarian cancer

It has been shown that OC can be an immunogenic tumor. First of all, it is characterized by the presence of tumor-infiltrating lymphocytes (TILs) (Clarke et al., 2009, Liu et al., 2020). The

presence of CD8+ TILs have been demonstrated to correlate with increased survival, while CD3+ T cells only seem to show prognostic significance in serous ovarian carcinomas (Clarke et al., 2009).

Besides this, according to immune infiltration and its prognostic value, three molecular OC subtypes have been identified. Cluster I (34.5%) is characterized by high levels of activated dendritic cells, macrophages M0, and activated mast cells. Cluster II (23.8%) displays high levels of resting CD4 memory T cells. Cluster III (41.7%) is more immunogenic than the other two clusters and shows high levels of resting dendritic cells, macrophages M1, activated NK cells, plasma cells, activated CD4 memory T cells, CD8 T cells, and regulatory T cells (Tregs). The clusters activate specific signaling pathways and have a different prognosis. Cluster I has a worse prognosis than Cluster III, Cluster II has the worst prognosis. The difference in the molecular characteristics of the three subtypes affects the immune infiltration pattern, and generates different responses to immunotherapy or anti-cancer drugs (Liu et al., 2020).
Tumor antigens, which help the immune system to identify tumor cells are potential candidates for their use in ovarian cancer therapy. In response to the secretion of tumor antigens by ovarian cancer cells the immune system mediates spontaneous antitumor responses specific to these antigens (Kandalaft et al., 2010; Mantia-Smaldone et al., 2012). The antigens are classified as tumor-associated antigens (*TAAs*) and universal tumor antigens. TAAs can be isolated not only from ascites or tumors, but also from normal cells. Currently, several TAAs associated with OC have been described and include *HER2/neu, p53, CA125, STn, FR-α*, *mesothelin, NY-ESO-1,* and *cdr-2.* Universal tumor antigens, including *hTERT,* and *survivin*, are those expressed in a variety of tumors and are not found in most normal human cells (Mantia-Smaldone et al., 2012).

1.2 Breast cancer

1.2.1 Epidemiology

Breast cancer (BC) is a heterogeneous disease developing solid tumors within the mammary gland (Badowska-Kozakiewicz et al., 2017). Apart from cancer of the lungs, it is the most common cancer in the world. In 2018, 2,088,849 new cases were diagnosed and 626,679 people died of BC (who.int, WHO 2018). Male BC accounts for less than 1% of all BC diagnoses worldwide (Yalaza et al., 2016). The median age for women diagnosed with BC is 62 years, men tend to be diagnosed at an older age than women. Their median age is about 67 years (Madeira et al., 2011).

According to the *American Cancer Society* (ACS), 90% of the people who receive a diagnosis of BC will live for at least another five years. This includes all types of BC at any stage of diagnosis (cancer.org, ACS 2018). Thanks to early detection by self-examination and, especially, by mammography, most BC cases in the developed world are diagnosed at an early stage.

1.2.2 Screening and diagnosis

Screening is a comprehensive program aimed at detecting malignant tumors as early as possible when there are no obvious clinical manifestations. Breast self-examination is an important tool that one can be performed regularly and at any age. According to the *WHO*, the only additional BC screening method that has proven to be effective is mammography screening for women without BC symptoms, who are not at a high risk of BC (WHO position paper on mammography screening). Screening should start at the age of 50 and thereafter every 2 years (mammographie-bayern.de).

In case of pathological screening mammography or symptoms, the patient is referred for further diagnosis. This includes physical examination, imaging techniques (mammography, ultrasound, magnetic resonance imaging), and biopsy. A biopsy is the only reliable way to confirm BC diagnoses. All algorithms for the clinical management of patients and their therapy include an immunohistochemical profile of the corresponding BC subtype (**Figure 6**; Badowska-Kozakiewicz et al., 2016; Goldhirsch et al., 2011).

In recent years, more and more molecular biological test procedures have been developed. These procedures include multigenic expression tests such as MammaPrint, Oncotype DX, and EndoPredict, which are intended for patients with hormone-dependent BC at the early stages of the disease. The expression of a number of genes in tumor tissue is measured and the risk of recurrence is indicated applying a risk score. MammaPrint analyses the activity of 70 genes, Oncotype DX 21 genes, and EndoPredict 12 genes (**Table 3**). These tests provide prognostic information about the risk of a possible relapse and can help to decide whether the patient will benefit from ChT or not (agendia.com, myriad.com, oncotypeiq.com).

Table 3. Indication of multigenic expression tests

MammaPrint	Oncotype DX	EndoPredict
• Stage I or II • ER+ or ER- • Invasive carcinoma • Tumor size <5.0 cm • Lymph node status: negative or positive (up to 3 nodes)	• Stage I, II, or IIIa • ER+ • HER2- • Lymph node status: negative or positive (up to 3 nodes)	• Stage I or II • ER+ • HER2- • Lymph node status: negative or positive (up to 3 nodes)

Estrogen-receptor status: positive (ER+) and negative (ER-)
Human epidermal growth factor status receptor 2: positive (HER2+) and negative (HER2-)

1.2.3 Risk factors

Many risk factors for BC have been identified. Reproductive factors (early menarche, late menopause, late age at first pregnancy and low parity) also favor this risk. Age over 40, alcohol consumption, obesity and too much dietary fat intake can also increase the risk of BC (Sun et al., 2017; Brewer et al., 2017; Lee et al., 2019). A significant role is also attributed to genetic factors such as the status of the BC type 1 susceptibility protein (*BRCA1*), the BC type 2 susceptibility protein (*BRCA*2), the tumor protein p53 (*TP53*), the phosphatase and tensin homolog (*PTEN*), and checkpoint kinase 2 (*CHEK2*) genes. The lifetime risk of developing BC in women with a mutation in the *BRCA*1 or *BRCA*2 gene is 60–80% (Badowska-Kozakiewicz et al., 2016; Young et al., 2009). Both mutations are predominantly responsible for different subtypes of BC. BC with a *BRCA*1 mutation is often characterized by a triple-negative phenotype, while for *BRCA*2 mutation it is more likely to be limited to estrogen receptor (ER) and/or to progesterone receptor (PR) positive tumors (De Talhouet et al., 2020). In case of an abnormal *CHEK2* gene, the lifetime risk of developing BC in women is up to 50%, whereas in case of a mutation *TP53* and *PTEN*, it is greater than 50%. Up to 10% all BCs are hereditary and are caused by abnormal genes. Currently, there are genetic tests to identify mutated *BRCA1* or *BRCA2* genes as well as mutations in the *CHEK2, PTEN*, *TP53* and many other genes *(ATM, BARD1, BRIP1, CDH1, NBN, NF1, PALB2, RAD51C, RAD51D, STK11, MSH2, MSH6, PMS2, EPCAM*) (breastcancer.org).

1.2.4 Classification

Classifications of breast tumors are based on different aspects, such as the histopathological type (**Figure 5**), the expression of proteins and genes (**Figure 6**), the stage of the tumor (**Table 4**), and the grade of the tumor (**Table 5**).

1.2.4.1 Histopathological classification

BC subtypes can be classified into carcinomas *in situ* and invasive (infiltrating) carcinomas **(Figure 5)**. For a long time, the term carcinoma *in situ* was used to describe a lesion that consists of cells that look like invasive carcinoma cells, featuring the accumulation of histologically altered cells without dissemination into the underlying tissue. It was assumed that, if left untreated, they would eventually progress into an invasive cancer (Ward et al., 2015). More recent data indicate that BC *in situ* does not always lead to the development of invasive carcinomas and can remain a non-invasive BC (van Seijen et al., 2019).

Carcinomas *in situ*, according to growth patterns and cytological features, can be subclassified into being ductal or lobular. Ductal carcinomas *in situ* (DCIS) are a heterogeneous group of diseases that account for approximately 25% of all diagnosed "breast cancers" and 85% of all breast carcinomas *in situ* (Cowell et al., 2013; Mullooly et al., 2017). Although it is a pre- or non-invasive disease, it is often considered an early form (stage 0) of BC. Up to 40% of DCIS develop into invasive carcinomas, if untreated (Cowell et al., 2013).

Traditionally, on the basis of the architectural features of the tumor, five generally recognized subtypes are distinguished: comedonic, ethmoid, micropapillary, papillary, and solid ones (Malhotra et al., 2010; van Seijen et al., 2019). Lobular carcinomas *in situ* (LCIS) account for 11.4% of all cases *in situ* and the lifetime risk of developing an invasive BC is 30-40% for women with LCIS (Mullooly et al., 2017; breastcancer.org).

Similar to *in situ* carcinomas, invasive carcinomas are as well classified into histological subtypes. The major invasive tumor types include no specific type, lobular, medullary, colloid (mucinous), papillary, tubular, adenoid cystic, inflammatory and carcinoma with metaplasia (Malhotra et al., 2010; Sinn et al., 2013; Rashmi et al., 2022).

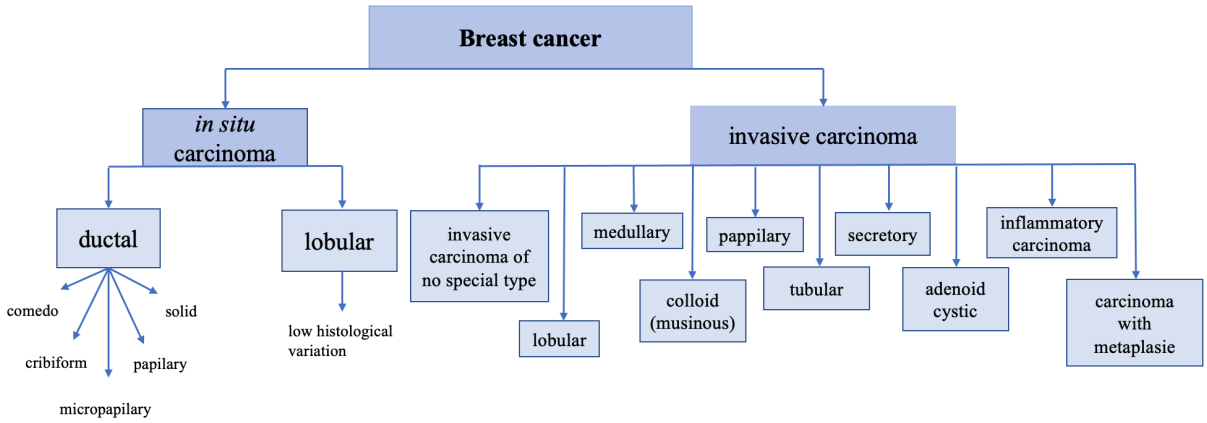

Figure 5. Histopathological classification of BC subtypes: carcinoma *in situ* include ductal (comedonic, ethmoid, micropapillary, papillary and solid) and lobular (low histological variation) subtypes. Invasive carcinoma includes no specific type, lobular, medullary, colloid (mucinous), papillary, tubular, adenoid cystic, inflammatory and carcinoma with metaplasia (Malhotra et al., 2010; Sinn et al., 2013; Rashmi et al., 2022).

This classification is based only on histology without the use of molecular markers that have shown predictive value (Malhotra et al., 2010).

1.2.4.2 Molecular classification

BC is further classified into subtypes based on the immunohistochemical detection of ER and PR, the detection of overexpression and/or the amplification of the human epidermal growth factor receptor 2 (HER2) oncogene, and a nuclear protein associated with cell proliferation (Ki-67) (**Figure 6**; Goldhirsch et al., 2011).

Around 75% of all BCs express ER and/or PR and are called ER-positive (or ER+) and PR-positive (or PR+), respectively (Schettini et al., 2016; Iqbal et al., 2014; cancer.org). Assessment of the presence of these two receptors is important for prognosis and management (Iqbal et al., 2014).

Up to 20% of BC show an overexpression/amplification of the HER2 (Schettini et al., 2016). Several methods are currently used for HER2 testing: IHC, fluorescence *in situ* hybridization (FISH), chromogenic *in situ* hybridization (CISH), and silver-enhanced *in situ* hybridization (SISH) (Gutierrez et al., 2011). Most commonly, IHC is applied, sometimes the HER2 status needs to be additionally tested after IHC with FISH to clarify the result. The IHC provides a score of 0 to +3. If the score is 0 to 1+ it is considered HER2-negative (HER2-). A score 3+ is considered as HER2-positive (HER2+). If the score is 2+, it is regarded borderline and needs to be further analyzed by FISH, which is a test for amplification of the HER2 gene (cancer.org).

Tumor proliferation is also a very important prognostic factor. Ki-67 is a nuclear protein that is an indicator of proliferation (Liang et al., 2020). The staining procedure measures the

percentage of tumor cells with positive nuclear staining from all tumor cells in a given histological field resulting in a Ki-67 index (Chung et al., 2016). Less than 10% is considered as low, 10-20% as borderline, and, if more than 20%, it is seen as high cell proliferation (breastcancer.org).

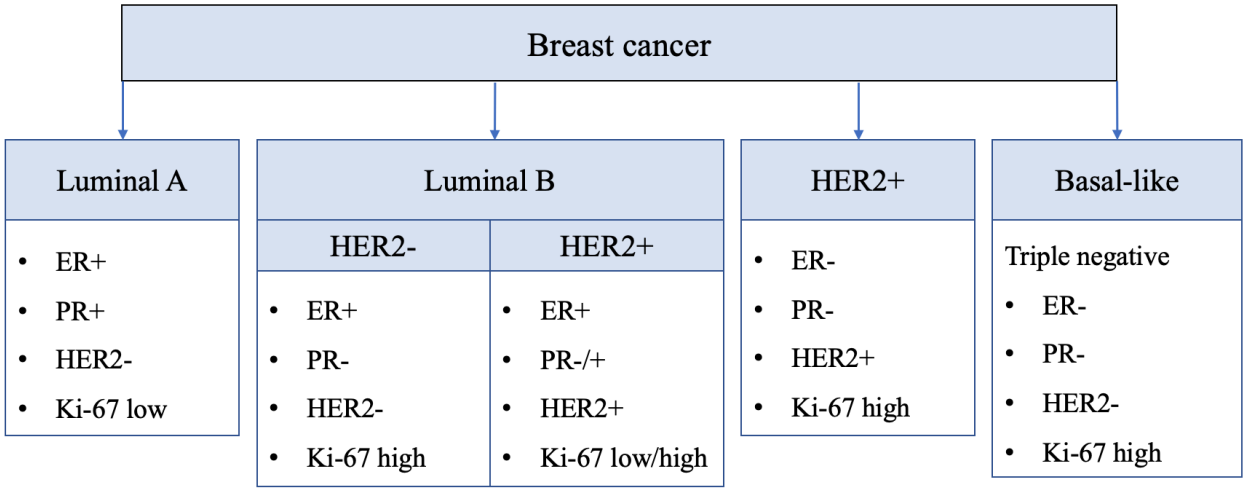

Figure 6. Molecular classification of BC subtypes: ER=estrogen receptor; HER2=human epidermal grown factor receptor; PR=progesterone receptor; Ki-67=nuclear protein associated with cell proliferation (Goldhirsch et al., 2011; Nascimento and Otoni, 2020).

Triple-negative BC (TNBC) lacks expression of the estrogen and progesterone receptors as well as overexpression of HER2 (William et al., 2010). Generally, TNBC accounts for about 12-17% of all BCs. This tumor-type is more aggressive than other breast carcinoma subtypes and is associated with a higher histopathological grade. It more often occurs in younger women (<50 years), and more likely shows distant recurrence and metastasis (Foulkes et al., 2010; Millikan et al., 2008; Nofech-Mozes et al., 2009). Also, very characteristic for TNBC is the absence of an association between the size of the primary tumor and the presence of metastases in the regional lymph nodes (Badowska-Kozakiewicz et al., 2016).

1.2.4.3 Tumor staging and grading

Any disease goes through various stages of its development. Stage classification helps to group specific symptoms that are related to one of the stages of the disease. Thanks to an individual stratification, it is easier to offer a special treatment (depending on the stage, various necessary treatment methods are used), and also allows to determine a prognosis of the disease. According to the *Cancer Research UK,* the TNM staging system is the most common way by which doctors stage BC. TNM stands for tumor, node, and metastasis (Cancer Research UK, 2020). The BC TNM classification includes the size of the tumors, involvement of lymph nodes and

the presence or absence of metastases. The TNM stage detection system, thus, provides information on tumor development (**Table 4**).

1.2.4.4 Treatment

BC treatment is always complex, depending on tumor subtypes and stage, and includes local (surgical and radiotherapy) and systemic (chemotherapy, endocrine therapy, molecular therapy) treatment (Dhankhar et al., 2010). The primary local therapy of choice is breast-conserving surgery (BSC), however, if this is impossible, mastectomy is necessary. Surgery of axillary lymph nodes is also usually carried out. Sentinel lymph node biopsy or axillary dissection is performed to control the spread of cancer and further decision about therapy. Postoperative radiotherapy is strongly recommended after BSC, as well as after mastectomy for high-risk patients. The systemic therapy includes either an adjuvant or a neoadjuvant approach. Adjuvant treatment is prescribed after the initial treatment to reduce the risk of cancer recurrence. Neoadjuvant treatment is indicated before surgery and can be applied for checking the sensitivity of the malignant tumor to ChT and/or for reduction its size. Usually, a combination of two or three drugs is used in ChT (anthracyclines, taxanes, cyclophosphamide, carboplatin, etc.). Multigenic expression tests such as Mammaprint, Oncotype DX and EndoPredict can help to determine which women will most likely benefit from ChT (Denkert et al., 2017).

To attack specific proteins that are involved in the growth and survival of cancer cells, targeted therapy is used, commonly in combination with traditional ChT (cancer.org; Cardoso et al., 2019). The targeted therapy shows a maximum impact on altered (tumor) cells with minimal impact on normal cells. This type of treatment is often associated with a good outcome because it is significantly less likely to result in untargeted side effects (Maddison et al., 2020). For example, there is the targeted therapy for HER2+ BC such as anti-HER2 monoclonal antibodies (trastuzumab, pertuzumab), and antibody-drug conjugates (trastuzumab, emtansin or TDM-1).

For hormone receptor-positive cancer an anti-hormonal (endocrine) therapy can be applied. It is a targeted treatment, which blocks hormones from attaching to receptors on cancer cells or by reducing the production of hormones. Tamoxifen, fulvestrant or aromatase inhibitors can be used (cancer.org; Cardoso et al., 2019).

PARP inhibitors (PARPi) (rucaparib, olaparib, niraparib, and talazoparib) are a type of targeted therapy that works by blocking the activity of the enzyme poly (ADP-ribose) polymerase, which is involved in the repair of DNA damage. In case of *BRCA1/2* mutations, PARPi proved to be effective. The inhibition of cyclin-dependent kinases (CDKs) (alvocidib, dinaciclib, seliciclib) in malignant cells provides another new strategy in the fight against cancer. CDKs

play a central role in the regulation of the cell cycle. Aberrant expression or altered activity of individual CDKs complexes lead to cells out of control of the cell cycle and malignant transformation (Law et al., 2015; Wesierska-Gadek J et al., 2004).

TNBC is lacking expression of estrogen and progesterone receptors and displays low expression of the HER2. Therefore, treatment options for TNBC are rather limited. Surgery and ChT, alone or in combination, are currently the only widely-used methods in therapy (Wahba et al., 2015). Still, TNBC has an immunologically active tumor microenvironment (which is characterized by a high proliferative activity), an increased immune cell infiltrate, and expression of androgen receptors, which could open up new avenues for the treatment for this aggressive subtype.

As research advances, new classes of drugs potentially effective in treating breast cancer are emerging. In addition, there exist several promising clinical approaches. They comprise anti-androgens and immune checkpoint inhibitors (Denkert et al., 2017). AR are expressed in around 70-90% cases of BC and play an important role in the pathogenesis of BC. Possibly AR may be a potential target for endocrine therapy for AR-positive BC patients (Anestis et al., 2020; Beniey et al., 2019). Immune checkpoints (PD-1/PD-L1 and CTLA-4/B7-1/B7-2) exert a natural brake on the immune system. Immune checkpoint inhibitors (pembrolizumab, atezolizumab) block it, which allows T-cells to recognize and attack tumors (cancer.gov). Presently, immune checkpoint inhibitors promise to supply new strategies for the treatment of BC (Beniey et al., 2019; Gaynor et al., 2020).

1.2.5 Immunology and breast cancer

BC displays low immunogenicity, especially when compared to tumors such as OC (Bates et al., 2018). However, in all BC subtypes tumor-infiltrated lymphocytes (TILs), which include B cells, T cells, dendritic cells (DCs), macrophages, neutrophils, monocyte and mast cells play an important role (Song et al., 2019). They do not only play a role in eliminating tumor cells, but also in the control of tumor growth, mediating response to ChT and generally improving clinical outcomes (Stanton and Disis, 2016; Denker et al., 2010). Most of the triple-negative and of HER2+ breast cancers refer to lymphocyte-predominant BC (LPBC), defined as tumors having high TIL levels (≥ 50%) and having the greatest survival benefit of each 10% increase in TILs. Hormone receptor-positive, HER2- tumors most likely show the lowest immune infiltrate (Stanton and Disis, 2016).

The phenotype of this infiltrate also determines the clinical outcome. The following TILs are associated with a favorable prognosis: CD8+ cytotoxic T lymphocytes (CTLs) with cytolytic

activity against cancer cells, CD4+ T-helper 1 (Th1) with facilitated antigen presentation through cytokine secretion and activation of antigen presenting cells. Unlike them GATA3+ T helper 2 (Th2) cells and FOXP3+ regulatory T lymphocytes (Tregs) can promote tumor growth and immune tolerance by impairing antigen presentation, activity, and cytotoxicity of other immune cells (Glajcar et al., 2019; Stanton and Disis, 2016). Depending on the number of deviations in the cell structure, different grading types are distinguished (**Table 5**; cancerresearchuk.or).

Table 4. TNM staging of BC

TX	Primary tumor cannot be assessed
T0	No evidence of primary tumor
T1	Tumor ≤ 20 mm
T2	Tumor > 20 mm but ≤ 50 mm
T3	Tumor > 50 mm
T4	Tumor of any size with direct extension into the chest wall and/or to the skin

T – primary tumor

pNX	Regional lymph nodes cannot be assessed
pN0	No regional lymph node metastasis
pN1	Metastases in 1-3 axillary lymph nodes and/or in internal mammary nodes
pN2	Metastases in 4-9 axillary lymph nodes
pN3	Metastases in ≥ 10 axillary lymph nodes

N – lymph node status

M0	No distant metastasis
M1	Distant metastasis

M - metastasis

Table 5. Grading of BC

GX	Grade cannot be assessed
G1	Low histological grade (favorable)
G2	Intermediate histological grade (moderately favorable)
G3	High histological grade (unfavorable)

G – histologic grade

1.3 Chemokines

1.3.1 General information about chemokines

Chemokines are a family of small chemoattractive cytokines characterized by a similar structure. The first chemokine was identified in 1977 by Walz and co-workers. It was the

procoagulant and angiostatic factor called platelet factor 4, now renamed CXCL4 (Walz et al., 1977). Chemokine genes are present in vertebrates from teleost fish up to humans (Yung et al., 2013). 48 chemokines in the human body have been identified (Blanchet et al., 2012).

These small, highly-conserved proteins (8 to 12 kDa) are involved in many biological processes (**Figure 7**). They play a vital role in cell migration through veins from the blood into tissue and vice versa. Chemokines are also significantly involved in the induction of cell movement in response to chemical (chemokine) gradients (Fernandez and Lolis, 2002; Miller and Mayo, 2017; Hughes and Nibbs, 2018).

The nomenclature of chemokines was initially created spontaneously, which caused major problems due to the presence of many synonyms. In 1999, one of the first systematic nomenclatures was introduced at the *Keystone Symposium on Chemokines and Chemokines Receptors* (Zlotnik et al., 2000). After some additions, a new classification was released (**Figure 8**). All chemokines have conserved amino acids that are important for creating their three-dimensional or tertiary structure, for example (in most cases) four cysteines (C), which upon forming distinct disulfide bonds create a "Greek key" shape. Intramolecular disulfide bonds are generally formed between the first and third as well as the second and fourth cysteine residues (numbers are given by the order in which they occur along the polypeptide chain from the N-end to the C-end) (chemeurope.com). Currently, chemokines are named according to the position of a cysteine residue in their primary structure and are grouped into four subfamilies (**Figure 8**). The names already include the subfamily name which the chemokine belongs to. The letter "L" means ligand, and the number stands according to the gene which encodes each chemokine (Nomiyama et al., 2008).

The chemokines signal through cell surface seven-transmembrane G protein-coupled receptors. In humans, 18 receptors have been identified. They are activated by different subfamilies: C (XCR1), CC (CCR1, CCR2, CCR3, CCR4, CCR5, CCR6, CCR7, CCR8, CCR9, CCR10), CXC (CXCR1, CXCR2, CXCR3, CXCR4, CXCR5, CXCR6), or CX_3C (CX_3CR1) (Arimont et al., 2017; Zlotnik and Yoshie, 2012). Their names depend on the class they bind. The receptors CXCR1, 2, 3, 4, 5, 6, 7 and 8 bind CXC, CCR1 through CCR10 bind CC, XCR1 binds the C, and CX3CR1 binds the CX3CL1 subfamily of chemokines (**Table 6**; Rossi and Zlotnik, 2000; Sánchez-Martín et al., 2013; Maravillas-Montero et al., 2015). In addition, four atypical receptors have been identified in humans (ACKRs: ACKR1, ACKR2, ACKR3/CXCR7, and ACKR4). They do not signal through G proteins and lack chemotactic activity (Arimont et al., 2017, Bachelerie et al., 2014).

Chemokines can activate more than one receptor, and many receptors can be activated by several different chemokines usually within a single class (**Table 6**; Yung et al., 2013), but also from other classes. For example, CCR3 can be activated by CXCL9, CXCL10, CXCL11, CCR5 by CXCL11, CXCR3 by CXC11 and CX3CR1 by CCL25 (Zlotnik and Yoshie, 2012). Activation of receptors can lead to a variety of additional cellular and tissue responses, including proliferation, differentiation, angiogenesis, extracellular matrix remodeling and tumor metastases (Ruffini et al., 2007).

Chemokines may also be classified by their function, including inflammatory or homeostatic ones (Yung et al., 2013). Inflammatory chemokines are activated when inflammatory cytokines, such as the tumor necrosis factor alpha (TNF-α), are released by the inflamed tissue, and they help to recruit leukocytes from the blood stream into the tissue. Homeostatic chemokines are constitutively expressed and mediate a proper immune cell composition, all of which express the corresponding receptor in various tissues in order to prepare for upcoming immune-relevant events (Oldham, University of Birmingham, UK; Zlotnik and Yoshie, 2000). Some members show characteristics of both groups such as CCL11, CCL17, CCL20, CCL22, XCL1, XCL2, CX3CL1 (Zlotnik and Yoshie, 2013).

Lately, cytokines are of great interest and the most studied function is the control of leukocyte migration. It is already known that some tumor cells produce different chemokines and express their receptors, which in many cases helps to enhance tumor growth (Hughes and Nibbs, 2018).

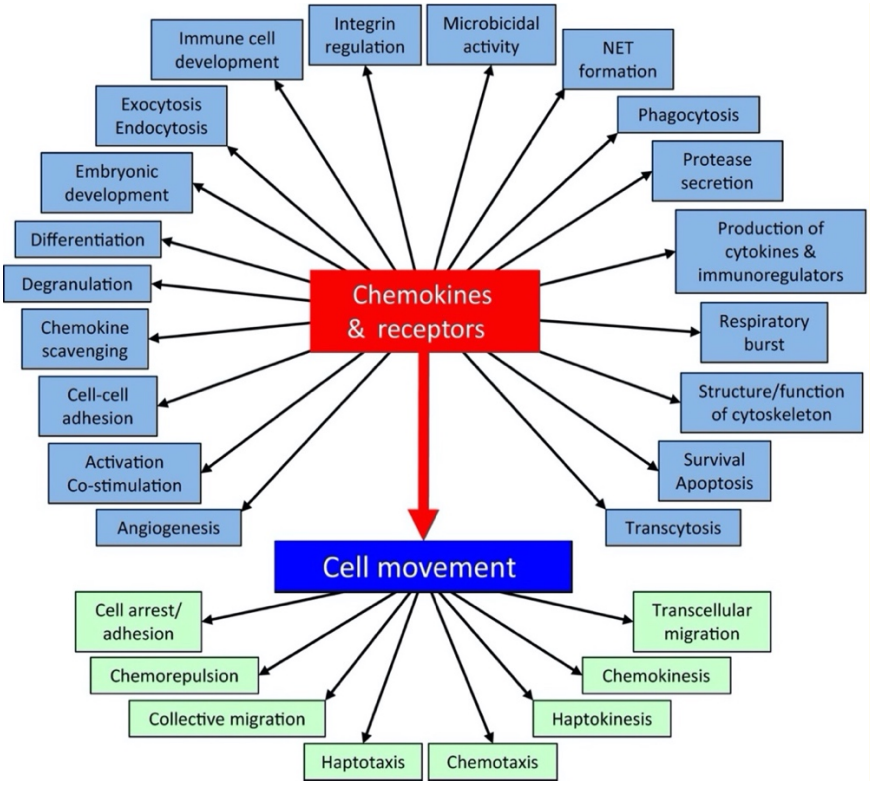

Taken from: Hughes and Nibbs, 2018.

Figure 7. Function of chemokines and their receptors

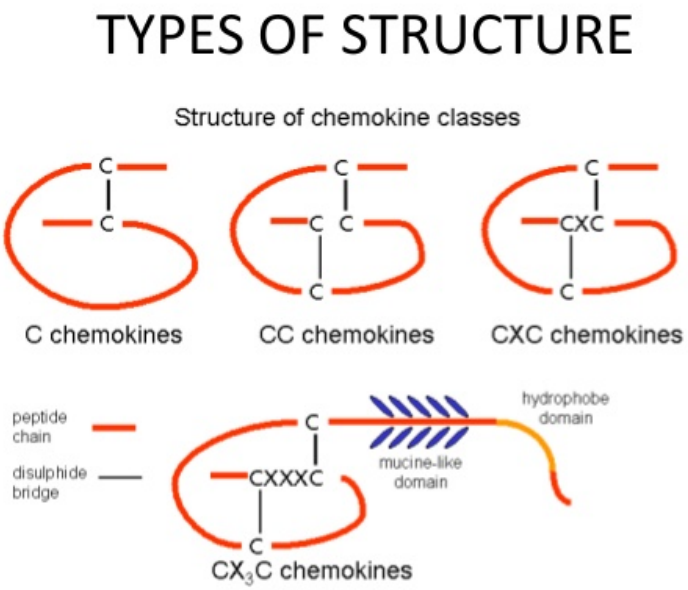

Taken from: presentation Dr. Kohidai

Figure 8. Different types of chemokine structures:

1. (X)C – missed the first or third cysteine;
2. CC- have two adjacent cysteines;
3. CXC- one amino acid separates the first two cysteines;
4. CX3C - has three amino acids between the two cysteines (Nomiyama et al., 2008).

1.3.2 C-X-C chemokines

The pleiotropic subfamily of the CXC chemokines comprises17 members. Most of the members of the CXC subfamily genes have been mapped to the human chromosome 4q. The main functions include the regulation of angiogenesis and the stimulation of migration of various immune cells such as cytotoxic lymphocytes (CTLs), natural killer (NK) cells, natural killer T (NKT) cells, and macrophages (Balestrieri et al., 2008; Tokunaga et al., 2017).

Depending on the presence or absence of the three-amino-acid sequence glutamic acid, leucine and arginine (Glu-Leu-Arg; the "ELR" motif), the C-X-C ligands can be dichotomized into angiogenic or angiostatic factors. The presence of the ERL sequence determines the ability to stimulate angiogenesis by acting on endothelial cells. The CXC chemokines encompassing the ELR amino acid motif (CXCL1-3, 5-8, 14 and 15) are angiogenic and bind to CXCR2, whereas non-ELR CXC chemokines (CXCL9-14) are mainly angiostatic and bind to CXCR3, CXCR5, CCR3, CXCR7 (Zlotnik and Yoshie, 2012; Kiefer and Siekmann AF, 2011; Vandercappellen et al., 2008). An exception is the angiogenic non-ELR CXCL12, which binds to CXCR4 and CXCR7 (Vandercappellen et al., 2008). Many of the ELR-containing CXC members have been shown to be chemotactic for neutrophils, while non-ELR CXC chemokines are chemotactic for lymphocytes.

Table 6. Human receptors and ligand-binding patterns of the seven-transmembrane domain G-protein-coupled human chemokine receptors within a single class

Receptor	Chemokine
XCR1	XCL1, XCL2
CX3CR1	CX3CL1
CCR1	CCL3, CCL5, CCL7, CCL8, CCL14, CCL15, CCL16, CCL23, CCL25
CCR2	CCL2, CCL7, CCL8, CCL11, CCL13, CCL16, CCL25
CCR3	CCL5, CCL7, CCL11, CCL13, CCL14, CCL15, CCL18, CCL24, CCL25, CCL28, CXCL9, CXCL10, CXC11
CCR4	CCL17, CCL22
CCR5	CCL3, CCL4, CCL5, CCL7, CCL8, CCL11, CCL14, CCL16, CCL26, CXCL11
CCR6	CCL20
CCR7	CCL19, CCL21
CCR8	CCL8, CCL16

CCR9	CCR9
CCR10	CCL27, CCL28
CXCR1	CXCL6, CXCL7, CXCL8
CXCR2	CXCL1, CXCL2, CXCL3, CXCL5, CXCL6, CXCL7, CXCL8
CXCR3	CXCL4, CXCL9, CXCL10, CXCL11, CXCL13, CCL11
CXCR4	CXCL12
CXCR5	CXCL13
CXCR6	CXCL16

Receptors CXCR1–CXCR3, CCR1–CCR5, CCR7, CCR8, CCR10 and XCR1 all bind several chemokines. By contrast, CCR6, CCR9, CX3CR1 and CXCR4–CXCR6 bind only one ligand each.

1.3.3 Angiostatic CXC (CXCL9, CXCL10, CXCL11) chemokines and their receptors

Angiogenesis plays a very important role in the development, growth, and metastatic potential of cancer. Regulation of angiogenesis by CXC chemokines plays a significant role in the development of malignant formations such as melanoma, pancreatic cancer, OC, gastrointestinal cancer, bronchogenic cancer, prostate cancer, glioblastoma, head and neck cancer, and renal cell cancer (Keeley et al., 2010). Interestingly, CXCL9, CXCL10 and CXCL11 are anti-angiogenic, which, on the one hand, may result in undersupplied, stagnating tumors, but, on the other one, in more aggressive tumor cells with a metastasizing potential (Bronger et al., 2019).

CXCR3 is highly expressed on Th1-type CD4+ T-cells, on innate lymphocytes such as NK cells and NKT cells, on plasmacytoid dendritic cells (DCs), and subsets of B-cells (Groom et al., 2011). For the first time, the human chemokine receptor CXCR3 was described in 1996 (Loetscher et al., 1998). Later, the CXCR3 receptor was named CXCR3-A, because two more variants were discovered: CXCR3-B and CXCR3-alt (Ehlert et al., 2004; Lasagni et al., 2003; Berchiche et al., 2016). CXCR3-A seems to promote proliferation, cell survival, chemotaxis, and mobilization of intracellular calcification, while CXCR3-B appears to mediate growth suppression, apoptosis, and inhibit angiogenesis. CXCR3-A is the receptor for CXCL9, CXCL10, CXCL11, while CXCR3-B acts as a functional receptor for CXCL4. The chemokine CXCL4 shares several activities with CXCL9, CXCL10, and CXCL11, including an angiostatic effect (Berchiche et al., 2016; Lasagni et al., 2003). In contrast to CXCR3-A and CXCR3-B, CXCR3-alt has been shown to bind exclusively to CXCL11 (Kuo et al., 2018).

The interferon-inducible non-ERL CXC members can be expressed by monocytes, endothelial cells, fibroblasts, and cancer cells. These chemokines belong to the inflammatory group and take their part in all types of inflammation, including autoinflammation, and cancer. The CXCL9, CXCL10 and CXCL11 chemokines primarily regulate cell migration of Th1 cells, natural killer cells, macrophages, dendritic cells, as well as hematopoiesis (Tokunaga et al., 2017). One of the decisive values for the induction of tumor regression is the ability of CXCR3 to stimulate Th-1 dependent immunity and inhibit angiogenesis (Balestrieri et al., 2008; Metzemaekers et al., 2018).

Chemokines interact differently with their receptors because they have different binding sites and display different affinities. Typically, CXCL11 has the highest affinity for CXCR3-A, while CXCL9 has the lowest. CXCL11 is also the most potent of the IFNγ-dependent ligands for CXCR3, based on its effects on intracellular calcium release and on the chemotactic response of cells expressing CXCR3-A (Cole et al., 1998).

1.3.4 CXCL11 expression and cancer

CXCL11 is a non-ELR CXC chemokine which is also called interferon-inducible T-cell alpha chemoattractant (I-TAC) and interferon-gamma-inducible protein 9 (IP-9). It is weakly expressed in healthy tissues such as thymus, spleen, and pancreas (Cole et al., 1998). It is dramatically upregulated by IFN-γ and IFN-β, and to a smaller extent by IFN-α (Rani et al., 1996). The gene encoding CXCL11 maps to chromosome 4 together with other members of the CXC chemokine family. CXCL11 is more effective than CXCL9 or CXCL10 in its ability to intracellularly mobilize calcium and as a chemotactic factor. It is also the main chemokine responsible for the internalization of CXCR3 (Sauty et al., 2001). Moreover, CXCL11 has much higher affinity to CXCR3 than either CXCL9 or CXCL10 (Cole et al., 1998).

The chemokine CXCL11 plays a very important role in cancer pathogenesis, as it supports the intensive infiltration of tumor antigen-reactive T-cells as a vital part in tumor eradication (Gao, Q. et al., 2019). The transfer of T-cells into the tumor depends on the pairing between the chemokine receptors on the effector cells and chemokines secreted by the tumor. CXCL11 is highly expressed in different solid tumors, including colorectal carcinomas (Gao et al., 2018) as well as lung cancer (Cole et al., 1998) and controls tumor growth, metastasis, and lymphocyte infiltration (Puchert et al., 2020).

2 Aim of the study

This study aimed at investigating the expression levels and clinical relevance of CXCL11 mRNA and protein expression in two different types of cancer, breast (BC) and ovarian (OC) cancer, respectively. We focused on rather homogenous patient cohorts, on the one hand the largest subgroup of OC, namely high-grade serous OC (HGSOC), and, on the other hand, the most aggressive subgroup of BC, triple-negative BC (TNBC).

The following steps were conducted to achieve our goal:

1. Determination of CXCL11 mRNA expression levels in advanced HGSOC and TNBC tissue samples by qPCR and analysis of their relation to clinical parameters and survival.
2. Immunohistochemical staining of tissue micro arrays followed by digital quantification of the CXCL11 protein expression levels in tissue of patients afflicted with advanced HGSOC and TNBC, respectively, and their relationship with clinical parameters and survival.
3. Monitoring of *in vitro* CXCL11 protein expression and secretion by ELISA in different ovarian cancer cell lines and comparison to the expression and secretion of CXCL9 and CXCL10, respectively.

3 Patients, materials and methods

3.1 Ovarian cancer patients

The study is based on the defined histology of the tumor and available follow-up information of OC patients. All patients declared written consent and tissue samples were derived from the Tumor Bank of the Medical Faculty/ Department of Pathology and Pathological Anatomy of the Technical University of Munich, Germany.

139 samples of advanced (FIGO stage III/IV) high-grade serous OC (HGSOC) were enrolled in the present study. All patients were operated in the period from 1991 to 2015 at the Department of Obstetrics and Gynecology in Klinikum Rechts der Isar, Technical University of Munich, Germany, in accordance with the standard stage-related guidelines. After surgery, adjuvant treatment based on platinum was performed on agreed recommendations at that time. Tumor tissues were collected during surgery and inspected for malignancy by pathologists. Validated HGSOC tumor tissues were stored in liquid nitrogen until RNA extraction. In total, RNA was isolated from 139 frozen tumor specimens of advanced HGSOC patients (cohort 1, n=139) and stored at -80 °C until analysis.

The Department of Pathology and Pathological Anatomy routinely works with formalin-fixed, paraffin-embedded (FFPE) tumors tissues. FFPE blocks were used for the preparation of the tissue microarrays (TMAs), encompassing 242 cases of tumor tissue of advanced HGSOC patients (cohort 2, n=242) and 108 cases of other types of OC, including low-grade serous OC (LGSOC), borderline OC, and mucinous OC (cohort 3, n=108). 75 patients of cohort 1 overlapped with cohort 2. The clinical data of the OC patients of cohort 1, 2 and 3 are depicted in **Tables 7**, **8,** and **9**, respectively. Clinical data for the non-serous and LGSOC patients were not available.

Table 7. Clinical data of advanced HGSOC patients (cohort 1)

Clinical parameters	Number	Percentage
All patients	139	
Excluded patients	16	
All patients after curation*	123	
Median observation time	41.4	
range	2-279 months	
Age		
≤ 60 years	53	43.1
> 60 years	70	56.9
Residual tumor mass		
0	63	52.1
> 0	58	47.9
Ascitic fluid volume		
≤ 500 ml	70	60.3
> 500 ml	46	39.7
Involved lymph node		
Yes	87	72.5
No	33	27.5
Metastasis		
Yes	32	24.1
No	101	75.9
Grading		
2	15	10.8
3	124	89.2
Progression-free survival events		
Yes	66	70.2
No	28	29.8
Overall survival events		
Yes	68	61.8
No	42	38.2

Due to missing data sets the cases do not always add up to 123. * Reasons for deletion: in the qPCR analyses one sample had the Ct value for HPRT 40; one sample had the $2^{-\Delta\Delta Ct}$ error progression% 37%, and 36% after repetition; for 14 samples the % STDEV of the $2^{-\Delta\Delta Ct}$ for two valid runs was higher than 47.1%.

Table 8. Clinical data of advanced HGSOC patients (cohort 2)

Clinical parameters	Number	Percentage
All patients	242	
Median age	62.5	
range	26-88 years	
Median observation time	44.6	
range	0-269 months	
Age		
≤ 60 years	92	38.0
> 60 years	150	62.0
Residual tumor mass		
0	102	44.2
> 0	129	55.8
Ascitic fluid volume		
Yes	74	52.5
No	67	47.5
Involved lymph node		
Yes	139	67.2
No	68	32.8
Metastasis		
Yes	46	29.7
No	109	70.3
Grading		
2	27	11.2
3	214	88.8
Progression-free survival events		
Yes	164	79.2
No	43	20.8
Overall survival events		
Yes	162	68.4
No	75	31.6

Due to missing data sets the cases do not always add up to 242. The IHC scores were provided by two independent observers. The difference of most scores was less than 10%, the remaining samples were reanalyzed and the average value of the three closest ones was taken. In case of repeated non-conformance, the measurement was carried out again, but this time jointly.

Table 9. Histological subtype composition of the non-HGSOC (cohort 3)

Ovarian cancer subtype	Number
Endometrioid carcinoma	29
Adenocarcinoma	15
Clear cell carcinoma	16
Mucinous carcinoma	23
Borderline tumor	17
Low-grade serous carcinoma	8
All patients	**108**

3.2 Breast cancer patients

104 samples of TNBC were enrolled in the present study with the prior written consent of the patients. All patients were operated on between 1991 to 2012 at the Department of Obstetrics and Gynecology in Klinikum Rechts der Isar, Technical University of Munich, Germany. After surgery, treatment was performed based on agreed recommendations at that time. Tumor tissues were collected during surgery, inspected for malignancy by pathologists, and validated tumor tissues of TNBC patients were stored in liquid nitrogen until RNA extraction. RNA was isolated from 104 frozen tumor specimens of TNBC (cohort 4, n=104) and stored at -80 °C until analysis.

For the preparation of TMAs, FFPE blocks were used, encompassing 146 cases of tumor tissue of TNBC patients (cohort 5, n=146) and 219 cases of other tumor BC subtypes (cohort 6, n=219). 48 patients of cohort 4 overlapped with cohort 5.

The clinical data of the BC patients of cohort 4, 5, and 6 are depicted in **Tables 10, 11,** and **12,** respectively.

Table 10. Clinical data of TNBC patients (cohort 4)

Clinical parameters	Number	Percentage
All patients	104	
Excluded patients	3	
All patients after curation*	101	
Median observation time	93.8	
range	4-286 months	
Age		
≤ 60 years	54	53.5
> 60 years	47	46.5
Involved lymph node		
Yes	11	10.9
No	90	89.1
Tumor size		
≤ 20mm	27	27.0
> 20mm	73	73.0
Grading		
2	10	9.9
3	91	90.1
Disease-free survival events		
Yes	42	42.9
No	56	57.1
Overall survival events		
Yes	36	36.0
No	64	64.0

Due to missing data sets the cases do not always add up to 101.
* Reasons for deletion: in the qPCR analyses one sample had the $2^{-\Delta\Delta Ct}$ error progression% 32%, and 33% after repetition; for two samples the % STDEV of the $2^{-\Delta\Delta Ct}$ for two valid runs war 53% and 55%.

Table 11. Clinical data of TNBC patients (cohort 5)

Clinical parameters	Number	Percentage
All patients	146	
Median age	57	
range	29-90 years	
Median observation time	92	
range	1-324 months	
Age		
≤ 60 years	88	60.3
> 60 years	58	39.7
Involved lymph node		
Yes	66	46.2
No	77	53.8
Tumor size		
≤ 20mm	45	32.8
> 20mm	92	67.2
Grading		
2	18	12.6
3	125	87.4
Disease-free survival events		
Yes	28	19.2
No	118	80.8
Overall survival events		
Yes	64	43.8
No	82	56.1

The IHC scores were provided by two independent observers. The difference of most scores was less than 10%, the remaining samples were reanalyzed and the average value of the three closest ones was taken. In case of repeated non-conformance, the measurement was carried out again, but this time jointly. Due to missing data sets the cases do not always add up to 146.

Table 12. Clinical data of BC patients (cohort 6)

Clinical parameters	Number	Percentage
All patients	219	
Median age	61.4	
range	28-97 years	
Median observation time	68.9	
range	1-164 months	
Age		
≤ 60 years	99	45.2
> 60 years	120	54.8
Involved lymph node		
Yes	82	37.4
No	137	62.5
Tumor size		
≤ 20mm	109	49.8
> 20mm	110	50.2
Grading		
2	135	61.6
3	84	38.4
ER status		
positive	219	9.4
negative	0	0
PR status		
positive	26	11.9
negative	193	88.1
HER2 status		
positive	136	62.7
negative	81	37.3
Disease-free survival events		
Yes	34	15.5
No	185	84.5
Overall survival events		
Yes	32	14.6
No	187	85.4

The IHC scores were provided by two independent observers. The difference of most scores was less than 10%, the remaining samples were reanalyzed and the average value of the three closest ones was taken. In case of repeated non-conformance, the measurement was carried out again, but this time jointly. ER-estrogen-receptor; PR-progesteron; HER-human epidermal growth factor receptor 2. Due to missing data sets the cases do not always add up to 219

3.3 Reagents

3.3.1 Cell culture

HEPES (4-(2-hydroxyethyl)-1-piperazineethanesulfonic acid)	#15630-056, Thermofisher, Paisley, UK
0.5% Trypsin-EDTA (10x)	#15400-054, Thermofisher, Paisley, UK
PBS (phosphate-buffered saline)	#141290-094, Gibso, Thermofisher, Paisley, UK
FBS (fetal bovine serum)	#10270-106, Invitrogen, Carlsbad, USA
DMSO (dimethyl sulfoxide)	#317275, Merck Chemicals, Darmstadt, Germany
RPMI Medium+ GlutaMax	#61870-010, Thermofisher, Paisley, UK
Insulin 10 mg/mL, pH 8.2	#SLBX8459, Sigma, Louis, MN, USA
Dulbecco's Modified Eagle Medium (DMEM) + GlutaMax4.5 g/l D-Glucose	#61965-026, Thermofisher, Paisley, UK
McCoy's Medium+ L glutamine	#16600-082, Thermofisher, Paisley, UK
L-arginine	A8094, Sigma, St. Louis, MN, USA
L-asparagine	A4159, Sigma, St. Louis, MN, USA

3.3.2 Complete medium for cell culture

OV-MZ-6	DMEM,10% FBS,10 mM HEPES
SKOV-3	McCoy's Medium,10% FBS, 5 ml 0.550 mM L-Arginine 0.272 mM L-Asparagine
Caov-3	DMEM with 10% FBS and 10 mM HEPES
OVCAR-3	RPMI Medium, 20% FBS, 5 ml HEPES, 0.550 mM L-Arginine 0.272 mM L-Asparagine, Insulin 10 mg/ml - 61,6 µl.

3.3.3 IHC

Tris-buffered saline, pH7.6	60.5 g Trizma Base, 700 ml H_2O, 90 g NaCl
Anti-CXCL11 antibody, 100 µg	ab9955, #GR35298-46, Abcam, Cambrige, United Kingdom
Tween-20	#P1379, Sigma-Aldrich GmbH, Taufkirchen, Germany
Citric acid	#C1909, Sigma-Aldrich GmbH, Taufkirchen, Germany
NaOH (sodium hydroxide)	#S-0899, Sigma-Aldrich GmbH, Taufkirchen, Germany
H_2O_2 30%	#9681.4, Carl Roth, Karlsruhe, Germa
HRP One-Step polymer anti-rabbit	#ZUC053-100, Zytomed Systems, Berlin, Germany

DAB (diaminobenzidine)	#DAB 5000 plus, Zytomed Systems GmbH, Berlin, Germany
Antibody diluent	#ZUC025-500, Lot R236, Zytomed Systems GmbH, Berlin, Germany
Hemalum Mayer	# T865-2, Carl Roth, Karlsruhe, Germany
Pertex (mounting medium)	#41-4012-00, Medite Pertex, Burgdorf, Germany
Xylene and isopropanol	Provided by Department of Pathology and Pathological Anatomy of the Technical University of Munich, Germany

3.3.4 qPCR

Brilliant III Ultra-Fast RT-PCR Master Mix with Low ROX	#600890, Agilent Technologies, USA
CXCL11 primers	Hs00171138_m1, Thermo Fisher Scientific, Germany
HPRT primers	Metabion, Martinsried, Germany
Universal ProbeLibray probes	Roche, Penzberg, Germany
AMV First Strand cDNA Synthesis Kit	#40885, Invitrogen, Darmstadt, Germany
RNeasy Plus Mini Kit	Qiagen, Hilden, Germany

3.3.5. ELISA

hTNF Alpha	#41525, PeproTech, London, UK
hIFN Gamma	#121527, PeproTech, London, UK
Reagent Diluent Concentrate	P227671, P&D Systems, Minneapolis, USA
RPMI Medium+ GlutaMax	#61870-010, Thermofisher, Paisley, UK
DMEM + GlutaMax 4.5 g/L D-glucose	#61965-026, Thermofisher, Paisley, UK
McCoy's Medium+ L glutamine	#16600-082, Thermofisher, Paisley, UK
PBS (phosphate-buffered saline)	#141290-094, Gibso, Thermofisher, Paisley, UK
Streptavidin HPR conjugant	P202818, Minneapolos, USA
TMB substrate kit	UK292741, ThermoScientific, Rockford, USA
hCXCL9 capture	DY392 #P160437, R&D Systems, MN, USA
hCXCL9 standard	DY392 #P160437, R&D Systems, MN, USA
hCXCL9 detection antibodies	DY392 #P160437, R&D Systems, MN, USA
hCXCL10 capture	DY266 #P225623 #P193981, R&D Systems, MN, USA
hCXCL10 standard	DY266 #P225623 #P193981, R&D Systems, MN, USA
hCXCL10 detection antibodies	DY266 #P225623 #P193981, R&D Systems, MN, USA
hCXCL11 capture	DY672 #237974 #220559, R&D Systems, MN, USA

hCXCL11 standard	DY672 #237974 #220559, R&D Systems, MN, USA
hCXCL11 detection antibodies	DY672 #237974 #220559, R&D Systems, MN, USA
Tween 20	Sigma, St. Louis, MN, USA

3.4 Machines and materials

Cell culture microscope	CK30, Olympus, Tokyo, Japan
Centrifuge	Rotina 420R, Andreas Hettich, Tuttlin, Germany
CO2 incubator Heracell 150i	Thermo Fisher Scientific, Waltham, MA, USA
Hamamatsu NanoZoomer Digital Pathology virtual microscope	U10074-01#40885, Hamamatsu, Japan
Nanodrop	Thermo Scientific, Peqlab, Erlangen, Germany
Multiscan^{tm} FC Photometer	30617387, Thermo Fisher Scientific, Waltham, MA, USA
MS2 Minishaker	IKA, Germany
Cell culture flask (25 cm, 75 cm, 125 cm)	Greiner Bio-one GmbH, Frickenhausen, Germany
Cryogenic tubes 1.5 ml	NALGENE Labware, Thermo Fisher Scientific, Roskilde, Denmark
Pipette Research plus	Eppendorf AG, Hamburg, Germany
Hemocytometer	mm, Neubauer, Blau Brand, Germany
bFilter-Tips, 1000 µl	#943540178, Qiagen, Hilden, Germany
Mx3000p 96-well plate	#401334, Agilent Technologies, Great Britain
Stratagene Mx3005P	Agilent Technologies, Boeblingen, Germany
Reaction tubes 1.5 ml	#9085012 SARSTE, Nümbrecht, Germany
Serological pipette	Greiner Bio-one GmbH, Frickenhausen, Germany
Pipette	Eppendorf Research plus, Hamburg, Germany
Tissue culture plates, 12 well	#353043, Falcon, Durham, USA
SafeSeal SurPhob tips	SurPhob, Biozym Scientific GmbH, Hessisch Oldendorf, Germany
Multipette plus	Eppendorf Research plus, Hamburg, Germany
Cover slips	rL 24x32 mm; Glass thickness 0.13-0.16
Cuvettes	Langenbrinck, Baden-Württemberg, Germany
Pressure cooker	WMF Perfect, Germany
Humid chamber	TissueGnostics, medical and biotech solution
pH meter	SCHOTT Instruments Analytics, Mainz, Germany

3.5 Quantitative PCR analysis

The qPCR assay for CXCL11 was established applying OC OV-MZ-6 cells.

3.5.1 RNA isolation from cell lines and tumor tissues

Total RNA was isolated from the cells of the cell line and tumor tissue, respectively, by using the RNeasy Mini Kit, following the manufacturer's instructions.

The concentration and purity of the isolated total RNA samples were spectrometrically assessed at 260/230 and 260/280 nm, respectively, applying the Nano Drop 2000c spectrophotometer and the Nano Drop 2000/2000c software (Thermo Fisher Scientific, Wilmington, DE, USA). Samples were stored at -80 °C until further use.

3.5.2 Reverse transcription and cDNA synthesis

For the generation of first-strand cDNA, 1 μg RNA was reverse transcribed with the Cloned AMV First Strand cDNA Synthesis Kit (Invitrogen, Darmstadt, Germany) following the manufacturer's instructions.

3.5.3 qPCR analysis applying Universal ProbeLibray probes

The method is based on introducing a target gene complementary DNA probe (8-9 nucleotides) during the amplification process. The probe is labeled with fluorescein (FAM) at the 5' end and with a dark quencher dye at the 3' end. The complementary of the probe, in addition to the gene-specific primer pair, significantly increases the specificity of the assay (**Table 13**).

Table 13. Primers and probes used for qPCR analysis

HPRT1 (NM_00194)	
Forward primer	5'-TGACCTTGATTTATTTTGCATACC-3'
Reverse primer	5'-CGAGCAAGACGTTCAGTCCT-3'
Probe	5'-FAM-GCTGAGGA-3'-dark quencher
Amplicon	102 bp
CXCL11 (NM_001302123.1)	
Primer/probe	Hs00171138_m1
Amplicon	64 bp

Assays detect the full-length sequence of the encoded proteins.

3.5.4 Standard dilution series for assay establishment

A series of dilutions were performed to evaluate the amplification efficiency of CXCL11 and HPRT assays. A two-fold dilution series for each gene was analyzed by qPCR in three independent experiments and was performed with the cDNA from OV-MZ-6 cells as template. cDNA was analyzed in five concentrations and after the measurement, a dilution curve was calculated depicting cDNA concentration (x-variable) and threshold cycle value (y-variable) according to linear regression analysis. The slope of the linear regression curve was used for the calculation of efficiency (**Figure 9**). E-value of two corresponds to 100%.

$$E = -1 + 10^{(-1/slope)}$$

Figure 9. Calculation of efficiency: E-efficiency.

The R^2 coefficient was analyzed to depict the quality of the regression curves (González-Bermúdez et al., 2019; Geng 2019; Liu 2019).

3.5.5 qPCR calculation methods

For qPCR 96-well plates were used and all reactions were executed in triplicates (input: 5 ng cDNA / well for clinical samples and cell lines). Negative controls were performed in triplicates as well, applying a no-template control (water only), genomic DNA (OV-MZ-6 cells) and a no-reverse transcriptase control (RNA only). The cycling program was performed following **Table 14.**

Table 14. qPCR cycling program

Step	Cycle	Temperature	Duration
Polymerase activation		95 °C	3 min
Denaturation	1	95 °C	15 sec
Annealing/Elongation	40	60 °C	1 min

In most cases, the qPCR was performed once. Cycle threshold values (Ct) were determined automatically for each marker by the MXPro software (version 4.10; standard evaluation settings).

Then, the following calculation were carried out:

1. the relative fold gene expression (**Figure 10**);
2. the relative error propagation (**Figure 11**);
3. the absolute error calculation (**Figure 12**).

$$\Delta Ct = Ct_{\text{sample}} - Ct_{\text{HPRT}}$$

$$\Delta\Delta Ct = \Delta Ct_{\text{sample}} - \Delta Ct_{\text{calibrator}}$$

Figure 10. The relative fold gene expression calculation: $2^{-\Delta\Delta Ct}$ method; Ct-Cycle threshold values; sample-CXCL11; calibrator-OV-MZ-6.

$$EP(\Delta CT) = \sqrt{\frac{(STDEV_{\text{sample}})^2 + (STDEV_{\text{HPRT}})^2}{2}}$$

$$EP(\Delta\Delta CT) = \sqrt{\frac{\left(EP_{\Delta CT_{\text{sample}}}\right)^2 + \left(STDEV_{\Delta CT_{\text{calibrator}}}\right)^2}{2}}$$

Figure 11. The relative error propagation calculation: EP-relative error propagation; Ct-Cycle threshold values; STREV-standard deviation; sample-CXCL11; calibrator-OV-MZ-6.

$$\text{Absolut error} = \ln 2 \times EP(\Delta\Delta CT) \times 2^{-\Delta\Delta Ct}$$

Figure 12. The absolute error calculation: EP-relative error propagation; Ct-cycle threshold values; ln-for natural logarithm.

Some results were excluded because of eventual detection limitation, the discrepancy of sample qualities and qPCR efficiencies. Samples were excluded in the following cases (Liu, 2018; Ahmed et al., 2016):

1. the Ct value for HPRT was >35;
2. the $2^{-\Delta\Delta Ct}$ error progression was >30% even after repetition;
3. the % STDEV of the $2^{-\Delta\Delta Ct}$ for two valid runs was higher than 47.1%.

3.6 IHC analysis of CXCL11 expression

IHC was performed on four µm thick paraffin sections obtained from patients treated at the Department of Pathology and Pathological Anatomy of the Technical University of Munich, Germany. Samples of cancer tissue were arranged on tissue micro arrays (TMA) in triplicate, samples of normal tissues, such as kidneys and lungs, were placed between tumor samples for comparison and orientation of histological samples.

3.6.1 IHC staining for CXCL11

Paraffin-embedded TMA slides were incubated overnight at 65 °C and then immersed twice in xylene for 10 min for deparaffinization. For rehydration, slides were immersed in a descending alcohol row (2 x 100% isopropanol, 1 x 96% ethanol, 1 x 70% ethanol) for five min each. The TMAs were washed with Tris-buffer/0.005% Tween 20 (TBST). For antigen retrieval, pressure cooking was used for four min in citrate buffer (citric acid 2.1 g, distilled H_2O 1 l, pH 6.0). After five min of washing with tap water and, then, in TBST five min each, the endogenous peroxidase activity was blocked for 20 min at room temperature (RT) with H_2O_2 3%. After rinsing for three min under tap water and five min with TBST, blocking of the antigens in the tissues was performed with goat serum 1:20 (5%) in antibody diluent for 10 min. Then, 120 µl 0.25 µg/ µl anti-CXCL11 antibody (ab9955) were applied and incubated in a wet chamber for 1 h at RT. Then, the slides were washed for five min with TBST and incubated for 30 min with 120 µl HRP One Step Polymer at RT. After the slides had been washed with TBST, DAB was added to the slides for eight min at RT. As a next step, the slides were washed with TBST and, then, counterstained with hematoxylin for two min and again washed for 10 min under running tap water. Then, they were transferred to distilled water for five min. For dehydration, the slides were subjected to an ascending alcohol series: one min 70% ethanol, three min 96% ethanol, twice three min 100 % isopropanol and twice three min xylene. As a last step, the slides were covered with Pertex.

3.6.2 Quantification of immunostaining

Stained TMA slides were scanned applying a NanoZoomer Digital Pathology virtual microscope (Hamamatsu) with a 100 × objective. For the analysis of the IHC staining intensity, the program ImageJ (Version 1.52), downloaded from the NIH website (https://imagej.nih.gov/ij), was used, including the IHC Profiler plugin, from the Sourceforge website (https://sourceforge.net). The digital slide viewer NDP.view2 U12388-01 was downloaded from the Hamamatsu website (hamamatsu.com). The image of each tumor core was saved and loaded into the software ImageJ. Applying the IHC Profiler plugin, color

deconvolution was performed to separate the antibody DAB signal from the hematoxylin counterstain. Guidelines for ImageJ and its plugin has previously been reported by Varghese and co-workers (**Figure 13**; Varghese et al., 2014; Liu, 2018).

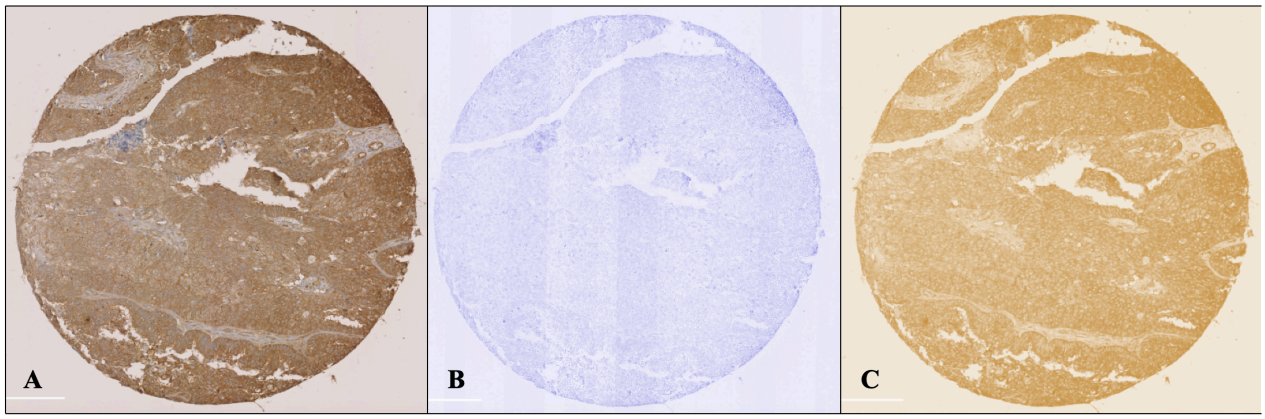

Figure 13. Color deconvolution
A: Ovarian cancer tissue with positive CXCL11 staining (DAB) Hematoxylin counterstain;
B: Hematoxylin staining only;
C: DAB staining only.

Tumor regions of interest on each TMA were manually selected by the agreement of two independent observers and the approval of a pathologist. Then, score assignments of the DAB images were performed (**Figure 14**).

$$\text{Score}=255-\sum_{i=1}^{n} \text{InD}_i \Big/ \sum_{i=1}^{n} A_i$$

Figure 14. Score assignment of the DAB images: InD – integrated the gray density; A – computed regions in pixels.

The pixel intensity values for the DAB staining ranged from 0 to 255, wherein 0 represented the darkest shade of the color and 255 represented the lightest shade of the color as a standard. For convenience, a subtraction of 255 minus the resulting mean value was added to the formula, thereby, the score positively associates with the DAB staining density (Liu, 2018).

The following criteria were applied for the analysis of the densiometric data:

1. values of both observers < 10% → average was taken
2. values of both observers > 10% → analysis was repeated
3. values of both observers > 10% after the second measurement → consent was formed

3.6.3 Cell culture

Table 15. Ovarian serous cancer cell lines

Cell Line Name	ATCC number	Disease
OV-MZ-6	none (Möbus et al., 1992)	Ovarian serous cystadenocarcinoma Derived from metastatic site: ascites
SKOV-3	HTB-77	Ovarian serous cystadenocarcinoma Derived from metastatic site: ascites
Caov-3	HTB-75	High-grade ovarian serous adenocarcinoma
OVCAR-3	HTB-161	High-grade ovarian serous adenocarcinoma. Derived from metastatic site: ascites

ATCC - American Type Culture Collection

Cryogenic flasks with cells (**Table 15**) from liquid nitrogen were swiftly thawed and transferred to a 15 ml Falcon tube containing five ml of complete medium (see chapter 3.3.2). After centrifugation for three min at 300 rpm and RT the supernatant was removed and four ml of fresh complete medium were added to the cells. Then, the cell suspension was transferred into a new cell culture flask for cultivation. Cells were adherently grown in different cell culture flasks, depending on their growth rate, with the complete medium in an incubator at the condition of 5% CO_2 (v/v), 95% humidity and 37 °C. Based on the growth rate the culture complete medium was replaced every 2-3 days and a cell passage was performed every 5-6 days. Briefly, the passage was performed by removing the medium, washing with PBS and detaching the cells with EDTA/PBS (1% w/v). Then, the cell suspension was centrifuged for three min at 300 rpm and RT, and subsequently the supernatant was removed. Finally, the cells were resuspended in fresh complete medium and the cell suspension was transferred to a new flask. The cells were cultured until a maximum confluence of 70% was reached.

For cell cryopreservation, a freezing medium (FBS containing 10% dimethylsulfoxide [DMSO]) was prepared. The cells were detached and collected in a Falcon tube. The freezing medium was applied to resuspend the cells ($1x10^6$ cells/ml) and, then, the cell suspension was transferred to cryogenic tubes. The cryogenic micro tubes were frozen at -80 °C, with a cool-down rate of 1 °C/min.

3.6.4 Cell stimulation

After cell cultivation, cells were counted with the hemocytometer and $2x10^5$ cells seeded in each well. After 24 h in an incubator, the complete medium was changed to a minimal medium (DMEM for OV-MZ-6 and Caov-3, McCoy' for SKOV-3 and RPMI for OVCAR-3). Following

a 24 h incubation, the minimal medium was removed, the cells washed with PBS, and directly proceeded to stimulation of the cells with interferon (IFN-γ) and tumor necrosis factor (TNF-α) as well as combinations thereof (**Figure 15**). 24 h later, the supernatant was collected and stored at -80 °C. Confluence was regularly documented.

A. SKOV-3, Caov-3, OVCAR-3

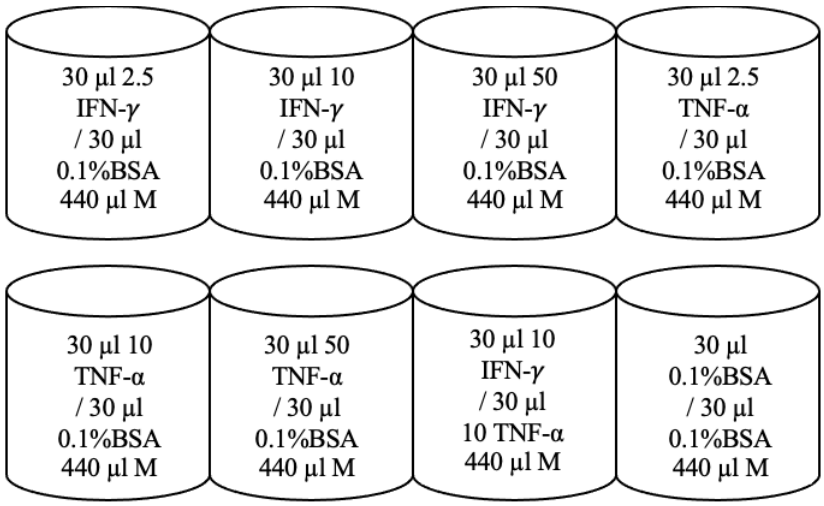

B. OV-MZ-6

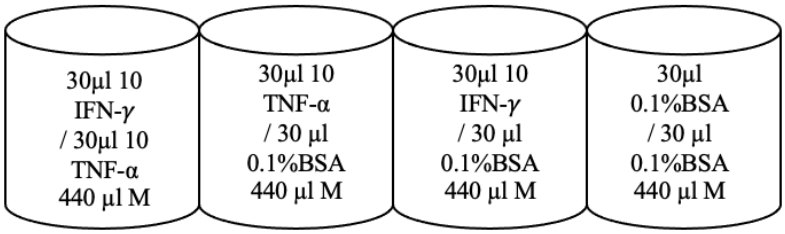

Figure 15. Assay layout for cell culture stimulation of OVCAR-3, Caov-3, SKOV-3, and OV-MZ-6 cells with the corresponding inflammatory cytokines: 2.5, 10 and 50 IFN-γ-concentration 2.5 ng/ml, 10 ng/ml and 50 ng/ml, respectively; 2.5, 10 and 50 TNF-α-concentration 10 ng/ml, 10 ng/ml and 50 ng/ml, respectively; M-minimal medium (DMEM for OV-MZ-6 and Caov-3, McCoy' for SKOV-3 and RPMI for OVCAR-3).

3.7 Protein quantification (enzyme-linked immunosorbent assay; ELISA)

A precise and sensitive way of measuring protein concentrations in solutions or tissue lysates is ELISA. Secretion of human CXCL9, CXCL10 and CXCL11 was measured in 100 µl of cell culture supernatant (sample) by commercially available kits according to manufacturer protocol (R&D Systems, see chapter 3.3.5). All measurements were taken in three separate analyses, each of which was performed in triplicate.

3.7.1 Sandwich ELISA

The sandwich ELISA quantifies antigens by applying two different target protein-specific antibodies. The first (capture antibody) immobilizes the protein of interest and the second antibody (detection antibody) is the target for the reporter molecule. Initially, 96 well plates were coated with the capture antibody (1:120 diluted in PBS), covered and incubated overnight at RT. Blocking was performed with 200 µl 1% BSA/PBS for two h at RT.

As a next step, 100 µl of supernatant sample or standard solution (8-fold dilution series) were added. The standard was determined in duplicates, samples in triplicate. After two h of incubation at RT, 100 µl of detection antibody (1:60 diluted in 1% BSA/PBS) were added. After another two h at RT, 100 µl of HRP-conjugated antibody directed to the detection antibody (appropriately diluted in 1% BSA/PBS) was added to each well. The covered plate was incubated for 20 min in darkness at RT. Then, 100 µl of TMB substrate solution were added to each well and again incubated for 20 min at RT in the dark. The last step was addition of 50 µl of "stop solution" (1M H_2SO_4). A thorough washing step with PBS-T 0.05% was performed between each incubation step. The result was evaluated spectrophotometrically. The signal accumulation was detected at 450 nm.

3.8. Statistics

All calculations were performed with the SPSS statistical analysis software (version 25.0; SPSS Inc., Chicago, IL, USA). For determination of the best cut-point, the X-tile software (version 3.6.1, Yale University, New Haven, CT) was used. In case a best cut-point could not be defined (resulting in significant results), CXCL11 expression was dichotomized into low and high expression by the median. P-values ≤ 0.05 were considered as statistically significant.

The relation of biological marker expression levels with clinicopathological parameters were evaluated applying the Chi-square test. The association of tumor biological factors and clinical parameters with patients' survivals were analyzed by Cox univariate and multivariate proportional hazards regression models and expressed as hazard ratio (HR) and its 95% confidence interval (95% CI). The multivariate Cox regression model was adjusted to established OC factors such as age, residual tumor mass, ascitic fluid volume and for established TNBC factors such as age, tumor size, lymph node status, and tumor grade.

Survival curves were plotted according to Kaplan-Meier, applying log-rank tests to test for differences. In order to determine the strength of association between two variables and the direction of the relationship were performed Pearson and Spearman correlation. In addition to the above methods descriptive statistics also were applied.

4 Results

4.1 CXCL11 in ovarian cancer

4.1.1 CXCL11 mRNA expression in advanced HGSOC

Amplification efficiency was determined by three independent experiments applying two-fold dilution series of the cDNA to quantify the gene of interest (CXCL11) and the reference gene (HPRT). Five serial dilution steps of cDNA derived from inflammatory cytokine-stimulated OV-MZ-6 cells (positive control) were analyzed:

1. Input: cDNA0 30 ng, cDNA1 15 ng, cDNA2 7.5 ng, cDNA3 3.75 ng, cDNA4 1.87 ng (**Figure 10. A**)
2. Input: cDNA0 100 ng, cDNA1 50 ng, cDNA2 25 ng, cDNA3 12.5 ng, cDNA4 6.25 ng (**Figure 10. B**)
3. Input: cDNA0 120 ng, cDNA1 60 ng, cDNA2 30 ng, cDNA3 15 ng, cDNA4 7.5 ng (**Figure 10. C**)

The cycles of threshold (Ct) values were plotted against the corresponding logarithm of the cDNA input. The amplification efficiency for each primer pair (Ct) and the logarithm of the initial cDNA concentrations were plotted to calculate the slope of the linear regression. In the three independent repetitions, the slope of the fitted lines for CXCL11 dilution series (slope: 1^{st} -2.99; 2^{nd} -3.26; 3^{rd} -2.95) was parallel with the ones of HPRT (slope: 1^{st} -3.50; 2^{nd} -2.80; 3^{rd} -3.27). The efficiencies of CXCL11 amplification (E: 1^{st}-2.16; 2^{nd}-2.03; 3^{rd}-2.18) were similar to the ones of HPRT (E: 1^{st}-1.93; 2^{nd}-2.27; 3^{rd}-2.02). As these correspond to an optimal qPCR efficiency of E=2, an efficiency correction was not necessary and the $2^{-\Delta\Delta Ct}$ method was applied for the calculation of relative CXCL11 mRNA expression (González-Bermúdez et al., 2019; Geng 2019; Liu 2019).

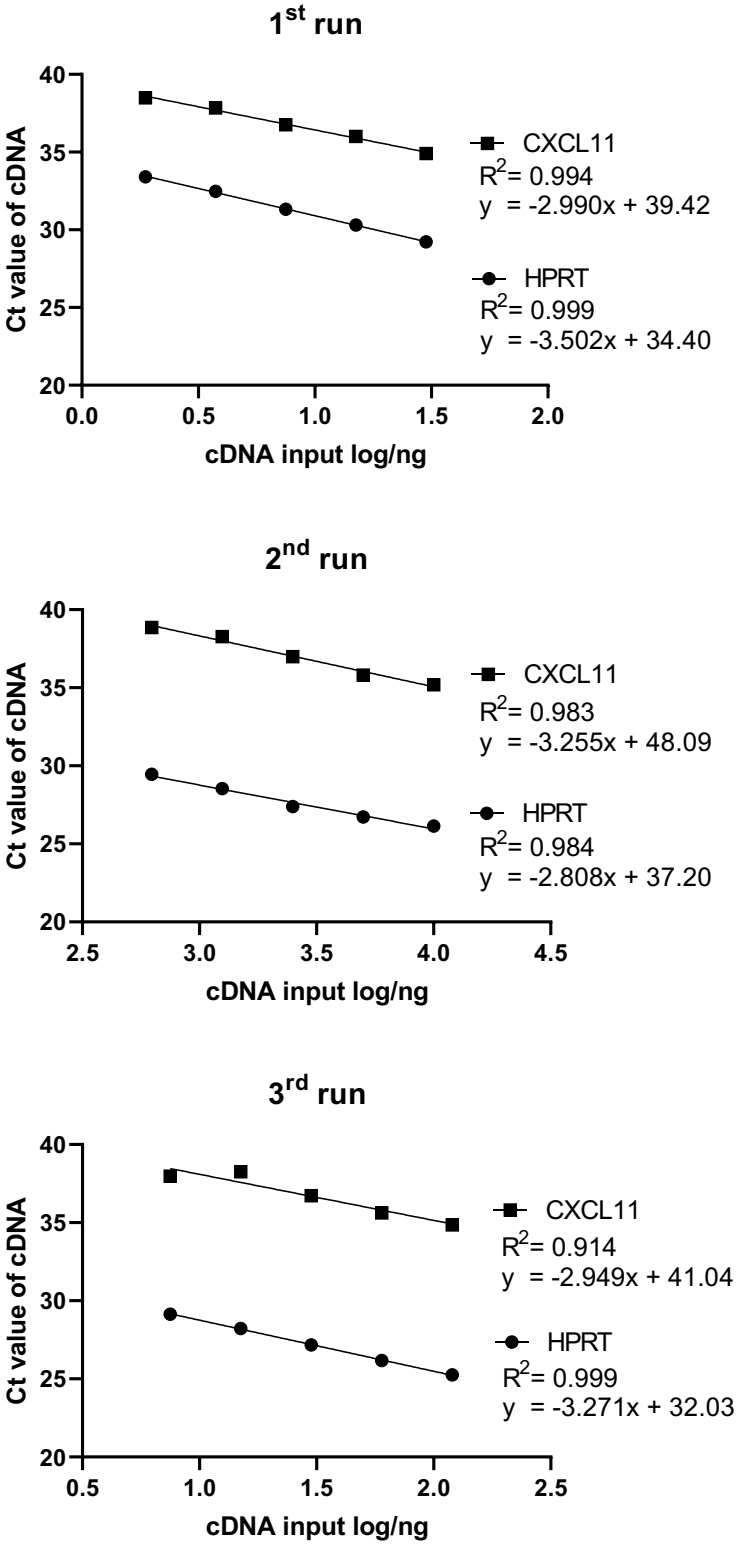

Figure 16. Amplification efficiency of the CXCL11 and HPRT qPCR assays: two-fold dilution series of cDNA were applied for CXCL11 and HPRT. Three different starting concentrations have been used (1st run: 30ng, 2nd run:100ng, 3rd run:120ng). Resulting CT values are plotted against the logarithm of the cDNA input. Each experiment was performed in triplicates.

For the analysis of CXCL11 mRNA expression levels, determined by qPCR, patient cohort 1 was evaluated (n=139; **Table 7**). According to our criteria (see Materials & Methods), 16 cases were excluded. 14 cases were excluded because the % STDEV of the $2^{-\Delta\Delta Ct}$ for two valid runs was higher than 47.1%, one case had the $2^{-\Delta\Delta Ct}$ error progression% which was >30% even after repetition, and one case the Ct value for HPRT was 40. The relative CXCL11 mRNA levels, normalized to the expression levels of the housekeeping gene HPRT, ranged from 0.06 to 235.57 (median 24.33). For further analysis, the remaining 123 cases were dichotomized concerning CXCL11 mRNA expression into low expression and high expression by the median (**Figure 17**).

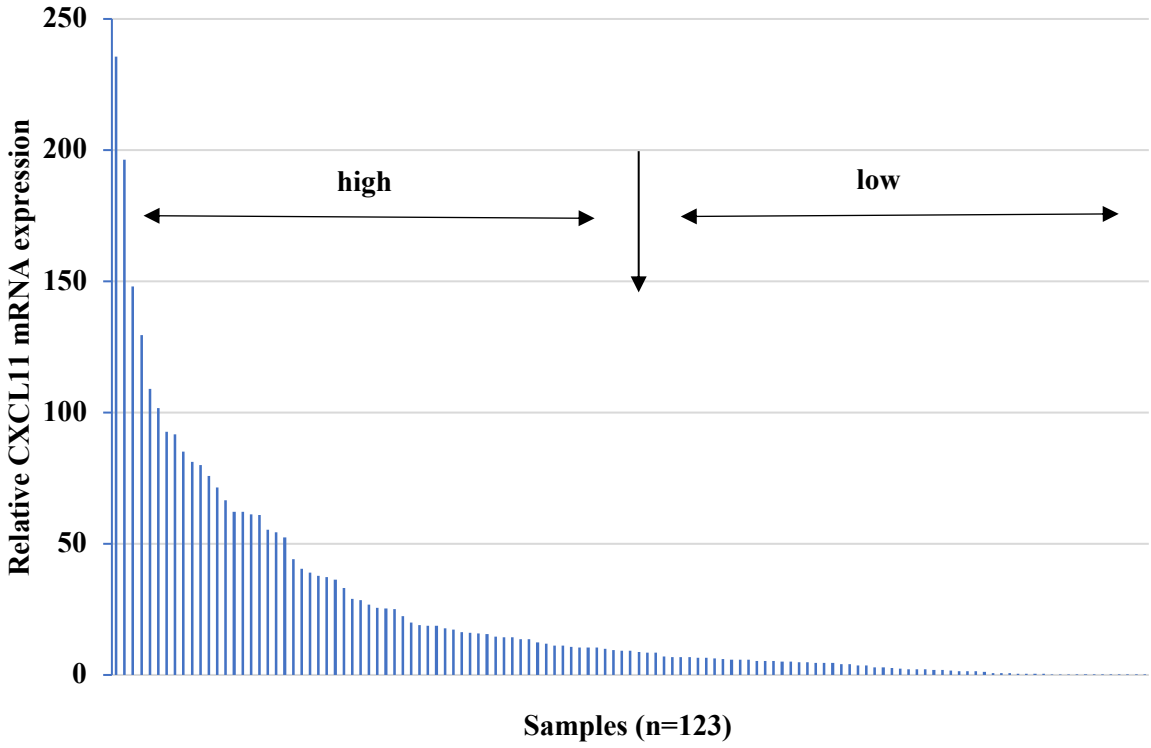

Figure 17. CXCL11 mRNA expression levels in tumor tissue of patients with advanced HGSOC: CXCL11 mRNA expression dichotomized into low expression and high expression by the 50th percentile.

Based on this categorization the association between CXCL11 mRNA expression levels and the established clinical parameters (age ≤ 60 vs. > 60 years; residual tumor mass yes vs. no; ascitic fluid volume ≤ 500 ml vs. > 500 ml) was investigated applying the Chi-square test. There was no significant association between clinical characteristics of advanced HGSOC patients and CXCL11 mRNA expression (**Table 16**).

Table 16. Association between clinical characteristics of advanced HGSOC patients (FIGO III/IV) and the tumor biological factor CXCL11

Clinical parameters	No. of patients	CXCL11 low/high
Age		P = 0.957
≤ 60 years	53	27/26
>60 years	70	36/34
Residual tumor mass		P = 0.770
0 mm	63	32/31
> 0 mm	58	31/27
Ascitic fluid volume		P = 0.543
≤ 500 ml	70	34/36
> 500 ml	46	25/21

n=123; cut-off: 50th percentile; statistics: Chi-square test, p≤0.05 is considered as statistically significant. Due to missing data sets, the cases do not always add up to 123.

4.1.1.1 Univariate Cox regression analysis of the clinical outcome in advanced HGSOC patients (FIGO III/IV) for clinical parameters and the tumor biological factor CXCL11

Table 17 demonstrates the association between clinical parameters and CXCL11 mRNA expression levels with patients' 5-year overall survival (OS) and progression-free survival (PFS). In univariate Cox regression analysis, the residual tumor mass represented a significant predictor for shorter OS (HR: 3.59, p<0.001) and PFS (HR: 2.43, p<0.001). The ascitic fluid volume represented a univariate predictor for PFS (HR: 1.68, p=0.049). Elevated CXCL11 mRNA expression was notably linked to longer OS (HR: 0.58, p=0.046), which was confirmed by Kaplan-Meier analysis (**Figure 18**). The result showed a significant association of elevated CXCL11 mRNA expression with OS (p=0.042), but not with PFS (p=0.600).

Table 17. Univariate Cox regression analysis of the clinical outcome in advanced HGSOC patients (FIGO III/IV) for clinical parameters and the tumor biological factor CXCL11

Clinical parameters	Overall survival 60 months			Progression-free survival 60 months		
	No.	**HR (95% CI)**	**P**	**No.**	**HR (95% CI)**	**P**
Age			0.459			0.678
≤ 60 years	45	1		39	1	
> 60 years	65	1.22 (0.72 - 2.09)		55	1.11 (0.68 - 1.83)	
Residual tumor mass			**<0.001**			**<0.001**
0 mm	57	1		52	1	
> 0 mm	51	3.59 (1.98 - 6.48)		42	2.43 (1.48 - 3.99)	
Ascitic fluid volume			*0.051*			**0.049**
≤ 500 ml	64	1		55	1	
> 500 ml	39	1.73 (1.00 - 3.00)		33	1.68 (1.00 - 2.82)	
CXCL11			**0.046**			0.607
low	55	1		44	1	
high	55	0.58 (0.33 - 0.99)		49	0.88 (0.54 - 1.43)	

HR-hazard ratio, CI-confidence interval; cut-off: 50th percentile; Cox regression analysis, p≤0.05 is considered as statistically significant. Due to missing data sets, the cases do not always add up to 123.

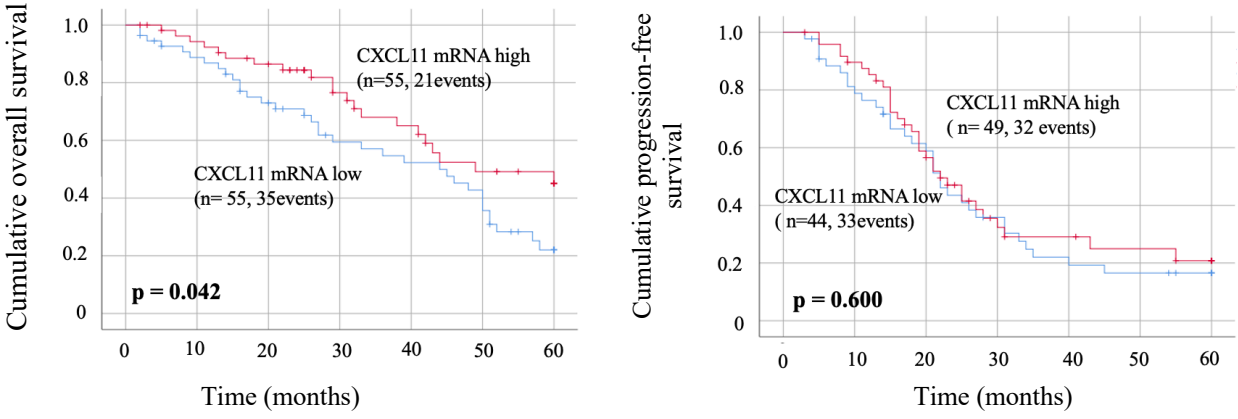

Figure 18. Elevated levels of CXCL11 mRNA are associated with longer overall survival in the cohort of advanced HGSOC patients (FIGO III/IV): Kaplan–Meier survival analysis, p≤0.05 is considered as statistically significant**.** Red curve: CXCL11 mRNA high expression levels, blue curve: CXCL11 mRNA low expression levels.

4.1.1.2 Association of CXCL11 mRNA expression with OS and DFS in multivariable Cox regression analysis

As a next step, the independent relationship of CXCL11 mRNA with OS and PFS was examined (**Table 18**). In the base model, only the residual tumor mass is representing a predictive marker for OS and PFS (HR: 3.52, p<0.001; HR: 2.30, p=0.004). Moreover, CXCL11 mRNA expression levels turned out remain as an independent factor for OS after addition to the base model (HR: 0.38, p=0.002).

Table 18. Multivariable Cox regression analysis of the clinical outcome in advanced HGSOC patients (FIGO III/IV) for clinical parameters and CXCL11

Clinical parameters	Overall survival 60 months			Progression-free survival 60 months		
	No	**HR (95% CI)**	**P**	**No**	**HR (95% CI)**	**P**
Age			0.513			0.899
≤ 60 years	42	1		37	1	
> 60 years	59	1.21 (0.68 - 2.15)		50	0.97 (0.57 - 1.64)	
Residual tumor mass			**< 0.001**			**0.004**
0 mm	56	1		51	1	
> 0 mm	45	3.52 (1.78 - 6.96)		36	2.30 (1.31 - 4.02)	
Ascitic fluid volume			0.870			0.431
≤ 500 ml	63	1		55	1	
> 500 ml	38	0.95 (0.50 - 1.78)		32	1.25 (0.71 - 2.20)	
CXCL11			**0.002**			0.459
low	51	1		41	1	
high	50	0.38 (0.20 - 0.69)		46	0.82 (0.49 - 1.38)	

CXCL11 mRNA was added to the base model (age, residual tumor mass, ascitic fluid volume); HR-hazard ratio, CI-confidence interval; cut-off: 50th percentile; multivariable Cox regression analysis, p≤0.05 is considered as statistically significant.

4.1.2 CXCL11 protein expression in advanced HGSOC patients

The relative CXCL11 protein expression was analyzed based on specific IHC staining and digital scoring. The scores were provided by two independent observers.

For the analysis of CXCL11 protein expression levels, patient cohort 2 was evaluated (n=242; **Table 8**). For this, CXCL11 protein expression levels were dichotomized into low and high by the 50th percentile (**Figure 19**).

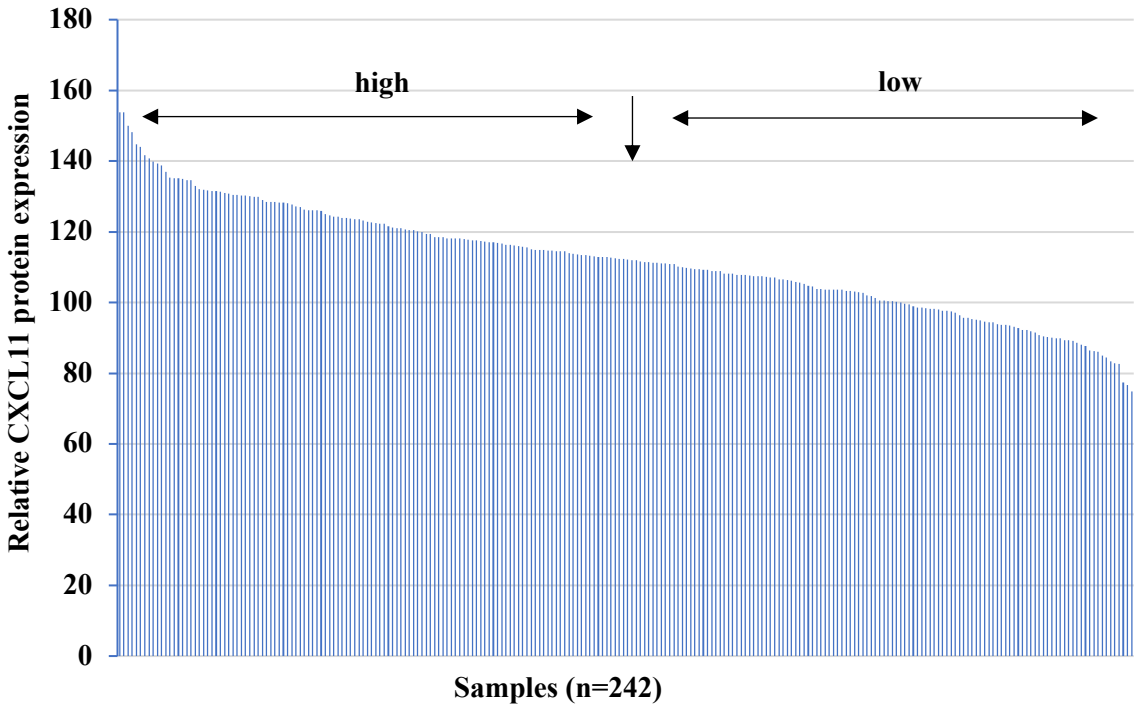

Figure 19. CXCL11 protein expression levels in tumor tissue of patients with advanced HGSOC: CXCL11 protein expression dichotomized into low expression and high expression by 50th percentile.

The association between CXCL11 protein expression levels and the established clinical parameters (age ≤ 60 vs. > 60 years, residual tumor mass yes vs. no, ascitic fluid volume ≤ 500 ml vs. > 500 ml) was investigated applying the Chi-square test. There was no significant association between clinical characteristics of advanced HGSOC patients and CXCL11 protein expression (**Table 19**).

Table 19. Association between clinical characteristics of advanced HGSOC patients (FIGO III/IV) and CXCL11 protein expression

Clinical parameters	No. of patients	CXCL11 low/high
Age		P = 0.692
≤ 60 years	93	45/48
>60 years	149	76/73
Residual tumor mass		P = 0.376
0 mm	102	55/47
> 0 mm	129	62/67
Ascitic fluid volume		P = 0.990
≤ 500 ml	74	31/43
> 500 ml	67	28/39

n=242; cut-off: 50th percentile; Chi-square test, p≤0.05 is considered as statistically significant. Due to missing data sets the cases do not always add up to 242.

4.1.2.1 Univariate Cox regression analysis of the clinical outcome in advanced HGSOC patients (FIGO III/IV) for clinical parameters and CXCL11 protein expression

In univariate Cox regression analysis for 5-year OS and DFS, residual tumor mass and ascitic fluid volume represented significant predictors for OS (HR: 3.66 and 2.45, p<0.001) and PFS (HR: 2.28 and 2.80, p<0.001) (**Table 20**). Elevated CXCL11 protein expression was not significantly linked to OS (HR: 1.10, p=0.586) and PFS (HR: 1.10, p=0.566), which was confirmed by Kaplan-Meier analysis (**Figure 20**).

Table 20. Univariate Cox regression analysis of the clinical outcome in advanced HGSOC patients (FIGO III/IV) for clinical parameters and CXCL11 protein expression

Clinical parameters	Overall survival 60 months			Progression-free survival 60 months		
	No.	HR (95% CI)	P	No.	HR (95% CI)	P
Age			0.738			0.149
≤ 60 years	88	1		79	1	
> 60 years	147	1.06 (0.75 -1.51)		124	1.27 (0.92 - 1.76)	
Residual tumor mass			**< 0.001**			**< 0.001**
0 mm	99	1		52	1	
> 0 mm	127	3.66 (2.46 - 5.44)		41	2.28 (1.65 - 3.16)	
Ascitic fluid volume			**< 0.001**			**< 0.001**
≤ 500 ml	72	1		55	1	
> 500 ml	63	2.45 (1.61 - 3.74)		32	2.80 (1.83 - 4.29)	
CXCL11			0.586			0.566
low	118	1		103	1	
high	118	1.10 (0.78 - 1.54)		101	1.10 (0.80 - 1.49)	

HR-hazard ratio, CI-confidence interval; cut-off: 50th percentile; Cox regression analysis, p≤0.05. is considered as statistically significant. Due to missing data sets the cases do not always add up to 242.

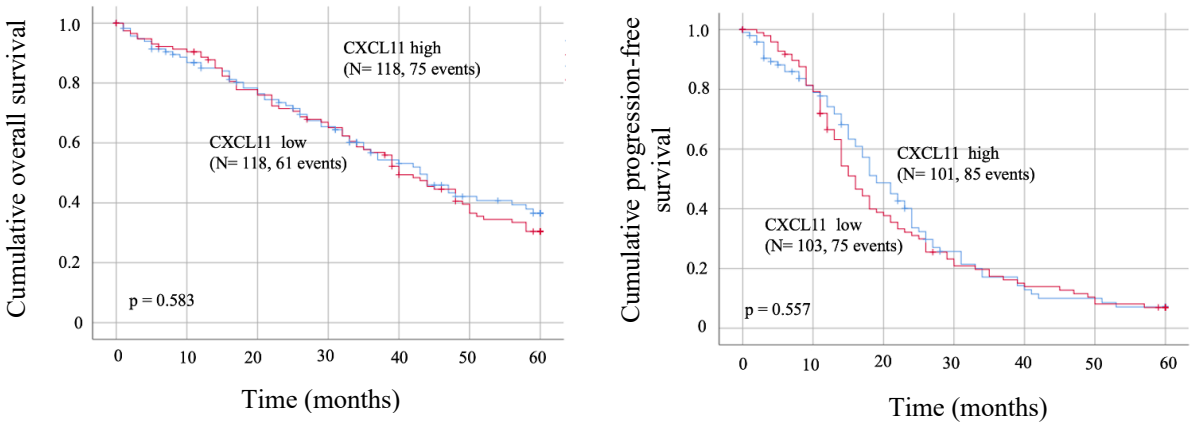

Figure 20. Elevated levels of CXCL11 protein are not associated with longer overall and progression-free survival in the cohort of advanced HGSOC patients (FIGO III/IV): Kaplan–Meier survival analysis, p≤0.05 is considered as statistically significant**.** Red curve: CXCL11 high level protein expression, blue curve: CXCL11 low level protein expression.

4.1.3 CXCL11 protein expression in other OC subtypes

Protein expression was determined by IHC in another cohort (cohort 3; n=108, **Table 9**), encompassing endometrioid carcinoma (n=29), adenocarcinoma (n=15), clear cell carcinoma (n=16), mucinous carcinoma (n=23), borderline OC (n=17) and LGSOC (n=8) cases (**Table 21**). There were no obvious distinct differences in CXCL11 protein expression in non-serous and LGSOC subtypes. The results are illustrated by applying a box plot (**Figure 21**).

Table 21. Characteristics of CXCL11 protein expression levels in the various OC subtypes

Ovarian cancer subtype	No.	Minimum	Maximum	Mean	Standard deviation
Endometrioid carcinoma	29	94.75	150.36	124.60	12.64
Adenocarcinoma	15	112.78	165.18	146.88	14.62
Clear cell carcinoma	16	96.02	153.10	127.22	16.37
Mucinous carcinoma	23	92.28	169.15	131.79	19.86
Serous borderline tumor	17	108.39	197.40	163.40	25.82
Low-grade serous OC	8	82.82	137.55	112.03	18.19

OC-ovarian cancer; No.-number of samples; descriptive statistics.

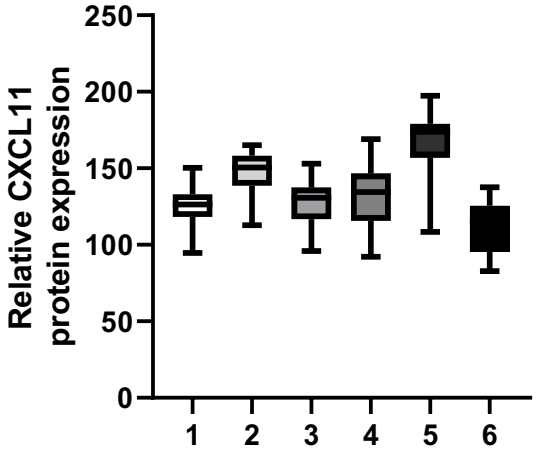

Figure 21. Box plot analysis of CXCL11 protein expression levels in different OC subtypes. 1-endometrioid carcinoma; 2-adenocarcinoma; 3-clear cell carcinoma; 4-mucinous carcinoma; 5-serous borderline tumor; 6-low-grade serous OC.

4.2 CXCL11 in breast cancer

4.2.1 CXCL11 mRNA in TNBC

For the analysis of CXCL11 mRNA expression levels in TNBC, which was determined by qPCR, patient cohort 4 was evaluated (n=104; **Table 10**). According to our criteria, three cases

were excluded. Two cases were excluded because the % STDEV of the $2^{-\Delta\Delta Ct}$ for two valid runs was 55% and 53%, respectively. One case had a $2^{-\Delta\Delta Ct}$ error progression% corresponding to 32% even after repetition. The relative CXCL11 mRNA levels, normalized to the expression levels of the housekeeping gene HPRT, ranged from 1.87-1077.40 (median 120.20). Most samples display high expression. Therefore, the remaining 101 samples were dichotomized into low and high expression by the tertials, T1 vs. T2+3 (**Figure 22**).

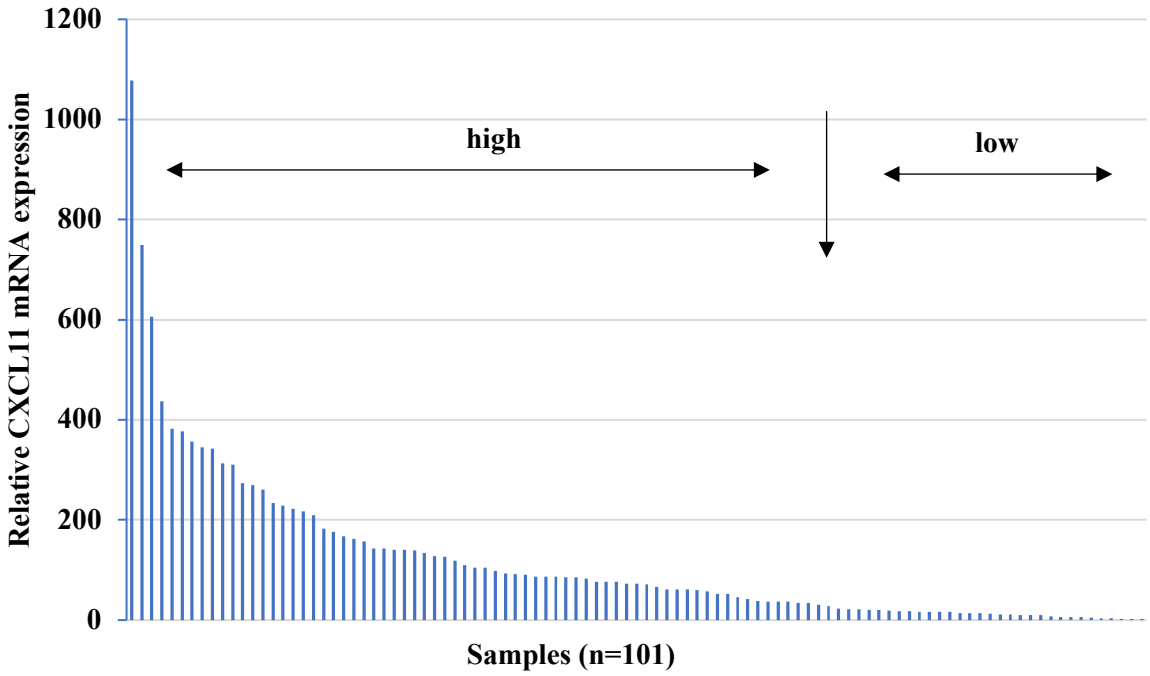

Figure 22. CXCL11 mRNA expression levels in tumor tissue of patients with TNBC: CXCL11 mRNA expression dichotomized into low expression and high expression by the 33rd percentile.

Based on this categorization, the association between CXCL11 mRNA expression levels and the established clinical parameters (age ≤ 60 vs. > 60 years, tumor size < 20 mm vs. ≥ 20 mm, lymph node status negative vs. positive, tumor grade 2 vs. 3/4) was investigated applying the Chi-square test. There is no significant association between clinical characteristics of TNBC and CXCL11 mRNA expression (**Table 22**).

Table 22. Association between clinical characteristics of TNBC patients and CXCL11 mRNA expression

Clinical parameters	No. of patients	CXCL11 low/high
Age		P = 0.485
≤ 60 years	54	16/38
>60 years	47	17/30
Tumor size		P = 0.966
< 20 mm	27	9/18
≥ 20 mm	73	24/49
Lymph node status		P = 0.686
negative	89	30/60
positive	11	3/8
Tumor grade		P = 0.603
grade 2	10	4/6
grade 3	91	29/62

n=101; cut-off: 33rd percentile; Chi-square test, p≤0.05. is considered as statistically significant. Due to missing data sets, the cases do not always add up to 101.

4.2.1.1 Univariate Cox regression analysis of the clinical outcome in TNBC with respect to clinical parameters and CXCL11 mRNA expression

The association between clinical parameters and CXCL11 mRNA expression levels with patients' OS and DFS (observation time: 15-years) is shown in **Table 23**. In univariate Cox regression analysis, the clinical factor age represented a significant predictor for OS (HR: 3.53, p<0.001) and DFS (HR: 2.75, p=0.003). The lymph node status represented a predictor for OS (HR: 4.47, p<0.001) and DFS (HR: 3.43, p=0.003). Moreover, elevated CXCL11 mRNA expression was notably linked to longer OS (HR: 0.50, p=0.046) and longer DFS (HR: 0.45, p=0.016).

Table 23. Univariate Cox regression analysis of the clinical outcome in TNBC patients with respect to clinical parameters and CXCL11 mRNA expression

Clinical parameters	Overall survival 180 months			Disease-free survival 180 months		
	No.	**HR (95% CI)**	**P**	**No.**	**HR (95% CI)**	**P**
Age			**<0.001**			**0.003**
≤ 60 years	53	1		53	1	
> 60 years	47	3.53 (1.68 – 7.44)		45	2.75 (1.41 – 5.34)	
Tumor size	27		0.292			0.410
≤ 20 mm	72	1		27	1	
> 20 mm		1.61 (0.66 - 3.91)		70	1.39 (0.64 – 3.04)	
Lymph node status			**<0.001**			**0.003**
negative	89	1		88	1	
positive	11	4.47 (2.01 - 9.96)		10	3.43 (1.50 - 7.84)	
Tumor grade			0.652			0.552
grade 2	10	1		10	1	
grade 3	90	1.31 (0.40- 4.32)		88	1.43 (0.44 - 4.67)	
CXCL11			**0.046**			**0.016**
low	32	1		32	1	
high	68	0.50 (0.25 - 0.99)		66	0.45 (0.24 - 0.86)	

HR-hazard ratio, CI-confidence interval; cut-off: 33rd percentile; Cox regression analysis, p≤0.05 is considered as statistically significant. Due to missing data sets, the cases do not always add up to 101.

The association between mRNA levels and survival parameters is visualized by the respective survival curves (**Figure 23**). The median OS and DFS for the patient group displaying low CXCL11 mRNA expression was reached after 105 months and 60 months, respectively, whereas the median OS and DFS for patients with high tumor-associated CXCL11 mRNA expression was not reached even after 180 months.

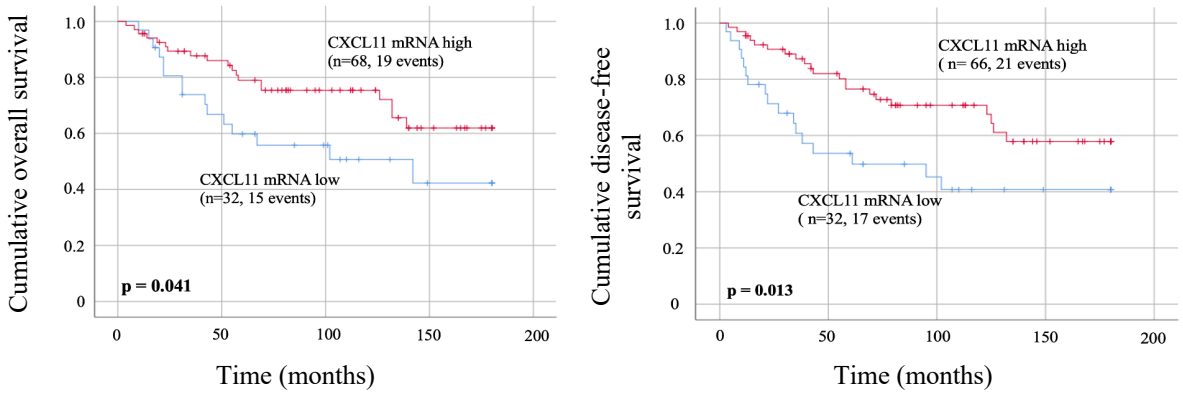

Figure 23. Elevated levels of CXCL11 mRNA are associated with longer overall survival and disease-free survival in the cohort of TNBC patients: Kaplan–Meier survival analysis, p≤0.05 is considered as statistically significant. Red curve: CXCL11 high level mRNA expression, blue curve: CXCL11 low level mRNA expression.

4.2.1.2 Association of CXCL11 mRNA expression with OS and DFS in multivariable analysis

An independent relationship of CXCL11 mRNA level and OS and DFS was studied by multivariable Cox hazard regression analysis (**Table 24**). In the base model age, tumor size, lymph node status and tumor grade were included. Here, age and lymph node status represented significant predictors for OS (HR: 4.28, p<0.001; HR: 4.75, p<0.001) and for DFS (HR: 3.11, p=0.001; HR: 3.41, p<0.005). After adding CXCL11 mRNA expression levels as additional factor to the base model, it turned out to represent an independent factor for OS (HR: 0.47, p=0.036) and DFS (HR: 0.42, p=0.010), as well.

Table 24. Multivariable Cox regression analysis of the clinical outcomes in TNBC patients with respect to clinical parameters and CXCL11

Clinical parameters	Overall survival 180 months			Disease-free survival 180 months		
		HR (95% CI)	P		HR (95% CI)	P
Age			**<0.001**			**0.001**
≤ 60 years	52	1		52	1	
> 60 years	47	4.28 (1.94 - 9.43)		45	3.11 (1.56 - 6.23)	
Tumor size			0.430			0.541
< 20 mm	27	1		27	1	
≥ 20 mm	72	1.44 (0.58 - 3.54)		70	1.28 (0.58 - 2.84)	
Lymph node status			**<0.001**			**0.005**
negative	88	1		87	1	
positive	11	4.75 (2.06 - 10.96)		10	3.41 (1.45 - 7.80)	
Tumor grade			0.828			0.636
grade 2	10	1		10	1	
grade 3	89	1.15 (0.34 - 3.92)		87	1.34 (0.40 - 4.48)	
CXCL11			**0.036**			**0.010**
low	32	1		32	1	
high	67	0.47 (0.23 - 0.95)		65	0.42 (0.21 - 0.81)	

CXCL11 mRNA was added to the base model (age, tumor size, lymph node status and tumor grade); HR-hazard ratio; CI-confidence interval; cut-off: 33rd percentile; multivariable Cox regression analysis; $p \leq 0.05$ is considered as statistically significant.

4.2.2 CXCL11 protein expression in TNBC

CXCL11 protein expression was analyzed by IHC applying tissue micro arrays of TNBC cohort encompassing 146 patients (cohort 5; n=146; **Table 11**) CXCL11 expression was dichotomized concerning low expression and high expression by the 40th percentile (**Figure 24**).

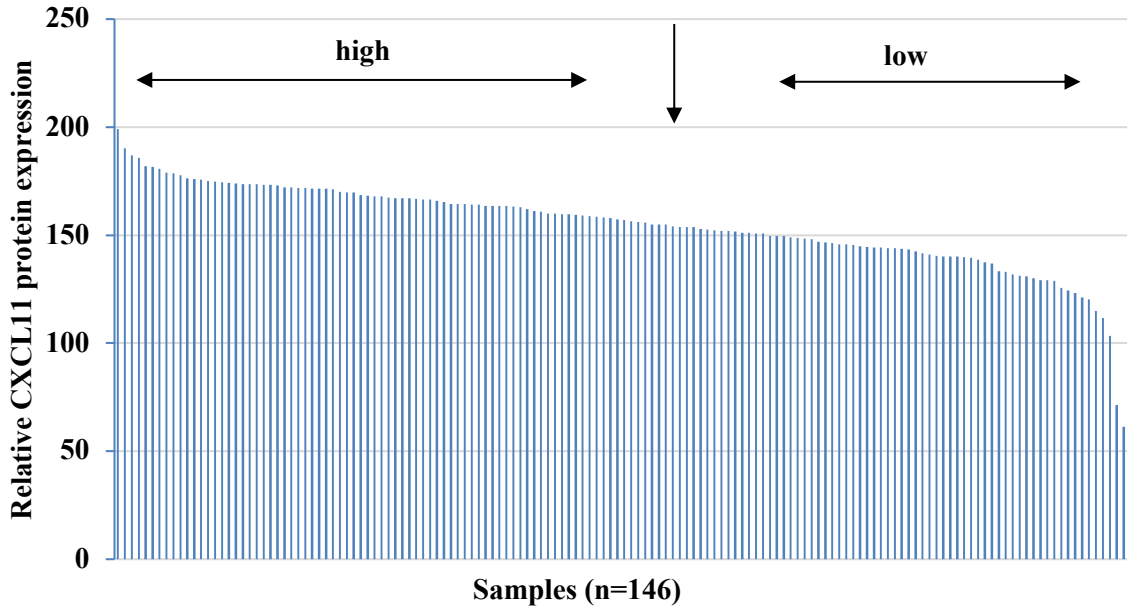

Figure 24. CXCL11 protein expression levels in tumor tissue of patients with TNBC: CXCL11 protein expression dichotomized into low expression and high expression by the 40th percentile.

The association between CXCL11 expression levels and the established clinical parameters (age ≤ 60 vs. > 60 years, residual tumor mass yes vs. no, ascitic fluid volume ≤ 500 ml vs. > 500 ml) was studied applying the Chi-square test. There was no significant association between clinical characteristics of TNBC patients and CXCL11 protein expression levels (**Table 25**).

Table 25. Association between clinical characteristics of TNBC patients and CXCL11 protein expression

Clinical parameters	No. of patients	CXCL11 Low/high
Age		P = 0.847
≤ 60 years	88	35/53
>60 years	58	24/34
Tumor size		P = 0.067
< 20 mm	45	23/22
≥ 20 mm	92	32/60
Lymph node status		P = 0.206
negative	77	27/50
positive	66	30/36
Tumor grade		P = 0.769
grade 2	18	8/10
grade 3	125	51/74

n=146; cut-off: 40th percentile; Chi-square test, p≤0.05 is considered as statistically significant. Due to missing data sets, the cases do not always add up to 146.

4.2.2.1 Univariate Cox regression analysis of the clinical outcome in TNBC patients with respect to clinical parameters and CXCL11 protein expression

In univariate Cox regression analysis with patients' OS and DFS (observation time: 15-years) age represented a significant predictor for OS (HR:1.71, p=0.036), lymph node status for OS and DFS (HR: 3.21, p<0.001 and HR: 3.22, p=0.004) (**Table 26**). Elevated CXCL11 protein expression was significantly associated with longer OS (HR: 0.51, p=0.009), which was confirmed by Kaplan-Meier analysis (**Figure 25**).

Table 26. Univariate Cox regression analysis of the clinical outcome in TNBC patients with respect to clinical parameters and CXCL11 protein expression

Clinical parameters	Overall survival 180 months			Disease-free survival 180 months		
	No.	**HR (95% CI)**	**P**	**No.**	**HR (95% CI)**	**P**
Age			**0.036**			0.699
≤ 60 years	87	1		86	1	
> 60 years	58	1.71 (1.04 – 2.82)		57	1.16 (0.54 – 2.51)	
Tumor size			0.418			0.955
≤ 20 mm	45	1		44	1	
> 20 mm	92	1.28 (0.70 - 2.35)		92	1.02 (0.45 – 2.36)	
Lymph node status			**<0.001**			**0.004**
negative	77	1		77	1	
positive	65	3.21 (1.84 - 5.59)		63	3.22 (1.44 - 7.18)	
Tumor grade			0.973			0.892
grade 2	18	1		18	1	
grade 3	124	0.99 (0.45- 2.17)		122	0.92 (0.28 - 3.07)	
CXCL11			**0.009**			0.592
low	59	1		59	1	
high	86	0.51 (0.31 - 0.84)		84	1.25 (0.56 - 2.77)	

HR-hazard ratio, CI-confidence interval; cut-off: 40^{th} percentile; Cox regression analysis, $p \leq 0.05$ is considered as statistically significant. Due to missing data sets, the cases do not always add up to 146.

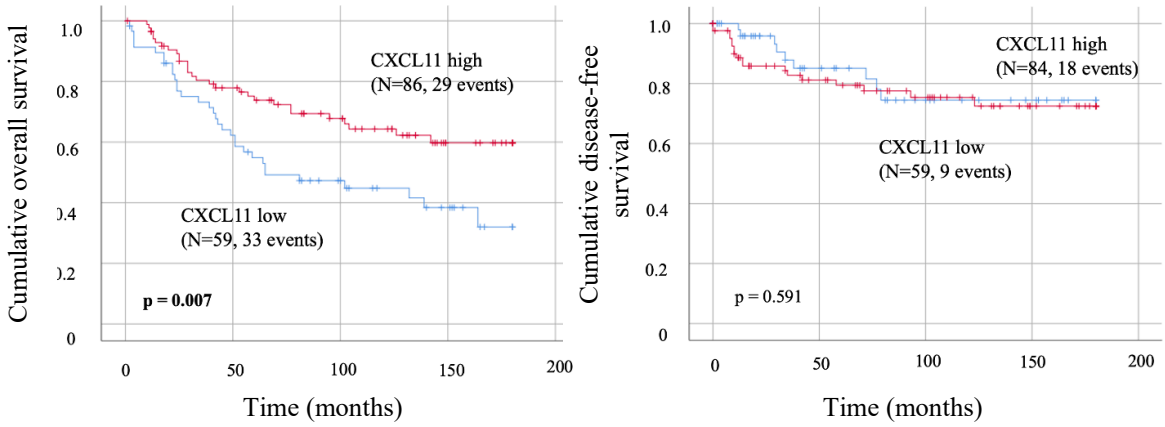

Figure 25. Elevated levels of CXCL11 protein are associated with longer overall survival in the cohort of TNBC patients: Kaplan–Meier survival analysis, p≤0.05 is considered as statistically significant**.** Red curve: CXCL11 high level protein expression, blue curve: CXCL11 low level protein expression.

4.2.2.2 Association of CXCL11 protein expression with OS and DFS in multivariable analysis

The independent relationship of CXCL11 protein levels with OS and DFS was examined by multivariable analysis (**Table 27**). In the base model, the lymph node status is representing a predictive marker for OS and DFS (HR: 3.38, p<0.001; HR: 3.16, p=0.008). After addition of CXCL11 protein expression levels to the base model, this biological factor showed a trend towards significance (p=0.054) concerning OS.

Table 27. Multivariable Cox regression analysis of the clinical outcome in TNBC patients with respect to clinical parameters and CXCL11 protein expression

Clinical parameters	Overall survival 180 months			Disease-free survival 180 months		
	No.	**HR (95% CI)**	**P**	**No**	**HR (95% CI)**	**P**
Age			0.165			0.674
≤ 60 years	81	1		80	1	
> 60 years	51	1.47 (0.85 – 2.51)		51	1.19 (0.54 - 2.61)	
Tumor size			0.561			0.526
< 20 mm	44	1		43	1	
≥ 20 mm	88	0.82 (0.41 – 1.61)		88	0.74 (0.29 – 1.89)	
Lymph node status			**<0.001**			**0.008**
negative	73	1		73	1	
positive	59	3.38 (1.85 – 6.16)		58	3.16 (1.35 – 7.42)	
Tumor grade			0.861			0.863
grade 2	17	1		17	1	
grade 3	115	1.08 (0.46 – 2.54)		11	1.12 (0.30 - 4.15)	
CXCL11			*0.054*			0.440
low	53	1		55	1	
high	79	0.58 (0.37- 1.0)		78	1.39 (0.61-3.17)	

CXCL11 protein was added to the base model (age, tumor size, lymph node status and tumor grade); HR-hazard ratio, CI-confidence interval; cut-off: 40th percentile; multivariable Cox regression analysis, p≤0.05, is considered as statistically significant.

4.2.3 CXCL11 protein expression in other BC subtypes

Supporting the idea that CXCL11 is expressed in breast cancer, an IHC analysis was carried out for other BC subtypes, i.e., HER2+ and/or ER/PR+ tumor types. Cohort 6 (n=219; **Table 12**) was dichotomized concerning low and high CXCL11 protein expression levels by the median (**Figure 26**).

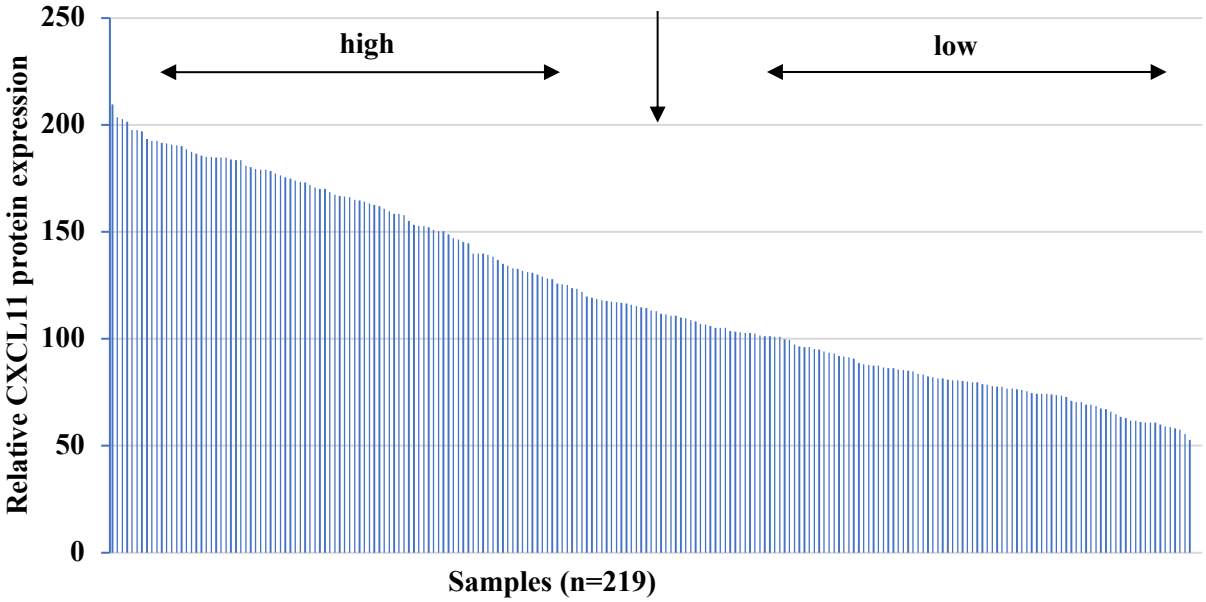

Figure 26. CXCL11 protein expression levels in tumor tissue of BC patients: CXCL11 expression dichotomized into low and high by median percentile.

The association between CXCL11 protein expression levels and the established clinical parameters (age ≤ 60 vs. > 60 years, residual tumor mass yes vs. no, ascitic fluid volume ≤ 500 ml vs. > 500 ml) was investigated applying the Chi-square test. There was no significant relation between clinical characteristics of BC patients and CXCL11 protein expression (**Table 28**).

Table 28. Association between clinical characteristics of BC patients and CXCL11 protein expression

Clinical parameters	No. of patients	CXCL11 Low/high
Age		P = 0.199
≤ 60 years	99	45/54
>60 years	120	65/55
Tumor size		P = 0.636
< 20 mm	109	53/56
≥ 20 mm	110	57/53
Lymph node status		P = 0.432
negative	137	66/71
positive	182	44/38
Tumor grade		P = 0.615
grade 2	135	66/69
grade 3	184	44/40

n=219; cut-off: 50th percentile; Chi-square test, p≤0.05 is considered as statistically significant. Due to missing data sets, the cases do not always add up to 219.

4.2.3.1 Univariate Cox regression analysis of the clinical outcome in BC patients with respect to clinical parameters and tumor biological factors

In univariate Cox regression analysis with respect to 15-year OS and DFS tumor size represented a significant predictor for OS (HR:3.85, p=0.002) and DFS (HR:3.60, p=0.024) (**Table 29**). Lymph node status showed a significance for DFS (HR: 2.67, p=0.005) and tumor grade for OS (HR: 2.04, 0.046). Elevated CXCL11 expression, however, was not significantly linked to OS and DFS, which was confirmed by Kaplan-Meier analysis (**Figure 27**).

Table 29. Univariate Cox regression analysis of the clinical outcome in BC patients with respect to clinical parameters and CXCL11

Clinical parameters	Overall survival 180 months			Disease-free survival 180 months		
	No.	**HR (95% CI)**	**P**	**No.**	**HR (95% CI)**	**P**
Age			*0.054*			0.895
≤ 60 years	99	1		120	1	
> 60 years	120	2.14 (0.99 – 4.62)		148	0.96 (0.49 – 1.88)	
Tumor size			**0.002**			**0.024**
≤ 20 mm	109	1		131	1	
> 20 mm	110	3.85 (1.66 - 8.90)		137	3.60 (1.63 – 7.96)	
Lymph node status			0.141			**0.005**
negative	137	1		137	1	
positive	82	1.68 (0.84 - 3.37)		82	2.67 (1.34 - 5.34)	
Tumor grade			**0.046**			0.180
grade 2	135	1		135	1	
grade 3	84	2.04 (1.01- 4.13)		84	1.56 (0.81 - 3.11)	
CXCL11			0.835			0.403
Low	110	1		110	1	
high	109	0.93 (0.46 - 1.87)		109	0.74 (0.37 - 1.49)	

HR-hazard ratio, CI-confidence interval; cut-off: 50th percentile; Cox regression analysis, p≤0.05 is considered as statistically significant. Due to missing data sets, the cases do not always add up to 219.

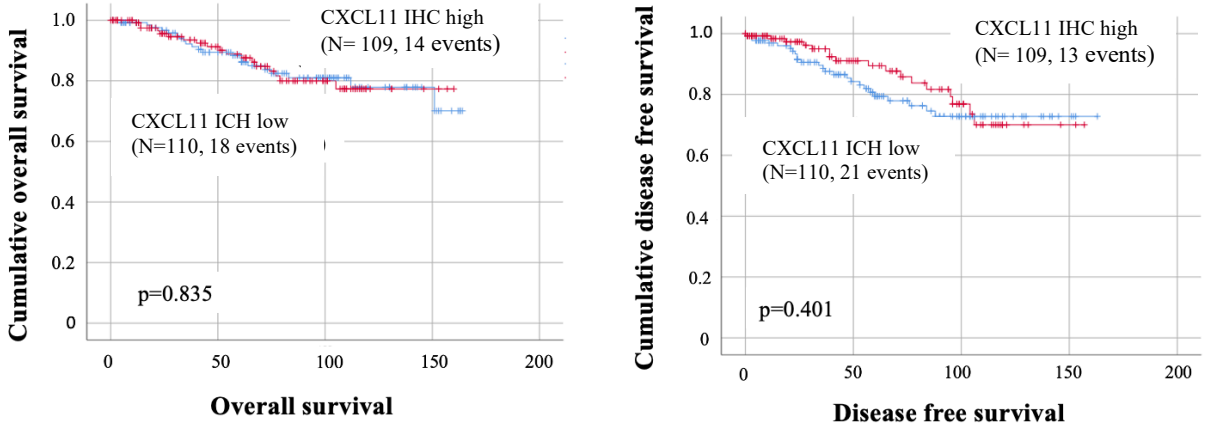

Figure 27. Elevated levels of CXCL11 protein are not associated with longer overall and disease-free survival in the cohort of patients encompassing different subtypes of BC: Kaplan–Meier survival analysis, p≤0.05 is considered as statistically significant. Red curve: CXCL11 high level protein expression, blue curve: CXCL11 low level protein expression.

4.3 Characterization of CXCL9-11 expression and secretion in ovarian cancer cell lines

The analysis of expression and secretion of CXCL9-11 into cell culture supernatants was performed via ELISA with and without prior stimulation of the cells with proinflammatory cytokines (IFN-γ, TNF-α). The following human ovarian cancer cell lines were used: OVCAR-3 (ATCC: HTB-161), Caov-3 (ATCC: HTB-75), SKOV-3 (ATCC: HTB-77), OV-MZ-6 (Möbus et. al 1992). The assays were performed in order to define whether ovarian cancer cell lines are capable of secreting chemokines and whether CXCL11 (**Figure 28**) is equivalently regulated in comparison to the other CXCR3 ligands, CXCL9 (**Figure 29**) and CXCL10 (**Figure 30**). Initially, tests with IFN-γ and TNF-α were performed individually using three different concentrations (2.5, 10, and 50 ng/ml). In general, a concentration-dependent induction of CXCL9, 10, and 11 was observed in most cell lines (**Table 30)**.

Table 30. Secretion of CXCL9, 10, and 11 into cell culture supernatants in human ovarian serous cancer cell lines after stimulation with different concentration of proinflammatory cytokines

	CXCL11			CXCL10			CXCL9		
	OVCAR-3	Caov-3	SKOV-3	OVCAR-3	Caov-3	SKOV-3	OVCAR-3	Caov-3	SKOV-3
2.5 IFN-γ	2.4	2.5	3.2	168.2	24.7	9.3	56.9	25.1	0
10 IFN-γ	6.4	2.8	6.2	228.9	20.6	22.6	78.5	23.1	0.6
50 IFN-γ	8.2	10.4	8.4	259.8	71.8	32.6	87.7	52.4	0
2.5 TNF-α	0	2.2	0	17.9	7.4	0.36	0	1.9	0
10 TNF-α	3.0	2.1	1.7	42.6	8.8	0.34	0	1.3	0
50 TNF-α	0	4.6	1.3	71.9	11.0	0	0	1.3	0

Concentration of the cytokines in the medium: 2.5, 10, 50 ng/ml IFN-γ, 2.5, 10, 50 ng/ml TNF-α. Experiments with OV-MZ-6 cells were not performed at all of these concentrations.

For the main experiments, a concentration of 10 ng/ml was used for both proinflammatory cytokines (**Table 31**).

The following results were obtained in the course of the *in vitro* experiments:

1. All four cell lines showed no or only very low chemokine baseline secretion into the cell supernatants.
2. CXCL11 is expressed upon stimulation by HGSOC cell lines (OVCAR-3, Caov-3, OV-MZ-6) but not by the clear cell ovarian cancer cell line (SKOV-3). The same result was found for CXCL9. SKOV-3 only expresses CXCL10.
3. The expression of CXCL11 is synergistically induced by the stimulation with IFN-γ and TNF-α, however the single stimulation with one of them alone is not sufficient to distinctly increase the CXCL11 secretion.

4. CXCL10 expression is sufficiently increased by stimulation with IFN γ and TNF-α, either one of them or together.
5. CXCL9 expression is induced by IFN-γ stimulation and is synergistically increased by IFN-γ and TNF-α stimulation.
6. Caov-3 shows the highest expression of CXCL11 compared to the other HGSOC cell lines although the expression of CXCL9 and CXCL10 in comparison is similar.
7. CXCL10 expression is highest in the OVCAR-3 cells, but all cell lines show CXCL10 secretion upon stimulation. Here both IFN-γ and TNF-α show an effect.

Table 31. Secretion of CXCL9, 10, and 11 into cell culture supernatants in human ovarian serous cancer cell lines after stimulation with proinflammatory cytokines

CXCL11 (pg/ml)

	OV-MZ-6	OVCAR-3	Caov-3	SKOV-3
IFN-γ	2.5	6.4	2.8	6.2
TNF-α	3.7	3	2.1	1.7
IFN-γ + TNF-α	117.1	46.5	169.5	3.6
BSA	4.3	0.3	0	0

CXCL10 (pg/ml)

	OV-MZ-6	OVCAR-3	Caov-3	SKOV-3
IFN-γ	96.1	228.9	20.6	22.6
TNF-α	34.3	42.6	8.8	0.3
IFN-γ + TNF-α	152.6	336.7	304.3	93.3
BSA	0	0.5	0	0

CXCL9 (pg/ml)

	OV-MZ-6	OVCAR-3	Caov-3	SKOV-3
IFN-γ	23.5	78.5	23.1	0.6
TNF-α	0.3	0	1.3	0
IFN-γ + TNF-α	65.5	90.5	116.4	1.7
BSA	0	0	1.2	0

Concentration of the cytokines in the medium: 10 ng/ml IFN-γ, 10 ng/ml TNF-α, 10 ng/ml IFN-γ/ 10 ng/ml TNF-α; control: 1% BSA.

For visibility, the results of the assays presented in the **Table 31.** are also shown in **Figures 28**, **29**, and **30**.

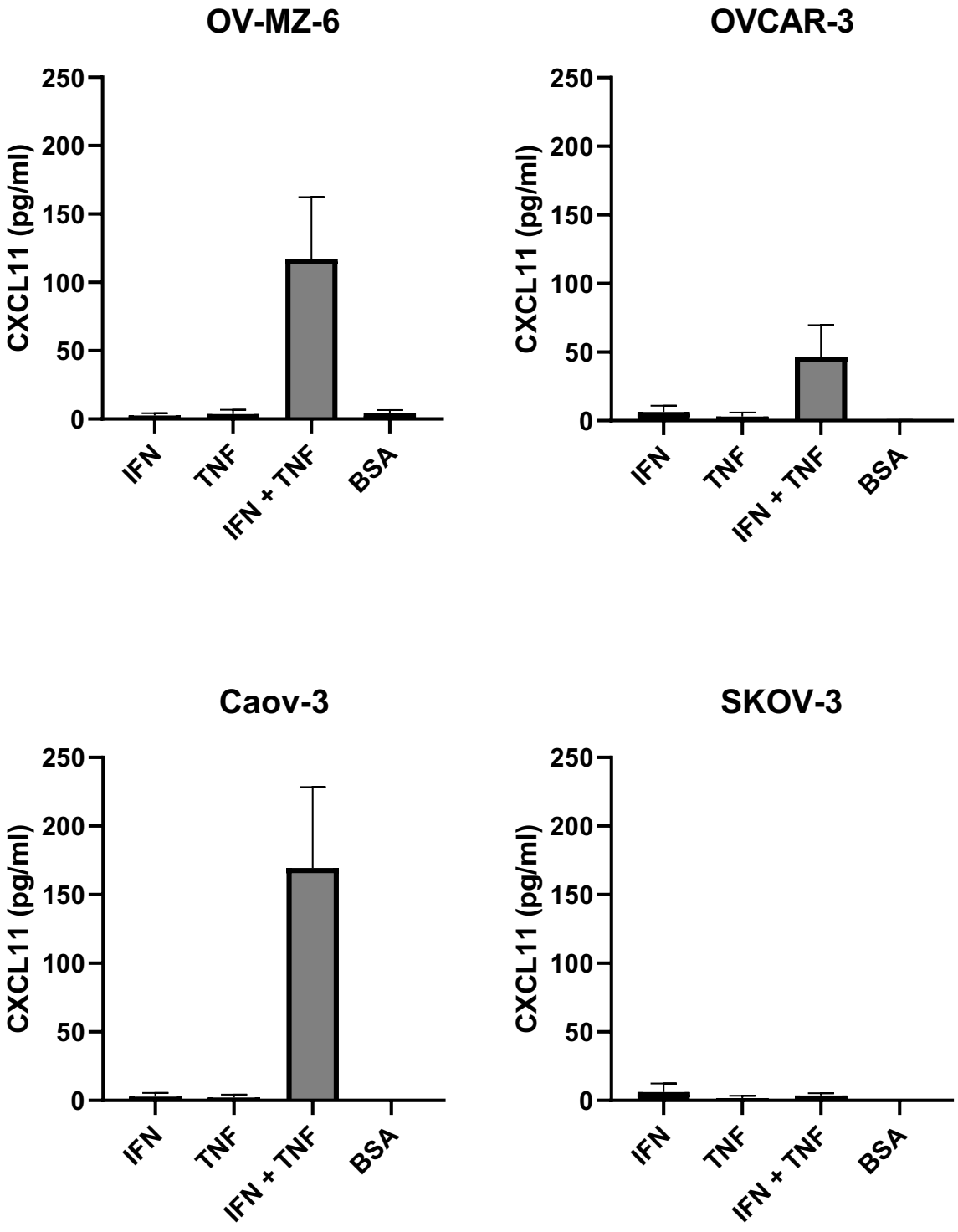

Figure 28. Induction of human CXCL11 expression in the human ovarian serous cancer cell lines after proinflammatory cytokines stimulation: (A) OV-MZ-6; (B) OVCAR-3 (HTB-161); (C) Caov-3 (HTB-75); (D) SKOV-3 (HTB-77). The following concentrations of cytokines containing medium were chosen to illustrate the data (from left to right): 10 ng/ml IFN-γ, 10 ng/ml TNF-α, 10 ng/ml IFN-γ/ 10 ng/ml TNF-α, 1% BSA.

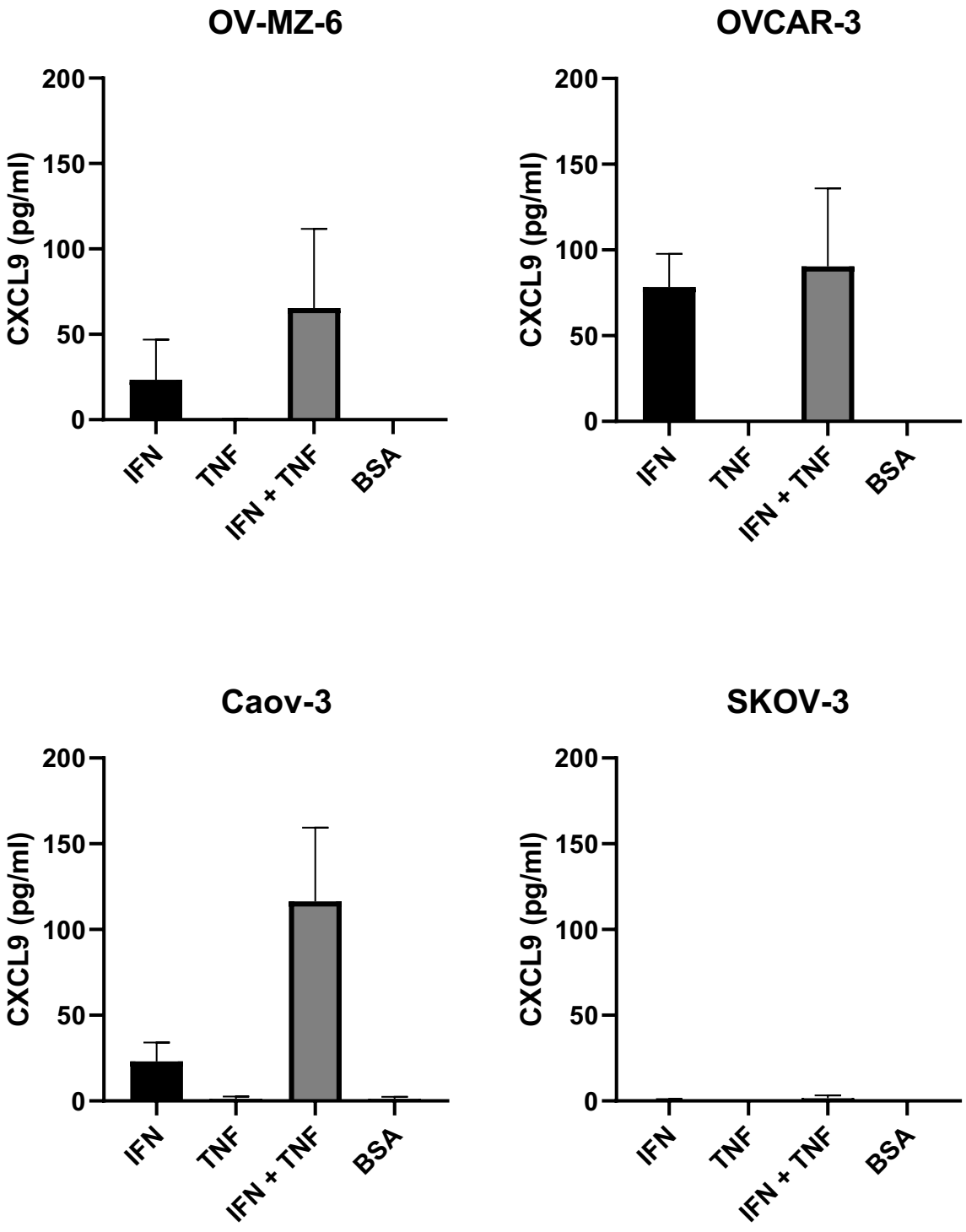

Figure 29. Induction of human CXCL9 expression in the human ovarian serous cancer cell lines after proinflammatory cytokines stimulation. (A) OV-MZ-6; (B) OVCAR-3 (HTB-161); (C) Caov-3 (HTB-75); (D) SKOV-3(HTB-77). The following concentrations of cytokines containing medium were chosen to illustrate the data (from left to right): 10 ng/ml IFN-γ, 10 ng/ml TNF-α, 10 ng/ml IFN-γ/ 10 ng/ml TNF-α, 1% BSA.

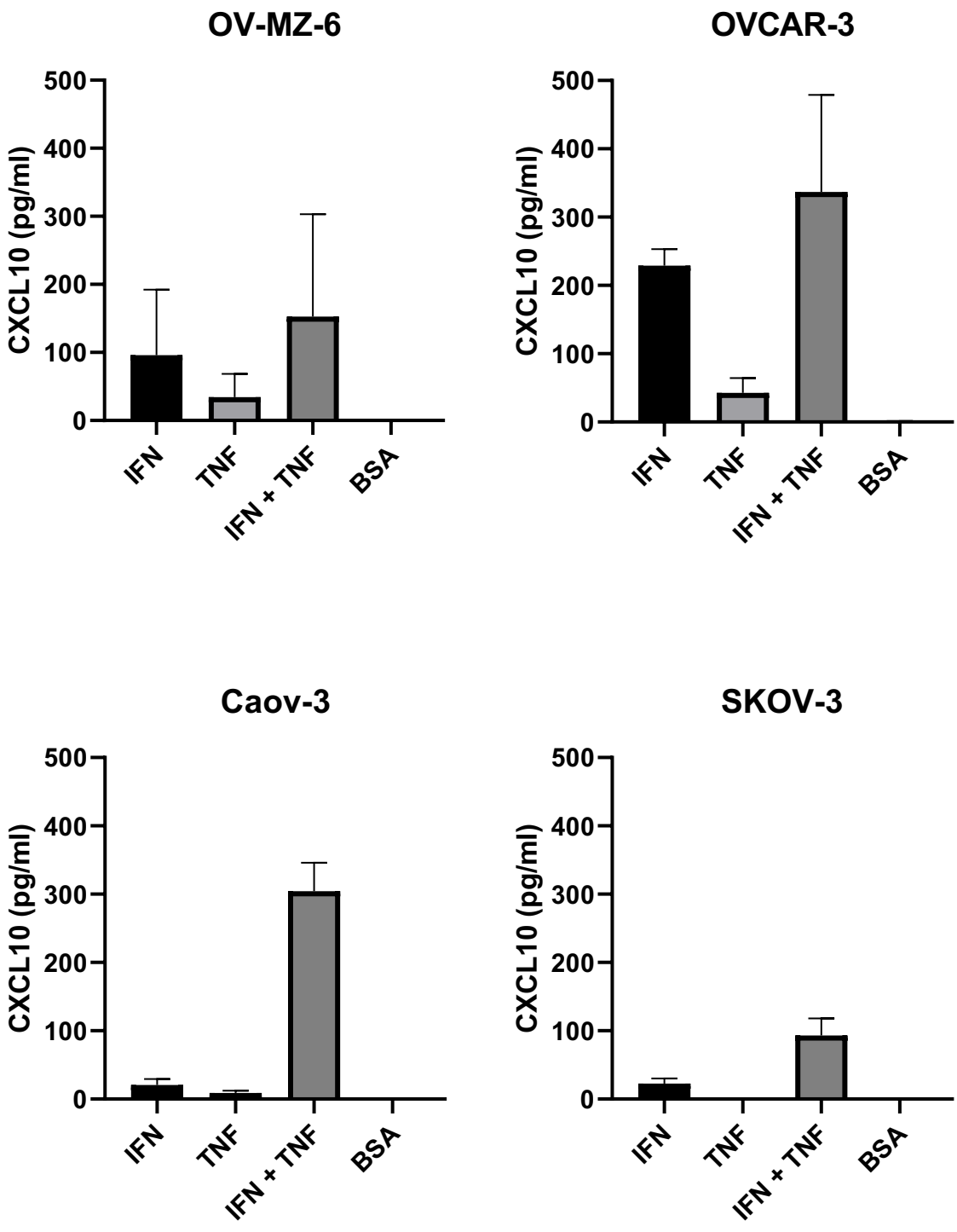

Figure 30. Induction of human CXCL10 expression in the human ovarian serous cancer cell lines after proinflammatory cytokines stimulation: (A) OV-MZ-6; (B) OVCAR-3 (HTB-161); (C) Caov-3(HTB-75); (D) SKOV-3 (HTB-77). The following concentrations of cytokines containing medium were chosen to illustrate the data (from left to right): 10 ng/ml IFN-γ, 10 ng/ml TNF-α, 10 ng/ml IFN-γ/ 10 ng/ml TNF-α, 1% BSA.

5 Discussion

Intense infiltration of T cells plays a key role in the host-specific anti-tumor response. Moreover, many targeted- and immunotherapies, also rely on a sufficient immune-cell infiltration in the tumor. Unfortunately, these cells are often unable to suppress the tumor due to a reduction in the number of infiltrating effector cells in the tumor-microenvironment (TME) (Rosenblum et al., 2010). Finding a way to increase the infiltration of anti-tumor immune cells is an urgent task to improve therapy response and the overall outcome of cancer patients.

CXCL11, together with CXCL9 and CXCL10, mainly regulates immune cell migration, differentiation, and activation of immune-effector cells such as T-cells, natural killer (NK) cells, and monocytic cells (Tokunaga et al., 2017). All three chemokines are ligands for the C-X-C chemokine receptor type 3 (CXCR3), which is expressed on many tumor-suppressive lymphocytes and, thereby, mediates their recruitment out of the bloodstream into the TME (Bronger et al., 2019; Cole et al., 1998). In lung cancer, it has been shown that the deficiency of early growth response protein 1 (Egr-1), interleukin-7 (IL-7), CCL21, and depletion of myeloid suppressor cells decreased the tumor load through enhanced expression of CXCL9 and CXCL10 (Ding et al., 2016; Caso et al., 2009; Wasuth et al., 2009; Sahin et al., 2012). This is presumably due to the anti-angiogenic role and involvement of tumor macrophages, CD4 and CD8+ T-lymphocytes as well as NK cells (Ding et al., 2016). Kondo and colleagues (2004) reported that intratumor expression of CXCL9 and CXCL10 in renal cell carcinoma correlated with an increased infiltration of anti-tumor CD8+ T cells, a reduced tumor size, and a rare recurrence after tumor resection. In patients with melanoma, overexpression of CXCL9 and CXCL10 was associated with the recruitment and migration of CD8+ T cells, which predicted a good patient prognosis (Harlin et al., 2009). In general, overexpression of the cytokines CXCL9 and CXCL10 has been shown to be associated with a higher number of tumor-infiltrating lymphocytes (TILs) and improved patient survival, e.g., in ovarian, breast, pancreatic, colorectal, lung, renal and several other cancers (Bronger et al., 2019; Qian et al., 2019; Mlecnik et al., 2010; Ding et al., 2016; Bronger et al., 2016; Kondo et al., 2004). CXCL11 is of special interest since it has a higher affinity towards its receptor CXCR3 as compared to CXCL9 and CXCL10, and in contrast to the latter, studies on the clinical relevance of CXCL11 tumor tissue levels are almost lacking (Cole et al., 1998). All in all, it is tempting to speculate that the chemokine CXCL11 is similar to CXCL9 and CXCL10 and has the same mode of regulation, mechanisms of action on tumor cells, targets, and improves survival of patients with malignant tumors.

At present, the data on the correlation between CXCL11 expression levels and survival parameters of tumor patients are quite contradictory. On the one hand, CXCL11 expression positively correlates with OS of patients with lung cancer (Gao et al., 2019), on the other hand, CXCL11 repression suppressed the metastatic ability in colorectal (Gao et al., 2018) and colon cancer (Liu et al., 2021). In the study conducted by Liu and colleagues (2021), real-time PCR and IHC analysis showed that high CXCL11 mRNA and protein expression correlated with differentiation status, depth of invasion, lymph node metastases, distant metastases, and advanced TNM stage in colorectal cancer. The same study showed that patients with a higher expression of CXCL11 had a lower survival rate (Liu et al., 2021). The inconsistency of the results can be explained by the regulation of angiogenesis by CXC chemokines, which leads to malnutrition, stagnant tumors, and also more aggressive tumor cells with metastatic potential (Bronger et al., 2019). CXCL11 overexpression in the TME enhances the recruitment of tumor-suppressive CD8+ T cells and correlates positively with antitumor cells such as memory B cells and negatively with M2 macrophages, activated CD4 memory T cells, and M1 macrophages. In addition to cancer-supporting cells, there is an increase in monocytes and a decrease in naïve CD4 T cells and activated mast cells (Gao et al., 2019; Yang et al., 2021). A recent study examining the relevance of CXCL11 in colorectal cancer showed that high expression of CXCL11 mRNA was associated with a higher proportion of anti-tumor immune cells (such as: CD8+ T cells, activated NK) and a lower proportion of protumor immune cells (such as: M0 macrophages, resting NK and monocytes) (Cao et al., 2021). From this, we can conclude that CXCL11 is associated with antitumor immunity, which partially explains the association of CXCL11 with a better prognosis. In addition, IHC analysis showed that patients with high levels of intratumoral CXCL11 had high infiltration by CD8+ T cells and CD56+ NK cells and a higher overall survival rate (Cao et al., 2021). In the present study, we demonstrate an association of increased CXCL11 expression in tumor tissue with a favorable patient prognosis which is in line with the proposed tumor-suppressive function of CXCL11.

5.1 Clinical relevance of CXCL11 in advanced HGSOC

Ovarian cancer (OC) is prone to recurrence, metastasis, and resistance. The mortality rate from OC is the highest among all gynecological malignancies and continues to grow (Guo et al., 2021). Patients with advanced OC have achieved long-term progression-free survival in recent years. This is primarily due to the targeted therapy with poly (ADP-ribose) polymerase inhibitors (PARPi) and bevacizumab (Guo et al., 2021). Using *in vivo* and *in vitro* experiments, it was confirmed that olaparib, which refers to PARPi, can increase the expression of CXCL11 in ovarian cancer cell lines (Shi et al., 2021). Despite advances in the treatment of epithelial

ovarian cancer (EOC), patient survival rates show modest improvements. The explanation for this can be the lack of effective prognostic markers leaving the patients with foremost late-stage disease and sub-optimal therapeutic windows. To date, new directions affecting carcinogenesis and disease progression need to be identified, and the discovery and development of new prognostic biomarkers and intensification of individualized therapy will be of great clinical importance. A large number of studies have found that CXC chemokines play an important role in tumorigenesis (Bronger et al., 2019; Qian et al., 2019; Mlecnik et al., 2010; Ding et al., 2016). Li with colleagues (2021), using the ONCOMINE database, showed that CXCL11 transcriptional levels in OC tissues were significantly elevated. According to the cancer genome atlas (TCGA) data in the gene expression profiling interactive analysis (GEPIA) database, high expression of CXCL11 may improve survival in patients with OC. This is confirmed also by the results of this study, which showed that increased levels of CXCL11 mRNA were associated with longer overall survival, an effect that was found to be significant and independent.

Ovarian cancer is considered an immunogenic tumor and is characterized by the presence of TILs, which are involved in the antitumor immune response and prognosis. This presents an opportunity for systemic immunotherapy, which uses the patient's immune system directly to destroy and target tumor cells (Clarke et al., 2009; Liu et al., 2020). Monoclonal antibodies, immune checkpoint inhibition, interleukin-2 (IL-2), and cancer vaccinations are strategies for immunologic therapy (cancerresearchuk.org). Monoclonal antibodies are based on the idea of selectively targeting tumor cells that express tumor-associated antigens. That holds great promise for treating ovarian cancer (cancerresearchuk.org). The 3 major mechanisms of tumor cell antibody-mediated cytotoxicity include antibody-dependent cellular cytotoxicity (ADCC), complement-dependent cytotoxicity (CDC), and antibody-dependent cellular phagocytosis (ADCP) (Li et al., 2021). ADCC initiates an immune response to antibody-coated cells for further recognition, mainly by NK cells, which leads to lysis of the target cells (Lo Nigro et al., 2019; Yonezawa et al., 2016). The ADCP response is closely related to tumor-associated macrophages (Li et al., 2021). CDC activates components of the complement cascade, which leads to the formation of a membrane attack complex on the cell surface and subsequent cell lysis (Meyer et al., 2014). The chemokine CXCL11 is known to be able to attract immune cells, including NK cells and macrophages, to the tumor, and is also overexpressed upon blocking the complement system in mouse models (Tokunaga et al., 2017; Downs-Canner et al., 2016). The results of immunotherapy highly depend on the condition (functionality and activity) of the immune system. Available data indicate the importance of CXC chemokines in tumor immunotherapy (Shi et al., 2021). In solid tumors, CXCL9, CXCL10, and CXCL11 are thought

to be responsible for tumor-suppressing lymphocytic infiltration (Dangaj et al., 2019). It is already known that CXCL9 and CXCL11 are associated with improved OS in patients with OC, by recruiting T- and B-lymphocytes and NK cells to suppress tumor growth, and CXCL11 expression is closely related to antigen-related genes, immune checkpoint-related genes, and PARPi therapy (Millstein et al., 2020; Yan et al., 2020; Shi et al., 2021; Guo et al., 2021). In advanced HGSOC overexpression of the chemokines, CXCL9 and CXCL10 is associated with increased infiltration of CD3+ T cells and significantly improved survival (Bronger et al, 2016). Kryczek and colleagues (2009) determined mRNA levels of the chemokines CXCL9 and CXCL10 using real-time reverse transcriptase polymerase chain reaction and protein levels using intracellular staining or ELISA kits in 201 patients with untreated ovarian carcinomas. It was found that CXCL9 and CXCL10 were positively associated with tumor-infiltrating CD8+ T cells and were also found to correlate with IL-17 levels, which also predicts improved patient survival (Kryczek et al., 2009). Moreover, CXCL9 levels together with CD8+ effector memory T cells can be important biomarkers for assessing the effectiveness of immune therapy and potentially represent therapeutic targets (Lieber et al., 2018). It is also known, that CXCL9, and CXCL11 recruit dendritic cells, which have the potential to play a major role in facilitating the infiltration of immune cells into the TME and the formation of an antitumor immune phenotype (Liu et al., 2021). Gene signatures should be used as biomarkers to improve the clinical outcome of patients with advanced OC, thereby optimizing personalized therapy (Zheng et al., 2021). However, the role of immune-related genes in the development of EOC has not been fully elucidated (Su et al., 2021). Currently, there is a need to develop a reliable risk model that could be used for prognostic prediction in EOC (Liu et al., 2021). CXCL11 already have shown promising results in a few immune-based prognostic risk models (Zheng et al., 2021; Su et al., 2021; Liu et al., 2021). Zheng and colleagues (2021) proposed a 11-gene TME-related risk model for HGSOC, which can improve the prognostic accuracy of clinical response to targeted therapies. Su and colleagues (2021) developed an immune-based prognostic risk model using nine immune-related genes, and also included CXCL11.

Currently, there are many studies aiming at confirming the clinical efficacy of immune checkpoint blockade (ICB) therapy in OC (Wang et al., 2021). At the same time, it is worth noting that remission after treatment with immune checkpoint inhibitors is observed only in 15% of patients with advanced and recurrent OC (Hamanishi et al., 2015; Varga et al., 2015). Given this, new approaches are needed to study possible agents that could interact with immune checkpoint inhibitors to improve clinical response. CXCL11 expression was found to be positively correlated with PD-L1 in colorectal cancer and colorectal adenocarcinoma (Cao et

al., 2021). It has also been reported that expression of CXCL11 is positively associated with TME and infiltrating immune cells and could be used as a potential biomarker for ICB therapy (Shi et al., 2021). CXCL11 expression significantly correlated with expression of the most significant immune checkpoint blockade-related genes, which have a profound effect on therapy (LAG3, ICOS, CTLA4, CD48, HAVCR2, PDCD1 (PD-1), PDCDILG2 (PD-L2), TIGIT, CD274 (PD-L1, and CD86) (Shi et al., 2021). Also, it was found that in response to exposure to compound 968, there was an increase in CXCL10 and CXCL11 by cancer cells, and an increase in T cell function and infiltration into tumors. Compound 968 is an allosteric glutaminase C inhibitor that inhibits the migration and proliferation of cancer cells without affecting their normal cell counterparts. An improvement in overall survival of mice was also observed after co-treatment with compound 968 and anti-PD-L1 antibody (Wang et al., 2021). The increase in T cell infiltration, probably through induction of CXCL10 and CXCL11 secretion by tumor cells, into tumors in response to compound 968, as well as the inhibition of glutaminase by compound 968, improved the treatment effect of ICB in ovarian cancer (Wang et al., 2021). CXCL9 expression has also been shown to be a very powerful marker to predict ICB therapy response in HGSOC and enable a successful therapy in a non-responding syngeneic mouse model for HGSOC (Seitz et al., 2022). This confirms that the role of CXCL9/CXCL10/CXCL11/CXCR3-mediated T-cell infiltration in the success of ICB therapy is very important.

All in all, overexpression of CXCL11 has shown promising results with regards to the prognosis of HGSOC. The results suggest that CXCL11 is a suitable prognostic biomarker with the potential to become a therapeutic target for cancer treatment.

5.2 Characterization of *in vitro* CXCL11 expression by ELISA in different human ovarian serous cancer cell lines and comparison to the expression CXCL9, CXCL10

CXCL11 is expressed at low levels under homeostatic conditions. This process is enhanced in response to stimulation by interferon-gamma (IFN-γ) and -beta (IFN-β), and weakly by -alpha (IFN-α). Moreover, it is synergistically enhanced by combination with tumor necrosis factor-alpha (TNF-α), which alone has no effect (Rani et al., 1996; Antonelli et al., 2013; Tensen et al., 1999; Tokunaga et al., 2017). From all CXCR3 ligands, TNF-α only affected CXCL10 secretion, which has already been reported (Bronger et al., 2016). A strong association has been observed between inflammatory processes and cancer development (Piotrowski et al., 2020). IFN-γ and TNF-α are proinflammatory cytokines, which are produced by inflammatory cells and play an important role in the immune system and the supervision of tumor growth (Shen et

al., 2018). In ovarian cancer, inflammation has a significant role in tumor development (Jia et al., 2018). Induction and secretion of chemokines of the CXCR3 system, in particular CXCL9 and 10, has been shown before for ovarian cancer cell lines, especially after the stimulation with proinflammatory cytokines (Bronger et al., 2016). Due to the strong redundancy of three similar ligands for the same receptor, the inductive potential of CXCL11 has not been systematically addressed in ovarian cancer cell lines. In the present work, it was demonstrated that in various ovarian cancer cell lines, CXCL11 is expressed after IFN-γ stimulation, and can be synergistically enhanced by TNF-α stimulation in the same way as CXCL9 and CXCL10. According to the Human Protein Atlas, CXCL9, 10 and 11 are prognostic and their high expression is favorable in ovarian cancer (proteinatlas.org). However, the average value in ovarian cancer tissues is variable. CXCL10 (63.1fragments per kilobase million (FPKM)) has the highest expression, followed by CXCL9 (13.6 FPKM) and then CXCL11 (8.7 FPKM) (proteinatlas.org). These data are consistent with the findings of the present study, where CXCL11 shows the lowest total concentration in comparison to CXCL9 and CXCL10.

The experiments carried out in this work demonstrate secretion of CXCL11 by various ovarian cancer cell lines in response to stimulation. Since CXCL11 secretion in TME *in vivo* can originate from several sources, such as fibroblasts or NK cells, it was important to show that tumor cells themselves can secrete chemokines. By *in vitro* assays, further studies need to show whether the identified tumor cells will provide sufficient amount of CXCL11 to alter immunological interactions in the TME and stimulate enhanced immune responses. Interestingly, laboratory mouse strains, e.g., C57BL/6 mice, generally carry a mutated, inactive CXCL11 gene, which is due to a single frameshift mutation. Therefore, *in vivo* data on the role of CXCL11 is almost completely lacking. Only very recently the mutations were corrected by the CRISPR/Cas9 technology, which may help to perform in vivo experiments helping to understand the tumorbiological role of CXCL11 (Dalit et al., 2022).

5.3 Clinical relevance of CXCL11 in TNBC

TNBC is an aggressive cancer that grows and spreads rapidly. There are very few treatment options because the cancer cells do not respond well to most known treatments (Yang et al., 2006). Surgery, cytotoxic chemotherapy, and PARPi are currently the therapy of choice, alone or together (Tarantino et al., 2022). Despite the availability of effective treatments, TNBC patients still have a mortality rate of about 40% of all breast cancer deaths. Together with the overall aggressive phenotype of this entity other factors contribute to the worse prognosis such as the lack of targeted therapy and potential resistance to chemotherapy (Wu et al., 2021).

Currently, none of the clinical targeted drugs are very effective in fighting against TNBC on their own (Singh et al., 2021). Despite the efficacy of chemotherapy treatment, unfortunately, 30-50% of patients will develop therapy resistance (Kim et al., 2018). Combining chemotherapy with PARPi significantly improves survival in patients with TNBC (Chen at al., 2021). PARPi therapy is effective in patients carrying mutations in *BRCA1/2* (Singh et al., 2021). Unfortunately, only about 15% of all people diagnosed with TNBC have these germline mutations (Hahnen et al., 2017). Therefore, there is an urgent need to identify effective prognostic markers, therapeutic targets, and develop a more effective method of treating TNBC. Increased knowledge of the tumor microenvironment allows us to discover new prognostic biomarkers, new therapeutic approaches, and new treatment concepts. In the present study. we demonstrate for the first time an association of increased CXCL11 expression in tumor tissue of TNBC with a favorable patient prognosis.

The outcome of therapy is highly dependent on immune cell infiltration (Bracci et al., 2013). ChT and PARPi strongly benefit from an increase in immune cells (Cole et al., 1998). In breast cancer tissue, immune cells are mainly represented by a population of T-lymphocytes (70%-80%), followed by B-lymphocytes, macrophages, NK cells, and antigen-presenting cells (Yu et. al., 2017; Ruffell et al., 2012; Coventry et al., 2015). TNBC represents a subtype of BC, which has increased levels of tumor-infiltrating lymphocytes (Beniey et al., 2019; Gaynor et al., 2020; Gao et al., 2020). Denkert and colleagues (2018) analyzed TIL concentrations and its relation to pathological complete response to neoadjuvant chemotherapy in 906 patients with TNBC. Pathological complete response was achieved in 80 (31%) of 260 patients with low levels of TILs (0-10% immune cells in stromal tissue within the tumor), 117 (31%) of 373 with intermediate levels of TILs (11-59%), and 136 (50%) of 273 with high levels of TILs (≥60%) (Denkert et al., 2018). The results demonstrate the key role of TILs for response to neoadjuvant chemotherapy in triple-negative breast cancer. TILs can also act as a biomarker for predicting the benefit of immunotherapy (Savas et al., 2016). As high levels of lymphocytic infiltration are not only associated with a better prognosis in patients with TNBC, but also play a role in response to therapy, the pathways responsible for this response need to be studied (Savas et al., 2016; Denkert et al., 2018). CXCR3 is mainly responsible for infiltration of TILs (Bronger et al., 2019; Cole et al., 1998). For BC, it was already shown that a high expression of the CXCR3 ligand CXCL9 correlated with a better response to chemotherapy (Specht et al., 2009). CXCL11, which has a higher affinity then the other chemokines towards to CXCR3, appears to play a critical role in this process, as it is closely related to survival and the presence of TILs

(Cole et al., 1998). From this, we suggest that CXCL11 can increase immune activation, thereby improving the outcome of therapy.

Due to the relatively high immunogenic potential of TNBC, immunotherapy becomes a promising treatment area (Beniey et al., 2019; Gaynor et al., 2020; Gao et al., 2020). Immune checkpoint inhibitors, an adoptive cellular immunotherapy, or a chimeric antigen immunotherapy offer new hope for patients suffering from TNBC (Emens 2021). Considering the KEYNOTE-086 (phase II) data, it was found that stromal TIL expression can predict response to immune checkpoint inhibitors (Adams et al., 2019; Qureshi et al., 2022). This study evaluated the response to the single agent pembrolizumab in two groups. In the group with previously treated metastatic TNBC and any PD-L1 status, the mean stromal TIL level in responders was 10% compared to 5% in non-responders (Adams et al., 2019). And in the group with previously untreated PD-L1 positive metastatic TNBC, the level of stromal TIL in responders was 50% compared with 15% in non-responders (Adams et al., 2019). In adopting CD8+ T cell therapy, large numbers of tumor-specific T cells are obtained from patients, expanded *in vitro*, and injected back into patients. CD8+ T cells play an important role in anti-tumor immunity, and their infiltration is associated with good prognosis of various types of cancer, including TNBC (Jin et al., 2020). Chimeric antigen receptor immunotherapy (CAR) alters T cells so that they can find and destroy cancer cells (cancer.gov). It was shown that lentivirus-infected epidermal growth factor receptor-CAR (EGFR-CAR) T cells reduce TNBC cell growth and tumorigenesis *in vitro* and *in vivo* (Qiu et al., 2022). Given the side effects of immunotherapy, it is necessary to identify prognostic biomarkers of response and resistance in order to improve patient selection. In summary, the results of this work, together with the proposed role of CXCL11, suggest that CXCL11 may be a suitable prognostic biomarker with the potential to become a therapeutic target for the treatment of TNBC.

The mechanism underlying the relationship between CXCL11 and the immune context requires further investigation. The study of CXCL11 and its role in cancer development could lead to new methods of diagnosis or individualization of patient treatment, opportunities for more effective immune therapies and improved efficacy of existing chemotherapy drugs. Future studies would be interesting to confirm the expression of CXCL11 in liquid biopsy samples from TNBC and ascites from HGSOC, as well as in patients' blood, and to identify a suitable pharmacological target to increase the intratumoral concentration of the chemokine (for example, via inhibition of cyclooxygenase, use of PARPi, etc.).

6 Summary

CXCL11 (C-X-C motif chemokine 11) is a small cytokine belonging to the C-X-C chemokine family. Together with CXCL9 and CXCL10, CXCL11 represents a ligand for the C-X-C chemokine receptor type 3 (CXCR3), which is mainly responsible for infiltration of tumor-suppressive lymphocytes. Overexpression of the cytokines CXCL9 and CXCL10 is associated with a higher number of tumor-infiltrating lymphocytes and improved patient survival, e.g., in breast, ovarian, colon, lung, and several other cancers. In contrast to CXCL9 and CXCL10, studies on the clinical relevance of CXCL11 tumor tissue levels are lacking. Therefore, the present project aimed at analyzing CXCL11 expression in homogeneous cohorts of advanced high-grade serous ovarian cancer (HGSOC) and triple-negative breast cancer (TNBC) and assessing their clinical relevance in these well-defined subgroups. CXCL11 mRNA expression levels were identified by quantitative PCR (qPCR) and protein expression levels by immunohistochemistry (IHC) in a cohort of patients suffering from HGSOC and TNBC, respectively. In addition, analysis of expression and secretion of CXCL9-11 into cell culture supernatants was performed *in vitro* via ELISA in selected ovarian cancer cell lines.

In HGSOC, CXCL11 mRNA expression was found to be rather low in approximately 50% samples. It was shown that an increased level of CXCL11 mRNA is associated with longer overall survival, and this impact turned out to be significant and independent (in univariate Cox regression analysis p=0.046; in multivariable Cox regression analysis p=0.002). For analysis of CXCL11 protein expression in tumor tissue, an ImageJ plus-based scoring system and IHC Profiler plugin were applied to assess the intensity of immunohistochemical staining. Here, there was no significant association of CXCL11 protein expression with disease outcome. The mRNA level indicates the amount of protein in the steady state (Liu et al., 2016), however, the correlation between mRNA and protein levels is only about 40% (Vogel and Marcotte, 2012). Many factors, including deficiencies in protein expression measurement (e.g. depending on the antibody used for staining) and/or IHC analysis, can affect the results of the assay. It is also important to note that unlike quantitative qPCR, IHC generates semi-quantitative data and can be considered a relatively subjective assay.

The analysis of expression and secretion of CXCL9 -11 into cell culture supernatants was performed via ELISA with or without stimulation of inflammatory cytokines (IFN- γ, TNF- α). The assay was deployed in order to define, whether the cell lines OVCAR-3 (ATCC: HTB-161), Caov-3 (ATCC: HTB-75), SKOV-3 (ATCC: HTB-77), and OV-MZ-6 (Möbus et. al., 1992), respectively, are capable of secreting chemokines upon stimulation and whether CXCL11 is equivalently regulated in comparison to the other CXCR3 ligands, CXCL9 and

CXCL10. Our experiment confirmed that in ovarian cancer cell lines, except in clear cell carcinoma cells (SKOV-3), CXCL11 is expressed in response to IFN-γ stimulation and can be synergistically amplified by TNF-α stimulation in the same manner as CXCL9 and CXCL10.

In TNBC, CXCL11 displayed a rather high mRNA expression in most of the samples (about 67%). Regarding its clinical relevance, CXCL11 mRNA expression levels turned out to represent a favorable prognostic factor in univariate Cox regression analysis for OS (p=0.046), but also for DFS (p=0.016). Moreover, this prognostic value of CXCL11 mRNA was independent of established clinical parameters according to multivariable Cox regression analysis of TNBC for both survival parameters (OS p=0.036, DFS p=0.010). The IHC assay showed a high level of protein expression in 60 % of the cases. Here, the elevated CXCL11 protein expression was linked to longer OS (p=0.009) and showed a trend towards to be significant an independent factor (p= 0.054).

Altogether, the present study shows promising results and demonstrates an association of elevated CXCL11 expression in tumor tissue with a favorable patient prognosis. Based on the results of this study and our assumption that the function of CXCL11 is similar to that of CXCL9 and CXCL10, respectively, CXCL11 should be included in the analysis along with the more studied CXCL9 and CXCL10 in the future.

In conclusion, for the first time, the clinical relevance of CXCL11 in two common, very aggressive subtypes of gynecological cancers - advanced HGSOC and TNBC - was investigated. CXCL11 may represent an attractive target for tumor therapies, demonstrating the potential to aid decision-making about systemic therapy for patients with poor prognosis in these tumors. Further research aimed at identifying potential cancer-related pathways in which CXCL11 is involved and will improve cancer treatment strategies and help patients suffering from these malignancies.

7 References

Adams S, Loi S, Toppmeyer D, Cescon DW, De Laurentiis M, Nanda R, Winer EP, Mukai H, Tamura K, Armstrong A, Liu MC, Iwata H, Ryvo L, Wimberger P, Rugo HS, Tan AR, Jia L, Ding Y, Karantza V, Schmid P. Pembrolizumab monotherapy for previously untreated, PD-L1-positive, metastatic triple-negative breast cancer: cohort B of the phase II KEYNOTE-086 study. *Ann Oncol.* 2019; 30:405-411.

Adams S, Schmid P, Rugo HS, Winer EP, Loirat D, Awada A, Cescon DW, Iwata H, Campone M, Nanda R, Hui R, Curigliano G, Toppmeyer D, O'Shaughnessy J, Loi S, Paluch-Shimon S, Tan AR, Card D, Zhao J, Karantza V, Cortés J. Pembrolizumab monotherapy for previously treated metastatic triple-negative breast cancer: cohort A of the phase II KEYNOTE-086 study. *Ann Oncol.* 2019; 30:397-404.

Ahmed N, Dorn J, Napieralski R, Drecoll E, Kotzsch M, Goettig P, Zein E, Avril S, Kiechle M, Diamandis EP, Schmitt M, Magdolen V. Clinical relevance of kallikrein-related peptidase 6 (KLK6) and 8 (KLK8) mRNA expression in advanced serous ovarian cancer. *Biol Chem.* 2016; 397:1265-1276.

Anestis A, Zoi I, Papavassiliou A, Karamouzis V. Androgen receptor in breast cancer-clinical and preclinical research insights. *Molecules.* 2020; 25:358.

Arimont M, Sun SL, Leurs R, Smit M, de Esch IJP, de Graaf C. Structural analysis of chemokine receptor-ligand interactions. *J Med Chem.* 2017; 60:4735-4779.

Aubrey BJ, Strasser A, Kelly GL. Tumor-suppressor functions of the TP53 pathway. *Cold Spring Harb Perspect Med.* 2016; 6:a026062.

Bachelerie F, Graham GJ, Locati M, Mantovani A, Murphy PM, Nibbs R, Rot A, Sozzani S, Thelen M. New nomenclature for atypical chemokine receptors. *Nat Immunol.* 2014; 15:207-8.

Badowska-Kozakiewicz AM, Budzik MP. Immunohistochemical characteristics of basal-like breast cancer. *Contemp Oncol.* 2016; 20:436-443.

Balestrieri ML, Balestrieri A, Mancini FP, Napoli C. Understanding the immunoangiostatic CXC chemokine network. *Cardiovasc Res.* 2008; 78:250-6.

Bates JP, Derakhshandeh R, Jones L, Webb TJ. Mechanisms of immune evasion in breast cancer. *BMC Cancer.* 2018; 18:556.

Beniey M, Haque T, Hassan S. Translating the role of PARP inhibitors in triple-negative breast cancer. *Oncoscience.* 2019; 6:287–288.

Berchiche YA, Sakmar TP. CXC chemokine receptor 3 alternative splice variants selectively activate different signaling pathways. *Mol Pharmacol.* 2016; 90:483-95.

Berek JS, Keho, ST, Kumar L, Friedlander M. Cancer of the ovary, fallopian tube, and peritoneum. *Int J Gynecol Obstet.* 2018; 143:59-78.

Blanchet X, Langer M, Weber C, Koenen RR, von Hundelshausen P. Touch of chemokines. *Front Immunol.* 2012; 3:175.

Bracci L, Schiavoni G, Sistigu A, Belardelli F. Immune-based mechanisms of cytotoxic chemotherapy: implications for the design of novel and rationale-based combined treatments against cancer. *Cell Death Differ.* 2014; 21:15-25.

Bray F, Ferlay J, Soerjomataram I, Siegel RL, Torre LA, Jemal A. Global cancer statistics 2018: GLOBOCAN estimates of incidence and mortality worldwide for 36 cancers in 185 countries. *CA Cancer J Clin.* 2018; 68:394-424.

Brewer HR, Jones ME, Schoemaker MJ, Ashworth A, Swerdlow AJ. Family history and risk of breast cancer: an analysis accounting for family structure. *Breast Cancer Res Treat.* 2017; 165:193–200.

Bronger H, Magdolen V, Goettig P, Dreyer T. Proteolytic chemokine cleavage as a regulator of lymphocytic infiltration in solid tumors. *Cancer Metastasis Rev.* 2019; 38:417-430.

Bronger H, Magdolen V, Goettig P, Dreyer T. Proteolytic chemokine cleavage as a regulator of lymphocytic infiltration in solid tumors. *Cancer Metastasis Rev.* 2019; 38:417-430.

Bronger H, Singer J, Windmüller C, Reuning U, Zech D, Delbridge C, Dorn J, Kiechle M, Schmalfeldt B, Schmitt M, Avril S. CXCL9 and CXCL10 predict survival and are regulated by cyclooxygenase inhibition in advanced serous ovarian cancer. *Br J Cancer.* 2016; 115:553-63.

Bronger H. Immunology and immune checkpoint inhibition in ovarian cancer - current aspects. *Geburtshilfe Frauenheilkd*. 2021; 81:1128-1144.

Cao Y, Jiao N, Sun T, Ma Y, Zhang X, Chen, Hong J, Zhang Y. CXCL11 Correlates with antitumor immunity and an improved prognosis in colon cancer. *Frontiers in Cell and Developmental Biology.* 2021; 9:646252.

Cardoso F, Kyriakides S, Ohno S, Penault-Llorca F, Poortmans P, Rubio IT, Zackrisson S, Senkus E. Early breast cancer: ESMO clinical practice guidelines for diagnosis, treatment and follow-up. *Ann Oncol.* 2019; 30:1194-1220.

Caso G, Barry C, Patejunas G. Dysregulation of CXCL9 and reduced tumor growth in Egr-1 deficient mice. *J. Hematol. Oncol.* 2009; 2:7.

Chen Z, Wang X, Li X, Zhou Y, Chen K. Deep exploration of PARP inhibitors in breast cancer: monotherapy and combination therapy. *J Int Med Res*. 2021; 49:300060521991019.

Chung YR, Jang MH, Park SY, Gong G, Jung WH. Korean breast pathology Ki-67 satudy group. Interobserver variability of Ki-67 measurement in breast cancer. *J Pathol Transl Med.* 2016; 50:129-137.

Clarke B, Tinker AV, Lee CH, Subramanian S, van de Rijn M, Turbin D, Kalloger S, Han G, Ceballos K, Cadungog MG, Huntsman DG, Coukos G, Gilks CB. Intraepithelial T cells and prognosis in ovarian carcinoma: novel associations with stage, tumor type, and BRCA1 loss. *Mod Pathol.* 2009; 22:393-402.

Cole KE, Strick CA, Paradis TJ, Ogborne KT, Loetscher M, Gladue RP, Lin W, Boyd JG, Moser B, Wood DE, Sahagan BG, Neote K. Interferon-inducible T cell alpha chemoattractant (I-TAC): a novel non-ELR CXC chemokine with potent activity on activated T cells through selective high affinity binding to CXCR3. *J Exp Med.* 1998; 187:2009-21.

Coventry BJ, Weightman MJ, Bradley J, Skinner JM. Immune profiling in human breast cancer using high-sensitivity detection and analysis techniques. *JRSM Open.* 2015; 6:1–12.

Cowell CF, Weigelt B, Sakr RA, Ng CK, Hicks J, King TA, Reis-Filho JS. Progression from ductal carcinoma in situ to invasive breast cancer: revisited. *Mol Oncol.* 2013; 7:859-69.

Dalit L, Alvarado C, Küijper L, Kueh AJ, Weir A, D'Amico A, Herold MJ, Vince JE, Nutt SL, Groom JR. CXCL11 expressing C57BL/6 mice have intact adaptive immune responses to viral infection. *Immunol Cell Biol.* 2022; 100:312-322.

De Talhouet S, Peron J, Vuilleumier A, Friedlaender A, Viassolo V, Ayme A, Bodmer A, Treilleux I, Lang N, Tille JC, Chappuis PO, Buisson A, Giraud S, Lasset C, Bonadona V, Trédan O, Labidi-Galy SI. Clinical outcome of breast cancer in carriers of BRCA1 and BRCA2 mutations according to molecular subtypes. *Sci Rep.* 2020; 10:7073.

Denkert C, Liedtke C, Tutt A, von Minckwitz G. Molecular alterations in triple-negative breast cancer-the road to new treatment strategies. *Lancet.* 2017; 389:2430-2442.

Denkert C, Loibl S, Noske A, Roller M, Müller BM, Komor M, Budczies J, Darb-Esfahani S, Kronenwett R, Hanusch C, von Törne C, Weichert W, Engels K, Solbach C, Schrader I, Dietel M, von Minckwitz G. Tumor-associated lymphocytes as an independent predictor of response to neoadjuvant chemotherapy in breast cancer. *J Clin Oncol.* 2010; 28:105-13.

Denkert C, Loibl S, Noske A, Roller M, Müller BM, Komor M, Budczies J, Darb-Esfahani S, Kronenwett R, Hanusch C, von Törne C, Weichert W, Engels K, Solbach C, Schrader I, Dietel M, von Minckwitz G. Tumor-associated lymphocytes as an independent predictor of response to neoadjuvant chemotherapy in breast cancer. *J Clin Oncol.* 2010; 28:105-13.

Denkert C, von Minckwitz G, Brase JC, Sinn BV, Gade S, Kronenwett R, Pfitzner BM, Salat C, Loi S, Schmitt WD, Schem C, Fisch K, Darb-Esfahani S, Mehta K, Sotiriou C, Wienert S, Klare P, André F, Klauschen F, Blohmer JU, Krappmann K, Schmidt M, Tesch H, Kümmel S, Sinn P, Jackisch C, Dietel M, Reimer T, Untch M, Loibl S. Tumor-infiltrating lymphocytes and response to neoadjuvant chemotherapy with or without carboplatin in human epidermal growth factor receptor 2-positive and triple-negative primary breast cancers. *J Clin Oncol.* 2015; 33:983-91.

Denkert C, von Minckwitz G, Darb-Esfahani S, Lederer B, Heppner BI, Weber KE, Budczies J, Huober J, Klauschen F, Furlanetto J, Schmitt WD, Blohmer JU, Karn T, Pfitzner BM, Kümmel S, Engels K, Schneeweiss A, Hartmann A, Noske A, Fasching PA, Jackisch C, van Mackelenbergh M, Sinn P, Schem C, Hanusch C, Untch M, Loibl S. Tumour-infiltrating lymphocytes and prognosis in different subtypes of breast cancer: a pooled analysis of 3771 patients treated with neoadjuvant therapy. *Lancet Oncol.* 2018; 19:40-50.

Dhankhar R, Vyas SP, Jain AK, Arora S, Rath G, Goyal AK. Advances in novel drug delivery strategies for breast cancer therapy. *Artif Cells Blood Substit Immobil Biotechnol.* 2010; 38:230-49.

Ding Q, Lu P, Xia Y, Ding S, Fan Y, Li X, Han P, Liu J, Tian D, Liu M. CXCL9: evidence and contradictions for its role in tumor progression. *Cancer Med.* 2016; 5:3246-3259.

Downs-Canner S, Magge D, Ravindranathan R, O'Malley ME, Francis L, Liu Z, Sheng Guo Z, Obermajer N, Bartlett DL. Complement inhibition: a novel form of immunotherapy for colon cancer. *Ann Surg Oncol.* 2016; 23:655-62.

Ehdaivand S. WHO classification of ovarian neoplasms. PathologyOutlines.com. 2020.

Ehlert JE, Addison CA, Burdick MD, Kunkel SL, Strieter RM. Identification and partial characterization of a variant of human CXCR3 generated by posttranscriptional exon skipping. *J Immunol.* 2004; 173:6234-40.

Emens LA. Immunotherapy in triple-negative breast cancer. *Cancer J.* 2021; 27:59-66.
Fernandez EJ, Lolis E. Structure, function, and inhibition of chemokines. *Annu Rev Pharmacol Toxicol.* 2002; 42:469-99.

Fields EC, McGuire WP, Lin L, Temkin SM. Radiation Treatment in Women with Ovarian Cancer: Past, Present, and Future. *Front Oncol.* 2017; 7:177.

Forgó E, Longacre TA. High grade serous carcinoma. PathologyOutlines.com. 2021.

Forgó E, Longacre TA. Low grade serous carcinoma. PathologyOutlines.com. 2021.

Foulkes WD, Smith IE, Reis-Filho JS. Triple-negative breast cancer. *N Engl J Med.* 2010; 363:1938-48.

Gadducci A, Cosio S. Therapeutic approach to low-grade serous ovarian carcinoma: state of art and perspectives of clinical research. *Cancers.* 2020; 12:1336.

Gajjar K, Ogden G, Mujahid MI, Razvi K. Symptoms and risk factors of ovarian cancer: a survey in primary care. ISR*N Obstet Gynecol.* 2012; 2012:754197.

Gao Q, Wang S, Chen X, Cheng S, Zhang Z, Li F, Huang L, Yang Y, Zhou B, Yue D, Wang D, Cao L, Maimela NR, Zhang B, Yu J, Wang L, Zhang Y. Cancer-cell-secreted CXCL11 promoted CD8+ T cells infiltration through docetaxel-induced-release of HMGB1 in NSCLC. *J Immunother Cancer.* 2019; 7:42.

Gao YJ, Liu L, Li S, Yuan GF, Li L, Zhu HY, Cao GY. Down-regulation of CXCL11 inhibits colorectal cancer cell growth and epithelial-mesenchymal transition. *Onco Targets Ther.* 2018; 11:7333-7343.

García-Teijido P, Cabal ML, Fernández IP, Pérez YF. Tumor-infiltrating lymphocytes in TNBC: the future of immune targeting. *Clin Med Insights Oncol*. 2016; 10:31-39.

Gaynor N, Crown J, Collins DM. Immune checkpoint inhibitors: Key trials and an emerging role in breast cancer. *Semin Cancer Biol.* 2022; 79:44-57.

Geng X, Liu Y, Diersch S, Kotzsch M, Grill S, Weichert W, Kiechle M, Magdolen V, Dorn J. Clinical relevance of kallikrein-related peptidase 9, 10, 11, and 15 mRNA expression in advanced high-grade serous ovarian cancer. *PLoS One.* 2017; 12:e0186847.

Glajcar A, Szpor J, Hodorowicz-Zaniewska D, Tyrak KE, Okoń K. The composition of T cell infiltrates varies in primary invasive breast cancer of different molecular subtypes as well as according to tumor size and nodal status. *Virchows Arch.* 2019; 475:13-23

Goldhirsch A, Wood WC, Coates AS, Gelber RD, Thürlimann B, Senn HJ; Panel members. Strategies for subtypes--dealing with the diversity of breast cancer: highlights of the St. Gallen international expert consensus on the primary therapy of early breast cancer 2011. *Ann Oncol.* 2011; 22:1736-47

González-Bermúdez L, Anglada T, Genescà A, Martín M, Terradas M. Identification of reference genes for RT-qPCR data normalisation in aging studies. *Sci Rep.* 2019; 9:13970.

Grabosch SM, Edwards RP. Ovarian Cancer Treatment Protocols 2019. Medscape.com.

Groom JR, Luster AD. CXCR3 in T cell function. *Exp Cell Res.* 2011; 317:620-631.

Guo W, Sun Z, Zhao N, Zhou Y, Ren J, Huang L, Ping Y. NOTCH2NLA silencing inhibits ovarian carcinoma progression and oncogenic activity in vivo and in vitro. *Ann Transl Med*. 2021; 9:1669.

Gutierrez C, Schiff R. HER2: biology, detection, and clinical implications. *Arch Pathol Lab Med.* 2011; 135:55-62.

Hahnen E, Hauke J, Engel C, Neidhardt G, Rhiem K, Schmutzler RK. Germline mutations in triple-negative breast cancer. *Breast Care (Basel)*. 2017; 12:15-19.

Hamanishi J, Mandai M, Ikeda T, Minami M, Kawaguchi A, Murayama T, Kanai M, Mori Y, Matsumoto S, Chikuma S, Matsumura N, Abiko K, Baba T, Yamaguchi K, Ueda A, Hosoe Y, Morita S, Yokode M, Shimizu A, Honjo T, Konishi I. Safety and antitumor activity of anti-PD-1 antibody, nivolumab, in patients with platinum-resistant ovarian cancer. *J Clin Oncol.* 2015; 33:4015-22

Harlin H, Meng Y, Peterson AC, Zha Y, Tretiakova M, Slingluff C, McKee M, Gajewski TF. Chemokine expression in melanoma metastases associated with CD8+ T-cell recruitment. *Cancer Res.* 2009; 69:3077-85.

Hughes CE, Nibbs RJB. A guide to chemokines and their receptors. *FEBS J.* 2018; 285:2944-2971.

Iqbal N, Iqbal N. Human epidermal growth factor receptor 2 in cancers: overexpression and therapeutic implications. *Mol Biol Int.* 2014; 2014:852748.

Jelovac D, Armstrong DK. Recent progress in the diagnosis and treatment of ovarian cancer. *CA Cancer J Clin.* 2011; 61:183-203.

Jia D, Nagaoka Y, Katsumata M. Inflammation is a key contributor to ovarian cancer cell seeding. *Sci Rep.* 2018; 12394.

Jin YW, Hu PZ. Tumor-infiltrating CD8 T cells predict clinical breast cancer outcomes in young women. *Cancers.* 2020; 12:1076.

Kaku T, Ogawa S, Kawano Y, Ohishi Y, Kobayashi H, Hirakawa T, Nakano H. Histological classification of ovarian cancer. *Med Electron Microsc.* 2003; 36:9-17.

Kamal R, Hamed S, Mansour S, Mounir Y, Abdel Sallam S. Ovarian cancer screening-ultrasound; impact on ovarian cancer mortality. *Br J Radiol.* 2018; 91:20170571.

Keeley EC, Mehrad B, Strieter RM. CXC chemokines in cancer angiogenesis and metastases. *Adv Cancer Res.* 2010; 106:91-111.

Kiefer F, Siekmann AF. The role of chemokines and their receptors in angiogenesis. *Cell Mol Life Sci.* 2011; 68:2811-30.

Kim C, Gao R, Sei E, Brandt R, Hartman J, Hatschek T, Crosetto N, Foukakis T, Navin NE. Chemoresistance evolution in triple-negative breast cancer delineated by single-cell sequencing. *Cell.* 2018; 173:879-893.e13.

Knipprath-Mészáros A, Heinzelmann-Schwarz V, Vetter M. Endocrine therapy in epithelial ovarian cancer (EOC) new insights in an old target: a mini review. *Cancer clinical trials.* 2018; 03:1-5.

Kondo T, Ito F, Nakazawa H, Horita S, Osaka Y, Toma H. High expression of chemokine gene as a favorable prognostic factor in renal cell carcinoma. *J Urol.* 2004; 171:2171-5.

Kryczek I, Banerjee M, Cheng P, Vatan L, Szeliga W, Wei S, Huang E, Finlayson E, Simeone D, Welling TH, Chang A, Coukos G, Liu R, Zou W. Phenotype, distribution, generation, and functional and clinical relevance of Th17 cells in the human tumor environments. *Blood.* 2009; 114:1141-9.

Kuo PT, Zeng Z, Salim N, Mattarollo S, Wells JW, Leggatt GR. The role of CXCR3 and its chemokine ligands in skin disease and cancer. *Front Med.* 2018; 5:271.

Lasagni L, Francalanci M, Annunziato F, Lazzeri E, Giannini S, Cosmi L, Sagrinati C, Mazzinghi B, Orlando C, Maggi E, Marra F, Romagnani S, Serio M, Romagnani P. An alternatively spliced variant of CXCR3 mediates the inhibition of endothelial cell growth induced by IP-10, Mig, and I-TAC, and acts as functional receptor for platelet factor 4. *J Exp Med.* 2003; 197:1537-49.

Law ME, Corsino PE, Narayan S, Law BK. CDK Inhibitors as Anticancer Therapeutics. *Molecular Pharmacology.* 2015, 88:846-852.

Lee K, Kruper L, Dieli-Conwright CM, Mortimer JE. The Impact of Obesity on Breast Cancer Diagnosis and Treatment. *Curr Oncol Rep.* 2019; 21:41.

Lee S, Rauch J, Kolch W. Targeting MAPK Signaling in cancer: mechanisms of drug resistance and sensitivity. *Int J Mol Sci.* 2020; 21:1102.

Li H, Somiya M, Kuroda S. Enhancing antibody-dependent cellular phagocytosis by Re-education of tumor-associated macrophages with resiquimod-encapsulated liposomes. *Biomaterials.* 2021; 268:120601.

Li W, Ma JA, Sheng X, Xiao C. Screening of CXC chemokines in the microenvironment of ovarian cancer and the biological function of CXCL10. *World J Surg Oncol.* 2021; 19:329.

Liang Q, Ma D, Gao RF, Yu KD. Effect of Ki-67 expression levels and histological grade on breast cancer early relapse in patients with different immunohistochemical-based subtypes. *Sci Rep.* 2020; 10:7648.

Lieber S, Reinartz S, Raifer H, Finkernagel F, Dreyer T, Bronger H, Jansen JM, Wagner U, Worzfeld T, Müller R, Huber M. Prognosis of ovarian cancer is associated with effector memory $CD8^+$ T cell accumulation in ascites, CXCL9 levels and activation-triggered signal transduction in T cells. *Oncoimmunology.* 2018; 7:e1424672.

Litchfield K, Reading JL, Puttick C, Thakkar K, Abbosh C, Bentham R, Watkins TBK, Rosenthal R, Biswas D, Rowan A, Lim E, Al Bakir M, Turati V, Guerra-Assunção JA, Conde L, Furness AJS, Saini SK, Hadrup SR, Herrero J, Lee SH, Van Loo P, Enver T, Larkin J, Hellmann MD, Turajlic S, Quezada SA, McGranahan N, Swanton C. Meta-analysis of tumor- and T cell-intrinsic mechanisms of sensitization to checkpoint inhibition. *Cell.* 2021; 184:596-614.e14.

Liu J, Tan Z, He J, Jin T, Han Y, Hu L, Song J, Huang S. Identification of three molecular subtypes based on immune infiltration in ovarian cancer and its prognostic value. *Biosci Rep.* 2020 ;40:BSR20201431.

Liu MJ, Guo H, Jiang LL, Jiao M, Wang SH, Tian T, Fu X, Wang WJ. Elevated RBP-Jκ and CXCL11 Expression in Colon Cancer is Associated with an Unfavorable Clinical Outcome. *Cancer Manag Res.* 2021; 13:3651-3661

Liu SY, Zhu RH, Wang ZT, Tan W, Zhang L, Wang YQ, Dai FF, Yuan MQ, Zheng YJ, Yang DY, Wang FY, Xian S, He J, Zhang YW, Wu ML, Deng ZM, Hu M, Cheng YX, Liu YQ. Landscape of immune microenvironment in epithelial ovarian cancer and establishing risk model by machine learning. *J Oncol*. 2021; 26:5523749.

Liu Y, Beyer A, Aebersold R. On the dependency of cellular protein levels on mRNA abundance. *Cell.* 2016; 165:535-50.

Liu Y, Preis S, Xiaocong G, Gong W, Kiechle M, Dreyer T, Magdolen V, Dorn J. Kallikrein-related peptidases in triple negative breast cancer: prognostic value of quantitatively assessed KLK8, KLK10 and KLK11 mRNA expression. 2021, preprint.

Lo Nigro C, Macagno M, Sangiolo D, Bertolaccini L, Aglietta M, Merlano MC. NK-mediated antibody-dependent cell-mediated cytotoxicity in solid tumors: biological evidence and clinical perspectives. *Ann Transl Med*. 2019; 7:105.

Loetscher M, Loetscher P, Brass N, Meese E, Moser B. Lymphocyte-specific chemokine receptor CXCR3: regulation, chemokine binding and gene localization. *Eur J Immunol.* 1998; 28:3696-705.

Lopez J, Banerjee S, Kaye SB. New developments in the treatment of ovarian cancer-future perspectives. *Ann Oncol.* 2013; 24:x69-x76.

Lu KH. Screening for ovarian cancer in asymptomatic women. *JAMA.* 2018; 319:557-558.

Madeira M, Mattar A, Passos RJ, Mora CD, Mamede LH, Kishino VH, Torres TZ, de Sá AF, dos Santos RE, Gebrim LH. A case report of male breast cancer in a very young patient: what is changing? *World J Surg Oncol.* 2011; 9:16.

Malhotra GK, Zhao X, Band H, Band V. Histological, molecular and functional subtypes of breast cancers. *Cancer Biol Ther.* 2010; 10:955-60.

Malpica A, Deavers MT, Lu K, Bodurka DC, Atkinson EN, Gershenson DM, Silva EG. Grading ovarian serous carcinoma using a two-tier system. *Am J Surg Pathol.* 2004; 28:496-504.

Mantia-Smaldone GM, Corr B, Chu CS. Immunotherapy in ovarian cancer. *Hum Vaccin Immunother.* 2012; 8:1179-1191.

Maravillas-Montero JL, Burkhardt AB, Hevezi PA, Martine JS, Zlotnik A. Cutting edge: GPR35/CXCR8 is the receptor of the mucosal chemokine CXCL17. *J Immunol*. 2015; 194:29-33.

Metzemaekers M, Vanheule V, Janssens R, Struyf S, Proost P. Overview of the mechanisms that may contribute to the non-redundant activities of interferon-inducible CXC chemokine receptor 3 ligands. *Front Immunol.* 2018; 8:1970.

Meyer S, Leusen JH, Boross P. Regulation of complement and modulation of its activity in monoclonal antibody therapy of cancer. *MAbs*. 2014; 6:1133-1144.

Miller MC, Mayo KH. Chemokines from a structural perspective. *Int J Mol Sci.* 2017; 18:2088.

Millikan RC, Newman B, Tse CK, Moorman PG, Conway K, Dressler LG, Smith LV, Labbok MH, Geradts J, Bensen JT, Jackson S, Nyante S, Livasy C, Carey L, Earp HS, Perou CM. Epidemiology of basal-like breast cancer. *Breast Cancer Res Treat.* 2008; 109:123-39.

Millstein J, Budden T, Goode EL, Anglesio MS, Talhouk A, Intermaggio MP, Leong HS, Chen S, Elatre W, Gilks B, Nazeran T, Volchek M, Bentley RC, Wang C, Chiu DS, Kommoss S, Leung SCY, Senz J, Lum A, Chow V, Sudderuddin H, Mackenzie R, George J; AOCS Group, Fereday S, Hendley J, Traficante N, Steed H, Koziak JM, Köbel M, McNeish IA, Goranova T, Ennis D, Macintyre G, Silva De Silva D, Ramón Y Cajal T, García-Donas J, Hernando Polo S, Rodriguez GC, Cushing-Haugen KL, Harris HR, Greene CS, Zelaya RA, Behrens S, Fortner RT, Sinn P, Herpel E, Lester J, Lubiński J, Oszurek O, Tołoczko A, Cybulski C, Menkiszak J, Pearce CL, Pike MC, Tseng C, Alsop J, Rhenius V, Song H, Jimenez-Linan M, Piskorz AM, Gentry-Maharaj A, Karpinskyj C, Widschwendter M, Singh N, Kennedy CJ, Sharma R, Harnett PR, Gao B, Johnatty SE, Sayer R, Boros J, Winham SJ, Keeney GL, Kaufmann SH, Larson MC, Luk H, Hernandez BY, Thompson PJ, Wilkens LR, Carney ME, Trabert B, Lissowska J, Brinton L, Sherman ME, Bodelon C, Hinsley S, Lewsley LA, Glasspool R, Banerjee SN, Stronach EA, Haluska P, Ray-Coquard I, Mahner S, Winterhoff B, Slamon D, Levine DA, Kelemen LE, Benitez J, Chang-Claude J, Gronwald J, Wu AH, Menon U, Goodman MT, Schildkraut JM, Wentzensen N, Brown R, Berchuck A, Chenevix-Trench G, deFazio A, Gayther SA, García MJ, Henderson MJ, Rossing MA, Beeghly-Fadiel A, Fasching PA, Orsulic S, Karlan BY, Konecny GE, Huntsman DG, Bowtell DD, Brenton JD, Doherty JA, Pharoah PDP, Ramus SJ. Prognostic gene expression signature for high-grade serous ovarian cancer. *Ann Oncol.* 2020; 33:1240-1250.

Momenimovahed Z, Tiznobaik A, Taheri S, Salehiniya H. Ovarian cancer in the world: epidemiology and risk factors. *Int J Womens Health.* 2019; 11:287-299.

Mullooly M, Khodr ZG, Dallal CM, Nyante SJ, Sherman ME, Falk R, Liao LM, Love J, Brinton LA, Gierach GL. Epidemiologic risk factors for in situ and invasive breast cancers among postmenopausal women in the national institutes of health-AARP diet and health study. *Am J Epidemiol.* 2017; 186:1329-1340.

Nascimento R. G. and Otoni K.M. “Histological and molecular classification of breast cancer: what do we know?”. *Mastology*. 2020.

Nofech-Mozes S, Trudeau M, Kahn HK, Dent R, Rawlinson E, Sun P, Narod SA, Hanna WM. Patterns of recurrence in the basal and non-basal subtypes of triple-negative breast cancers. *Breast Cancer Res Treat.* 2009; 118:131-7.

Nomiyama H, Hieshima K, Osada N, Kato-Unoki Y, Otsuka-Ono K, Takegawa S, Izawa T, Yoshizawa A, Kikuchi Y, Tanase S, Miura R, Kusuda J, Nakao M, Yoshie O. Extensive expansion and diversification of the chemokine gene family in zebrafish: identification of a novel chemokine subfamily CX. *BMC Genomics.* 2008; 9:222.

Oldham K. University of Birmingham, UK. Chemokines: introduction. https://www.immunology.org/public- information/bitesized-immunology/receptors-and-molecules/ chemokines-introduction.

Pantelidou C, Sonzogni O, De Oliveria Taveira M, Mehta AK, Kothari A, Wang D, Visal T, Li MK, Pinto J, Castrillon JA, Cheney EM, Bouwman P, Jonkers J, Rottenberg S, Guerriero JL, Wulf GM, Shapiro GI. PARP inhibitor efficacy depends on CD8+ T-cell recruitment via intratumoral STING pathway activation in BRCA-deficient models of triple-negative breast cancer. *Cancer Discov.* 2019; 9:722-737.

Pfaffl MW. Quantification strategies in real-time polymerase chain reaction. Quantitative real-time PCR. *Appl Microbiol.* 2012; 53-62.

Pilie PG, Gay CM, Byers LA, O'Connor MJ, Yap TA. PARP Inhibitors: extending benefit beyond BRCA-mutant cancers. *Clin Cancer Res.* 2019; 25:3759-3771.

Piotrowski I, Kulcenty K, Suchorska W. Interplay between inflammation and cancer. *Rep Pract Oncol Radiother.* 2020; 25:422-427.

Pogge von Strandmann E, Reinartz S, Wager U, Müller R. Tumor-Host Cell Interactions in Ovarian Cancer: Pathways to Therapy Failure. *Trends Cancer.* 2017; 3:137-148.

Przewoznik M, Hömberg N, Naujoks M, Pötzl J, Münchmeier N, Brenner CD, Anz D, Bourquin C, Nelson PJ, Röcken M, Mocikat R. Recruitment of natural killer cells in advanced stages of endogenously arising B-cell lymphoma: implications for therapeutic cell transfer. *J Immunother.* 2012; 35:217-22.

Puchert M, Obst J, Koch C, Zieger K, Engele J. CXCL11 promotes tumor progression by the biased use of the chemokine receptors CXCR3 and CXCR7. *Cytokine.* 2020; 125:154809.

Qiu D, Zhang G, Yan X, Xiao X, Ma X, Lin S, Wu J, Li X, Wang W, Liu J, Ma Y, Ma M. Prospects of immunotherapy for triple-negative breast cancer. *Front Oncol.* 2022; 11:797092.

Qureshi S, Chan N, George M, Ganesan S, Toppmeyer D, Omene C. Immune checkpoint inhibitors in triple negative breast cancer: the search for the optimal biomarker. *Biomark Insights.* 202; 17:11772719221078774.

Rani MR, Foster GR, Leung S, Leaman D, Stark GR, Ransohoff RM. Characterization of beta-R1, a gene that is selectively induced by interferon beta (IFN-beta) compared with IFN-alpha. *J Biol Chem.* 1996; 271:22878-84

Rashmi R, Prasad K, Udupa CBK. Breast histopathological image analysis using image processing techniques for diagnostic purposes: A methodological review. *J Med Syst. 2022;* 46:7.

Rose M, Burgess JT, O'Byrne K, Richard DJ, Bolderson E. PARP inhibitors: clinical relevance, mechanisms of action and tumor resistance. *Front Cell Dev Biol.* 2020; 8:564601.

Rosenblum JM, Shimoda N, Schenk AD, Zhang H, Kish DD, Keslar K, Joshua M. Farber JM, Fairchild RL. CXC Chemokine Ligand (CXCL) 9 and CXCL10 Are Antagonistic Costimulation Molecules during the Priming of Alloreactive T Cell Effectors. *J Immunol.* 2010; 184:3450-3460

Rossi D, Zlotnik A. The biology of chemokines and their receptors. *Annu Rev Immunol.* 2000; 18:217-42.

Ruffell B, Au A, Rugo HS, Esserman LJ, Hwang ES, Coussens LM. Leukocyte composition of human breast cancer. *Proc. Natl. Acad. Sci. USA.* 2012; 109:2796–2801.

Ruffini PA, Morandi P, Cabioglu N, Altundag K, Cristofanilli M. Manipulating the chemokine-chemokine receptor network to treat cancer. *Cancer.* 2007; 109:2392-404.

Sahin H, Borkham-Kamphorst E, Kuppe C, Zaldivar MM, Grouls C, Al-samman M, Nellen A, Schmitz P, Heinrichs D, Berres ML, Doleschel D, Scholten D, Weiskirchen R, Moeller MJ, Kiessling F, Trautwein C, Wasmuth HE. Chemokine Cxcl9 attenuates liver fibrosis-associated angiogenesis in mice. *Hepatology.* 2012; 55:1610-9.

Salehi F, Dunfield L, Phillips KP, Krewski D, Vanderhyden BC. Risk factors for ovarian cancer: an overview with emphasis on hormonal factors. *J Toxicol Environ Health B Crit Rev.* 2008; 11:301-21.

Sanchez-Martín L, Sanchez-Mateos P, Cabanas C. CXCR7 impact on CXCL12 biology and disease. *Trends Mol Med.* 2013; 19:12-22.

Sapiezynski J, Taratula O, Rodriguez-Rodriguez L, Minko T. Precision targeted therapy of ovarian cancer. *J Control Release.* 2016; 243:250-268.

Sauty A, Colvin RA, Wagner L, Rochat S, Spertini F, Luster AD. CXCR3 internalization following T cell-endothelial cell contact: preferential role of IFN-inducible T cell alpha chemoattractant (CXCL11). *J Immunol.* 2001;167:7084-93.

Savas P, Salgado R, Denkert C, Sotiriou C, Darcy PK, Smyth MJ, Loi S. Clinical relevance of host immunity in breast cancer: from TILs to the clinic. *Nat Rev Clin Oncol.* 2016; 13:228-41.

Schettini F, Buono G, Cardalesi C, Desideri I, D e Placido S, Del Mastro L. Hormone receptor/human epidermal growth factor receptor 2-positive breast cancer: Where we are now and where we are going. *Cancer Treat Rev.* 2016; 46:20-6.

Seitz S, Dreyer TF, Stange C, Steiger K, Bräuer R, Scheutz L, Multhoff G, Weichert W, Kiechle M, Magdolen V, Bronger H. CXCL9 inhibits tumour growth and drives anti-PD-L1 therapy in ovarian cancer. *Br J Cancer.* 2022.

Shi Z, Zhao Q, Lv B, Qu X, Han X, Wang H, Qiu J, Hua K. Identification of biomarkers complementary to homologous recombination deficiency for improving the clinical outcome of ovarian serous cystadenocarcinoma. *Clin Transl Med.* 2021; 11(5):e399.

Shi Z, Zhao Q, Lv B, Qu X, Han X, Wang H, Qiu J, Hua K. Identification of biomarkers complementary to homologous recombination deficiency for improving the clinical outcome of ovarian serous cystadenocarcinoma. *Clin Transl Med*. 2021; 11:e399.

Singh DD, Parveen A, Yadav DK. Role of PARP in TNBC: mechanism of inhibition, clinical applications, and Resistance. *Biomedicines*. 2021; 9(11):1512.

Sinn HP, Kreipe H. A Brief Overview of the WHO classification of breast tumors, 4th edition, focusing on issues and updates from the 3rd Edition. *Breast Care (Basel)*. 2013; 8:149-154.

Song J, Deng Z, Su J, Yuan D, Liu J, Zhu J. Patterns of immune infiltration in HNC and their clinical implications: a gene expression-based study. *Front Oncol.* 2019; 9:1285.

Sparano JA, Lee MC. Breast cancer staging. Medscape.com. 2019.

Specht K, Harbeck N, Smida J, Annecke K, Reich U, Nährig J, Langer R, Mages J, Busch R, Kruse E, Klein-Hitpass L, Schmitt M, Kiechle M, Höfler H.Expression profiling identifies genes that predict recurrence of breast cancer after adjuvant CMF-based chemotherapy. *Breast Cancer Res Treat.* 2009; 118:45–56.

Stanton SE, Disis ML. Clinical significance of tumor-infiltrating lymphocytes in breast cancer. *J Immunother Cancer.* 2016; 4:59.

Su T, Zhang P, Zhao F, Zhang S. A novel immune-related prognostic signature in epithelial ovarian carcinoma. *Aging.* 2021; 13:10289-10311.

Sun YS, Zhao Z, Yang ZN, Xu F, Lu HJ, Zhu ZY, Shi W, Jiang J, Yao PP, Zhu HP. Risk factors and preventions of breast cancer. *Int J Biol Sci.* 2017; 13:1387-1397.

Sundar S, Neal RD, Kehoe S. Diagnosis of ovarian cancer. *BMJ.* 2015;351:h4443.

Tarantino P, Corti C, Schmid P, Cortes J, Mittendorf EA, Rugo H, Tolaney SM, Bianchini G, Andrè F, Curigliano G. Immunotherapy for early triple negative breast cancer: research agenda for the next decade. *NPJ Breast Cancer.* 2022; 8:23.

Tensen CP, Vermeer MH, van der Stoop PM, van Beek P, Scheper RJ, Boorsma DM, Willemze R. Epidermal interferon-gamma inducible protein-10 (IP-10) and monokine induced by gamma-interferon (Mig) but not IL-8 mRNA expression is associated with epidermotropism in cutaneous T cell lymphomas. *J Invest Dermatol.* 1998; 111:222-6.

Tokunaga R, Zhang W, Naseem M, Puccini A, Berger MD, Soni S, McSkane M, Baba H, Lenz HJ. CXCL9, CXCL10, CXCL11/CXCR3 axis for immune activation - a target for novel cancer therapy. *Cancer Treat Rev.* 2018; 63:40-47.

van Seijen M, Lips EH, Thompson AM, Nik-Zainal S, Futreal A, Hwang ES, Verschuur E, Lane J, Jonkers J, Rea DW, Wesseling J; PRECISION team. Ductal carcinoma in situ: to treat or not to treat, that is the question. *Br J Cancer.* 2019; 121:285-292.

Vandercappellen J, Van Damme J, Struyf S. The role of CXC chemokines and their receptors in cancer. *Cancer Lett.* 2008; 267:226-44.

Vang R, Shih IeM, Kurman RJ. Ovarian low-grade and high-grade serous carcinoma: pathogenesis, clinicopathologic and molecular biologic features, and diagnostic problems. *Adv Anat Pathol.* 2009; 16:267-82.

Varga A, Piha-Paul SA, Ott PA, Mehnert JM, Berton-Rigaud D, Johnson EA, Cheng JD, Yuan S, Rubin EH, Matei DE. Antitumor activity and safety of pembrolizumab in patients with PD-L1 positive advanced ovarian cancer: Interim results from a phase Ib study. *J. Clin. Oncol.* 2015; 33:5510.

Varghese F, Bukhari AB, Malhotra R, De A. IHC Profiler: an open-source plugin for the quantitative evaluation and automated scoring of immunohistochemistry images of human tissue samples. *PLoS One.* 2014; 9:e96801.

Vinayak S, Ford JM. PARP inhibitors for the treatment and prevention of breast cancer. *Curr Breast Cancer Rep.* 2010; 2:190-197.

Vogel C, Marcotte EM. Insights into the regulation of protein abundance from proteomic and transcriptomic analyses. *Nat Rev Genet.* 2012; 13:227-32.

Wahba HA, El-Hadaad HA. Current approaches in treatment of triple-negative breast cancer. *Cancer Biol Med.* 2015; 12:106-16.

Walz DA, Wu VY, de Lamo R, Dene H, McCoy LE. Primary structure of human platelet factor 4. *Thromb Res.* 1977; 11:893-8.

Wang JJ, Siu MKY, Jiang YX, Leung THY, Chan DW, Wang HG, Ngan HYS, Chan KKL. A combination of glutaminase inhibitor 968 and PD-L1 blockade boosts the immune response against ovarian cancer. *Biomolecules*. 2021; 11:1749.

Ward EM, DeSantis CE, Lin CC, Kramer JL, Jemal A, Kohler B, Brawley OW, Gansler T. Cancer statistics: breast cancer in situ. *CA Cancer J Clin.* 2015; 65:481-95.

Wasmuth HE, Lammert F, Zaldivar MM, Weiskirchen R, Hellerbrand C, Scholten D, Berres ML, Zimmermann H, Streetz KL, Tacke F, Hillebrandt S, Schmitz P, Keppeler H, Berg T, Dahl E, Gassler N, Friedman SL, Trautwein C. Antifibrotic effects of CXCL9 and its receptor CXCR3 in livers of mice and humans. *Gastroenterology.* 2009; 137:309-19.

Wei SU, Li H, Zhang B. The diagnostic value of serum HE4 and CA-125 and ROMA index in ovarian cancer. *Biomed Rep.* 2016; 5:41-44.

Wesierska-Gadek J, Gueorguieva M, Wojciechowski J, Horky M. Cell cycle arrest induced in human breast cancer cells by cyclin-dependent kinase inhibitors: a comparison of the effects exerted by roscovitine and olomoucine. *Pol J Pharmacol.* 2004; 56:635-41.

Wu Q, Siddharth S, Sharma D. Triple negative breast cancer: a mountain yet to be scaled despite the triumphs. *Cancers (Basel)*. 2021; 13:3697.

Yalaza M, İnan A, Bozer M. Male Breast Cancer. *J Breast Health.* 2016; 12:1-8

Yan S, Fang J, Chen Y, Xie Y, Zhang S, Zhu X, Fang F. Comprehensive analysis of prognostic gene signatures based on immune infiltration of ovarian cancer. *BMC Cancer.* 2020; 20:1205.

Yang J, Hong S, Zhang X, Liu J, Wang Y, Wang Z, Gao L, Hong L. Tumor Immune Microenvironment Related Gene-Based Model to Predict Prognosis and Response to Compounds in Ovarian Cancer. *Front Oncol.* 2021; 13;11:807410.

Yang X, Chu Y, Wang Y, Zhang R, Xiong S. Targeted in vivo expression of IFN-gamma-inducible protein 10 induces specific antitumor activity. *J Leukoc Biol.* 2006; 80:1434-44.

Yin L, Duan JJ, Bian XW, Yu SC. Triple-negative breast cancer molecular subtyping and treatment progress. *Breast Cancer Res.* 2020; 22:61.

Yonezawa A, Chester C, Rajasekaran N, Kohrt H. Harnessing the innate immune system to treat cancer: enhancement of antibody-dependent cellular cytotoxicity with anti-CD137 Ab. *Chinese Clinical Oncology.* 2016; 5:5.

Young SR, Pilarski RT, Donenberg T, Shapiro C, Hammond LS, Miller J, Brooks KA, Cohen S, Tenenholz B, Desai D, Zandvakili I, Royer R, Li S, Narod SA. The prevalence of BRCA1 mutations among young women with triple-negative breast cancer. *BMC Cancer.* 2009; 9:86.

Yu LY, Tang J, Zhang CM, et al. New Immunotherapy Strategies in Breast Cancer. *Int J Environ Res Public Health.* 2017; 14:68

Yung SY, Farber JM. Chemokines: handbook of biologically active peptides (second edition). *Academic Press.* 2013.

Zhang C, Li Z, Xu L, Che X, Wen T, Fan Y, Li C, Wang S, Cheng Y, Wang X, Qu X, Liu Y. CXCL9/10/11, a regulator of PD-L1 expression in gastric cancer. *BMC Cancer.* 2018; 18:462.
Zheng M, Long J, Chelariu-Raicu A, Mullikin H, Vilsmaier T, Vattai A, Heidegger HH, Batz F, Keckstein S, Jeschke U, Trillsch F, Mahner S, Kaltofen T. Identification of a novel tumor microenvironment prognostic signature for advanced-stage serous ovarian cancer. *Cancers*. 2021; 13:3343.

Zlotnik A, Yoshie O. Chemokines: a new classification system and their role in immunity. *Immunity.* 2000; 12:121-7.

Zlotnik A, Yoshie O. The chemokine superfamily revisited. *Immunity.* 2012; 36:705-16.

8 Acknowledgements

I would like to thank the following people, without whom I would not have been able to complete this research.

First of all, I would like to express my deep and sincere gratitude to my supervisor, Prof. Victor Magdolen, for giving me the opportunity to do research research and providing invaluable guidance throughout the study. His vision, sincerity and motivation have inspired me. It was a great privilege and honor to work in his team and study under his guidance.

I also want to thank to my second research supervisor, Dr. rer. nat. Tobias Dreyer, for providing invaluable support. He has taught me the methodology to carry out the research and to present the research works as clearly as possible. Without his guidance and persistent help this thesis would not have been possible.

I wish to show my gratitude to the whole Klinische Forschergruppe der Frauenklinik des Klinikums rechts der Isar, especially Caixia Zhu, Jeanny Probst, Daniela Hellmann, Rosalinda Bräuer, Stefanie Seitz and Christoph Stange for teaching and supporting me.

Last but not least, my sincerest to my mother Irina Vedmetskaya for her love, support and sacrifices for my education and preparing me for the future. I am very grateful to my husband Jörg-Christof Bauer for his love, understanding, and constant support.